UNIVERSITA' DEGLI STUDI DELL'INSUBRIA

DOTTORATO DI RICERCA IN SCIENZE DELLA VITA E BIOTECNOLOGIE
XXXIV CICLO

THE ROLE OF VOLATILE ORGANIC COMPOUNDS IN PLANT RESPONSE TO ENVIRONMENTAL STRESSES

Tesi di dottorato di:
Ilaria Mancini
Matr. 739041

Docente guida: Prof. Marcella Bracale
Tutor: Dott. Guido Domingo

Dip. Biotecnologie e Scienze della Vita - Università degli Studi dell'Insubria

Anno accademico 2021-2022

CONTENTS

CHAPTER THREE

CHAPTER ONE

VOLATILE ORGANIC COMPOUNDS AND PLANT STRESS: INTRODUCTION TO THE TOPIC

Biogenic Volatile Organic Compounds (BVOCs) are secondary metabolites produced by living organisms and released in the ecosystem. They are characterized by having low molecular weight (>30-300 Da), lyophilic properties (octanol-water partition coefficient >1) and high vapor pressure at ambient conditions (Widhalm et al. 2015).

Terrestrial ecosystems are both the source and the sink of these molecules, which, by releasing up to 1000-1300 Tg/year of carbon as VOCs, heavily promote the global carbon cycle (Millet et al. 2018, Tani and Mochizuchi 2021).

120 Pg/year of carbon is fixed through photosynthesis and partially re-emitted in the atmosphere as reactive carbon compounds (Kesselmeier et al. 2002). These latter include mostly hydrocarbons (e.g. methane, ethene, propene), terpenoids (e.g. isoprene); oxygenated compounds (e.g. methanol, acetone, methyl-ethyl-ketone), carbon monoxide and, in few cases, sulphur and nitrogen compounds. The persistence (lifetime) in atmosphere may vary from 4.8 h (isoprene) to about 45h (ethanol) and reflects the degree of reactivity (Penuelas and Llusià 2001). Most of these compounds (e.g. methane) are oxidized as CO_2 in atmosphere while others (e.g. nitrogen oxides) react with other chemicals. In both cases, the atmospheric chemistry is altered, influencing the climate and living organisms (Guenther 2002, Rinnan et al. 2014). Examples of VOCs-derived climate forcer are ozone (O_3) and secondary organic aerosol (SOA) (Cotrozzi et al. 2019, Farmer and Riches 2020); together they form photochemical smog which can affect human health and crop yield quality (Chuwah et al. 2015, Nuvolone et al. 2018, Zhang et al. 2019).

So far, more than 1700 species of different plant VOCs have been isolated and characterized according to their chemical structure. They represent the 1% of the total secondary metabolites known in plants (Pichersky and Gershenzon 2002, Maffei et al. 2011).

VOLATILE BIOSYNTHESIS

The larger group of VOCs are terpenoids (mono-, di-, homo-, hemi- and sesquiterpenes), followed by phenylpropanoids, benzenoids, fatty acid derivates (including Green Leaf Volatiles or GLVs), and derivates from branched-amino acid biosynthesis as well as aliphatic hydrocarbons such as aldehydes, alcohols, alkanes, esters, and ketones (Dudareva et al. 2013). VOCs are not only released from leaves, but also from non-green tissues as roots, flowers, and fruits in different quantity and quality (Rodríguez et al. 2013). Epidermal cells (non-green tissues), secretory cells of storage structures as glandular trichomes (leaves) and mesophyll cells are the most typical sites of VOCs biosynthesis (Widhalm et al. 2015).

A simplified scheme of the biosynthetic pathways of the major VOCs groups, which will be described in some detail below, is reported in Fig. 1.

Terpenoids, also called isoprenoids, are the most abundant VOCs in nature and include both volatiles and non-volatiles compounds (Abbas et al. 2017).

Volatile terpenoids are hemiterpenes (C_5) monoterpenes (C_{10}) and sesquiterpenes (C_{15}), while the non-volatile terpenoids (>C_{15}) comprise key molecules as phytohormones [abscisic acid (ABA), gibberellins (GAs), cytokinins (CKs) and brassinosteroids (BRs)], photosynthetic pigments (chlorophylls, carotenoids, lycopene, strigolactones), quinones and membrane components (sterols) (Maffei et al. 2011).

There are two pathways for terpenoid biosynthesis in plant cells: the 2-*C*-methyl-D-erythritol 4-phosphate (MEP) for hemiterpenes (C_5, e.g. isoprene), monoterpenes (C_{10}), diterpenes (C_{20}), homoterpenes (C_{11}, e.g. 4,8-dimethylnona-1,3,7-triene -DMNT-) and tetraterpenes (C_{40}) including chlorophyll derivates, and the mevalonate (MVA) pathway for sesquiterpenes, sterols (C_{27}–C_{29}), homoterpene (C_{16}, e.g. 4,8,12-trimethyltrideca-1,3,7,11-tetraene -TMTT-) and triterpenes (C_{30}) (Fig.1) (Tholl et al. 2011, Bergman et al. 2019).

The MEP pathway is located in plastids, while the MVA pathway in distributed among cytosol, endoplasmic reticulum (ER), and peroxisomes (Dudareva et al. 2013).

Interestingly, most organism (archaea, fungi and animals) present only the MVA pathway, with photosynthetic eukaryotes and some bacteria representing the only exceptions (Pérez-Gil and Rodríguez-Concepción 2013, Hoshino and Gaucher 2018).

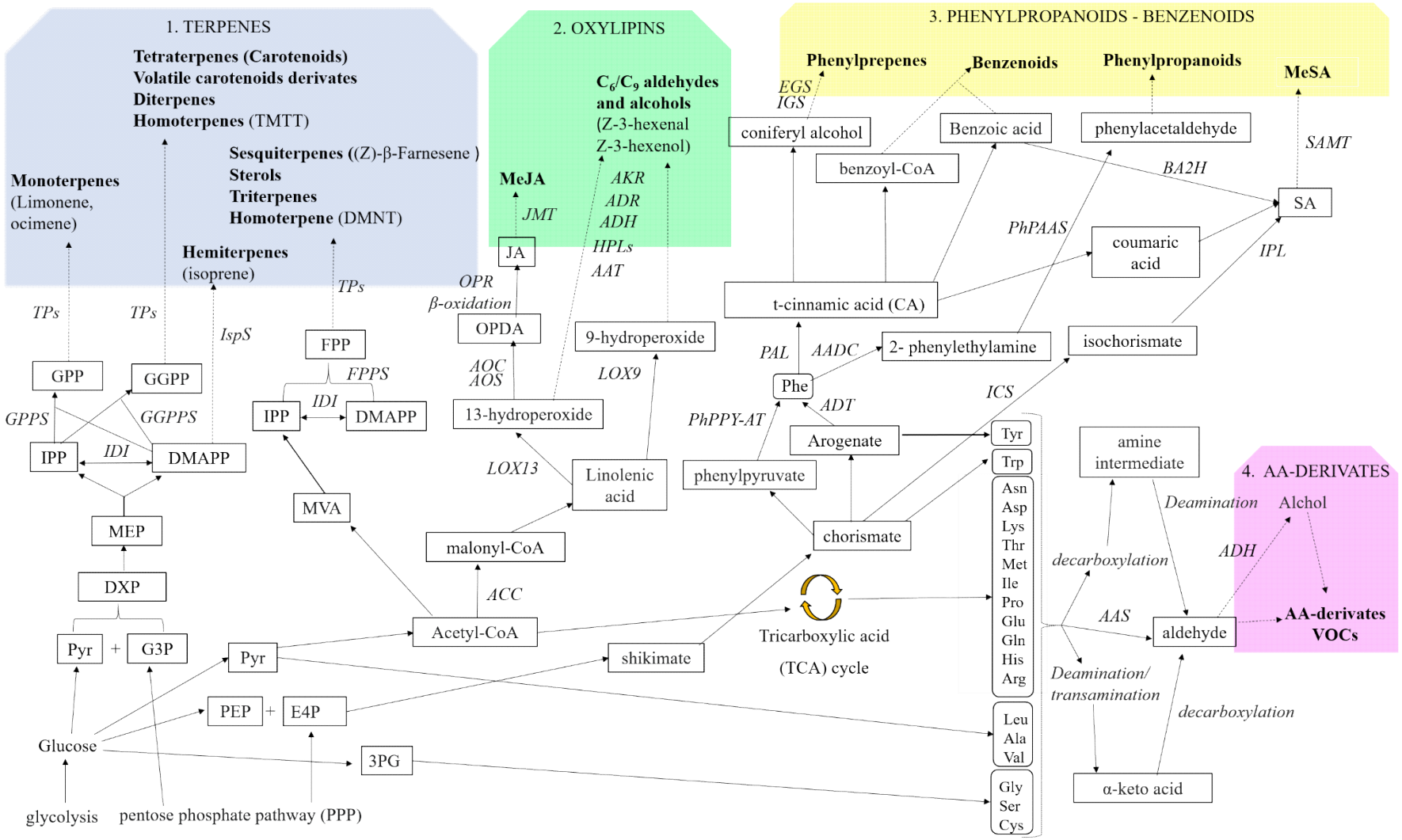
1. TERPENES
Tetraterpenes (Carotenoids)
Volatile carotenoids derivates
Diterpenes
Homoterpenes (TMTT)
Sesquiterpenes ((Z)-β-Farnesene)
Sterols
Triterpenes
Homoterpene (DMNT)
Monoterpenes
(Limonene,
ocimene)
Hemiterpenes
(isoprene)
TPs
TPs
TPs
IspS
GPP
GGPP
FPP
GPPS
GGPPS
FPPS
IPP
IDI
DMAPP
IPP
IDI
DMAPP
MEP
DXP
Pyr
+
G3P
MVA
2. OXYLIPINS
C6/C9 aldehydes
and alcohols
(Z-3-hexenal
Z-3-hexenol)
MeJA
JMT
JA
AKR
ADR
ADH
HPLs
AAT
OPR
β-oxidation
OPDA
9-hydroperoxide
AOC
AOS
LOX9
13-hydroperoxide
LOX13
Linolenic
acid
malonyl-CoA
ACC
Acetyl-CoA
3. PHENYLPROPANOIDS - BENZENOIDS
Phenylprepenes
Benzenoids
Phenylpropanoids
MeSA
EGS
IGS
coniferyl alcohol
Benzoic acid
phenylacetaldehyde
SAMT
benzoyl-CoA
BA2H
SA
PhPAAS
coumaric
acid
IPL
t-cinnamic acid (CA)
PAL
AADC
2- phenylethylamine
isochorismate
Phe
ADT
ICS
PhPPY-AT
Arogenate
Tyr
Trp
phenylpyruvate
chorismate
Asn
Asp
Lys
Thr
Met
Ile
Pro
Glu
Gln
His
Arg
Tricarboxylic acid
(TCA) cycle
shikimate
Pyr
PEP
+
E4P
Glucose
3PG
Leu
Ala
Val
Gly
Ser
Cys
glycolysis
pentose phosphate pathway (PPP)
amine
intermediate
4. AA-DERIVATES
Deamination
Alchol
ADH
decarboxylation
AAS
aldehyde
AA-derivates
VOCs
Deamination/
transamination
decarboxylation
α-keto acid

Fig. 1 Simplified scheme of the principal biosynthetic pathways leading to the formation of Terpenes (1), oxylipins (2), phenylpropanods – benzenoids (3) and amino acid (AA)-derivates (4); Annotations: Pyr, pyruvate; G3P, glyceraldehyde 3-phosphate; MEP, methyl-D-erythritol 4-phosphate; MVA, mevalonate; DXP, 1-deoxy-D-xylulose 5-phosphate; DMAPP, dimethylallyl diphosphate; IspS, isoprene synthase; GGPPS, Geranylgeranyl pyrophosphate Synthase; GPPS, Geranyl pyrophosphate Synthase; GPP, geranyl diphosphate; GGPP, geranylgeranyl diphosphate; TPSs, terpene synthases/cyclases; IDI, isopentenyl diphosphate isomerase; IPP, isopentenyl diphosphate; FPP, Farnesyl diphosphate; PEP, phophoenolpyruvate; E4P, D-erythrose 4-phosphate; JMT, carboxyl methyltransferase; ADT, arogenate dehydratase; PAL, L-phenylalanine ammonia lyase; FPPS, Farnesyl pyrophosphate synthase; 3PG, 3- phosphoglycerate; AAS, aldehyde synthase; ADH, Alcohol dehydrogenase*;* LOX*,* lipoxygenase; AADC, aromatic amino acid decarboxylase; PhPPY-AT, phenylpyruvate aminotransferase; PhPAAS Phenylacetaldehyde synthase; ACC, acetyl-CoA carboxylase; AOS, allene oxide synthase; AOC, allene oxide cyclase; OPDA, 2-oxophytodienoic acid; HPL, hydroperoxide lyase; AAS, aldehyde synthase; ADH, alcohol dehydrogenase alcohol; AAT, acyltransferase; ADR, aldehyde reductase; AKR, aldo-keto reductase; ICS, isochorismate synthase; IGS, isoeugenol synthase; EGS, eugenol synthase; BA2H, benzoic acid 2-hydroxylase; SAMT, salicylic acid carboxyl methyltransferase; IPL, isochorismate pyruvate lyase; SA, salicylic acid; JA, jasmonic acid; MeSA, methyl salicylate; MeJA, methyl jasmonate.

It has been assumed that retaining both pathways is advantageous to tackle sessile-life style challenges, while pathway's compartmentalization simplifies the mobilization of compounds for different functions, facilitating the management of simultaneous environmental stimuli (Vranová et al. 2013).

The plastidic MEP pathway is composed of seven enzymatic reactions; the first require pyruvate (Pyr) and glyceraldehyde 3-phosphate (G3P) condensation to produce 1-deoxy-D-xylulose 5-phosphate (DXP) (Fig.1); Pyr and G3P are provided by glycolysis and pentose phosphate pathway (PPP), respectively.

The isomerization of DXP forms the MEP intermediate. MEP is then converted to isopentenyl diphosphate (IPP) and its isomer dimethylallyl diphosphate (DMAPP), the common substrates of all terpenoids. Geranylgeranyl pyrophosphate Synthase (GGPPS) and Geranyl pyrophosphate Synthase (GPPS) convert IPP and DMAPP respectively to geranyl diphosphate (GPP), and geranylgeranyl diphosphate (GGPP). The subsequent action of enzymes as terpene synthases/cyclases (TPSs) forms the final terpene products (Phillips et al. 2008, Dudareva et al.

2013). The only exception is represented by isoprene, which is synthesized directly from DMAPP by the action of isoprene synthase (IspS) (Fig.1).

On the other hand, MVA pathway relies on Acetyl-CoA supply, which is converted to MVA through three enzymatic reactions; three additional steps are required to convert MVA to IPP. Farnesyl diphosphate (FPP) is than formed from IPP and DMAPP condensation by the action of Farnesyl pyrophosphate synthase (FPPS); sesquiterpenes are then synthetized through TPS enzymes (Fig.1).

IPP can be also reversibly converted to DMAPP thanks to isopentenyl diphosphate isomerase (IDI) in both MEP and MVA compartments. The MEP and MVA routes, despite their physical separation, interact through metabolic cross-talk (Hemmerlin et al. 2003). In fact, when using a MVA pathway inhibitor (lovastatin), the monitored level of sterol decreased, while MEP-dependent compounds (chlorophylls) increased in Arabidopsis seedlings. After 96 h of treatment, the level of sterols increased back to control levels. Similarly, when MEP pathway was inhibited with fosmidomycin, chlorophyll levels dropped while sterols production increased. However, the level of chlorophylls, after some fluctuations, never recovered. This fact suggests that the metabolic exchange among MVA and MEP pathways is likely unidirectional (Laule et al. 2003).

Phenylpropanoid (C_6-C_2) and benzenoid (C_6-C_1) compounds, including phenylpropenes (C_6-C_3), originates from the aromatic amino acid phenylamine (Phe) (Dudareva et al. 2013). Phe is also the substrate of curcuminoids, stilbenoids, and lignin (Koeduka 2014).

The first step of shikimate pathway and Phe synthesis (Fig.1), occurring in plastids, consists of phophoenolpyruvate (PEP) and D-erythrose 4-phosphate (E4P) condensation to shikimate (three enzymatic reactions) and the subsequent formation of chorismite (three enzymatic reactions) (Maeda and Dudareva 2012, Widhalm and Dudareva 2015).

Phe synthesis then remains in plastids and proceed through the arogenate pathway, in which chorismate is converted to arogenate (two enzymatic reactions) and the latter in Phe through arogenate dehydratase (ADT) (Qian et al. 2019).

Alternatively, Phe can be synthetized in cytosol through the phenylpyruvate pathway, consisting of the chorismate conversion to phenylpiruvate (two enzymatic reactions). The phenylpyruvate aminotransferase (PhPPY-AT*)* then converts phenylpyruvate in Phe. The major carbon flux is

directed through the arogenate pathway, whereas less is known about the phenylpyruvate pathway. So far, only the gene encoding for PhPPY-AT has been found in plants (Qian et al. 2019).

Since PEP and E4P derive from glycolysis and pentose phosphate pathways respectively, as well as the MEP-dependent metabolites, the shikimate and MEP pathways compete for carbon (Dudareva et al. 2013). Once Phe is synthesized, L-phenylalanine ammonia lyase (PAL) deaminates it into t-cinnamic acid.

From t-cinnamic acid, phenylpropanoid/benzenoid compounds are formed through different routes: phenylpropenes (C_6-C_3) are synthetized via CoA-dependent non-oxidative route, which is located in peroxisomes; phenylpropanoids via CoA-independent route and benzoic acids via combination of both β-oxidative and non-oxidative CoA-dependent routes, both located in cytosol. The CoA-dependent β-oxidative pathway is analogous to the β -oxidation of fatty acids and some branched-chain amino acids (Fig.1).

The initial biosynthetic steps in phenylpropene production is shared with the lignin biosynthetic pathway up to the coniferyl alcohol stage. The latter is then transformed by the action of acyl transferase, into coniferyl acetate, the common phenylpropenes precursor. Specific enzymes then convert coniferyl acetate in the final product; eugenol synthase (EGS) and isoeugenol synthase (IGS) for example synthetize eugenol and isoeugenol (Atkinson 2016).

The benzenoids (C_6-C_1) synthesis begins with activation of CA to cinnamoyl-CoA, which results, through three enzymatic reactions, in the formation of benzoyl-CoA. The second non-oxidative routes imply cinnamic acid conversion into benzaldehyde and its oxidation into benzoic acid. Benzoic acid and benzoyl-CoA are precursors of benzenoids as methylbenzoate and benzylbenzoate respectively (Dudareva et al. 2013). Differently from benzenoids and phenylpropenes, phenylpropanoids (C_6-C_2) [(phenylethanol, phenylethylbenzoate (Niinemets et al. 2013)] derived from Phe directly. By the action of aromatic amino acid decarboxylase (AADC), Phe is transformed to 2- phenylethylamine. Phenylacetaldehyde synthase (PhPAAS) then converts 2- phenylethylamine into phenylacetaldehyde, precursor of phenylpropanoids as phenylethylbenzoate.

Phe is also precursor of methyl salicylate (MeSA), a benzoate ester known for its role as airborne signal and inductor of defence mechanisms (Zhao et al. 2010). Depending on plant species, SA

synthesis occurs via benzoic acid 2-hydroxylase (BA2H*)* or via coumaric acid directly through the oxidative chain shortening (Malinowski et al. 2007, Dempsey and Klessig 2017).

Alternatively, SA is synthetized via isochorismate pathway, where isochorismate synthase (ICS) converts chorismate into isochorismate; the latter form SA and pyruvate by the action of isochorismate pyruvate lyase (IPL) (Dempsey and Klessig 2017). Finally, SA methylation is catalysed by salicylic acid carboxyl methyl-transferase (SAMT) (Zhao et al. 2010).

Another class of plant VOCs comprises fatty acid derivatives (oxylipins) and are synthetized from the unsaturated linolenic acid (C_{18}) through the 'lipoxygenase (LOX) pathway' (Fig. 1). Linolenic acid synthesis is complex and begins in plastids with the Acetyl-CoA carboxylation step to form malonyl-CoA; this reaction is leaded by acetyl-CoA carboxylase (ACC). The last step happens in ER and implies the oleic acid conversion to linoleic (Cagliari et al. 2011). Fatty acids (phospholipids in the ER and galactolipids in plastids) are the structural components of the cellular membranes.

Lipoxygenase enzymes, which catalyse the addition of molecular oxygen to polyunsaturated fatty acids, including linoleic acid, initiate the oxylipins biosynthesis (Porta and Rocha-Sosa 2002). Lipoxygenase (9 - 13) form 9-hydroperoxy and 13-hydroperoxy intermediates (Fig.1).

The 13-hydroperoxide is a precursor of methyl jasmonate (MeJA), which is produced when allene oxide synthase (AOS) and allene oxide cyclase (AOC) convert 13-hydroperoxide to 2-oxophytodienoic acid (cis -OPDA); OPDA is than reduced and β-oxidized to jasmonic Acid JA. Finally, carboxyl methyltransferase (JMT) converts JA to its volatile and methylated form, the MeJA (Cheong and Do Choi 2003). Both 9- and 13-hydroperoxide lead to C_6/C_9 aldehydes and alcohols (i.e. hexenal, (Z)-3-nonenal) by the action of hydroperoxide lyases (HPL), alcohol dehydrogenases (ADH), alcohol acyltransferase (AAT), (ADR), aldehyde reductase or aldo-keto reductase (AKR) enzymes (Ameye et al. 2018a) (Fig. 1).

The final major VOCs group includes compounds derived from amino acids as alanine, valine, leucine, isoleucine, tryptophan, cysteine, and methionine, or their intermediates (i.e. indole-3-glycerol phosphate). Such amino acids are converted to form aldehydes, alcohols, esters, acids, nitrogen- and sulfur-containing compounds. Typically, amino acids can be initially transaminated or decarboxylated to form amine or α-ketoacid intermediates; further decarboxylation and deamination steps lead to aldehyde synthesis. The latter can be also directly

formed through aldehyde synthase (AAS) enzyme activity. From aldehyde, other VOCs (acids, alcohols, and esters) are synthetized though further reduction, oxidation or esterification steps (Schwab et al. 2008, Gonda et al. 2010). For example, alcohols derive from the aldehyde reduction step by the oxidoreductase alcohol dehydrogenase (ADH*)* (Reineccius, 2006). Amino acids-derived volatiles typically form fruit aromas and flavor (Schwab et al. 2008, Rosenkranz and Schnitzler 2016).

Sulfur-containing volatiles (methanethiol, dimethyl disulfide, *S*-methyl thioacetate, propanthial *S*-oxide, methional, methanethiol) derive from methionine and cysteine and are responsible for the odour of onions, garlic, potatoes and cabbage; leucine and phenylalanine instead, are precursor of VOCs released by strawberry, tomato and grape, as 3-methylbutanal, 3-methylbutanol and 3-methylbutanoic acid, phenylacetaldehyde, -phenylethanol (Schwab et al. 2008).

Isoleucine is a probable precursor of 4,5-Dimethyl-3-hydroxy-2(5*H*)-furanone (sotolon) from dried fenugreek seeds *Trigonella foenum-graecum* L. (Schwab et al. 2008).

VOLATILE INTRACELLULAR TRANSPORT: FROM BIOSYNTHESIS SITE TO ATMOSPHERE

Newly synthetized VOCs must travel through plasma membrane, hydrophilic cell wall and eventually cuticle in order to be released (Fig. 2).

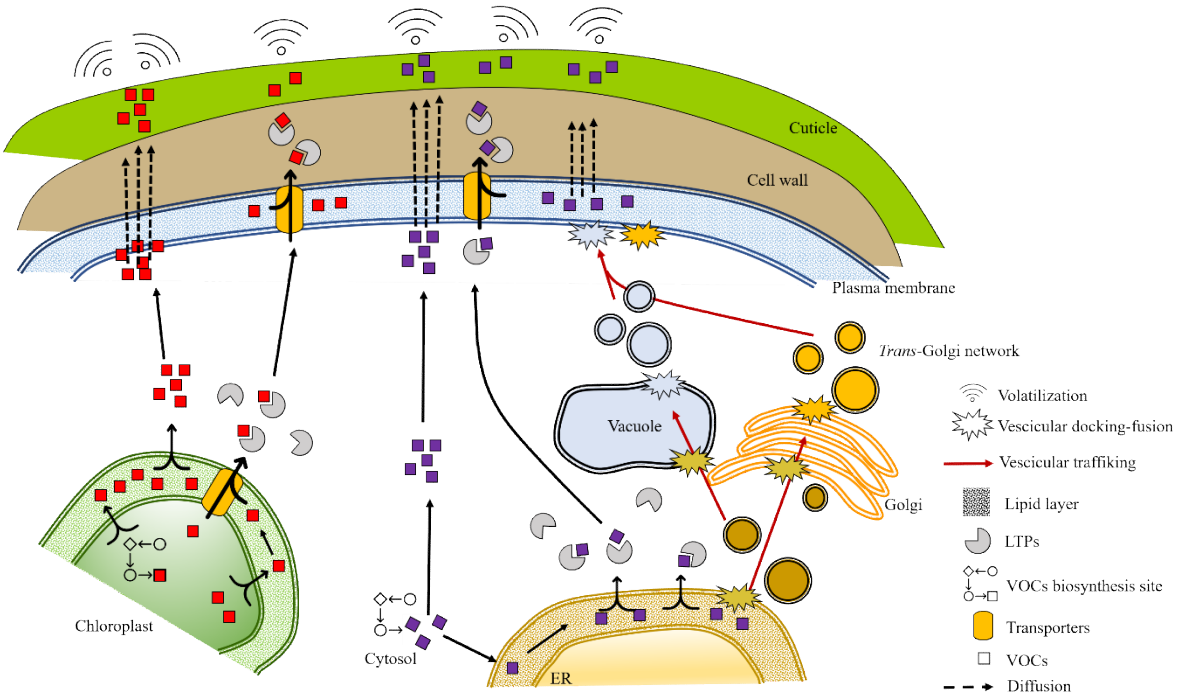

Fig. 2 VOC subcellular translocation scheme in plant cells. VOCs can diffuse (dashed arrows), transported by facilitated protein carriers (Lipid Transport proteins) or via vesicle trafficking (red arrows). Membrane-bound transporters export VOCs through the plasma membrane. Lipid transfer proteins (LTPs) can aid in the transport of VOCs in aqueous regimes such as the cytosol and cell wall. VOCs must diffuse through the cuticle prior to release into the atmosphere.

Due to their physical and chemical properties (low-molecular weight, lipophilicity, and high vapor pressure), in absence of barriers to diffusion as hydrophilic matrix, they can cross membranes freely and evaporate in atmosphere (Pichersky et al. 2006).

One mechanism of release implies the accumulation of VOCs in dedicated structures as extracellular peltate glandular trichomes, or resins ducts (Kainulainen et al. 1996, Loreto and

Schnitzler 2010, Glas et al. 2012, Zhao and Erbilgin 2019). The release of these VOCs is caused by the disruption of storage structures that usually follow the herbivore attack (Dalin et al. 2008). Glandular trichomes are found in 30% of all vascular plants (Glas et al. 2012), especially Lamiaceae as peppermint (*Mentha x piperita*), basil (*Ocimum basilicum*), and lavender (*Lavandula spp.*).

In trichomes, VOCs are synthesized in glandular secretory cells and transported directionally into the subcuticular storage space, which is embraced by cell wall materials; in this way volatiles are trapped until release by mechanical damage. Trichome-borne compounds are often dominated by volatile terpenoids and phenylpropanoids and represent the first line of defense against herbivores and microorganisms (Andama et al. 2020). The involvement of these structures allow the accumulation of secondary metabolites with anti-mycotic or anti-bacterial activity, or their precursors, while avoiding self-toxicity (Tissier et al. 2017).

Alternatively, in mesophyll, VOCs passively or actively diffuse from the biosynthesis site through plasma membrane, cell wall and cuticle (Adebesin et al. 2017) (Fig.2).

Among all membrane layers from biosynthesis site to atmosphere, cuticle imposes the higher resistance and could represent the limiting factor for VOCs emission (Widhalm et al. 2015).

In order to diffuse in hydrophobic environments, VOCs must accumulate in significant concentrations. For small molecules as isoprene, which diffuses very spontaneously, a hyper concentration does not really occur. For bigger molecules (e.g. phenylpropanoid-benzenoids, C_{10}-C_{15} terpenes) and non-volatile compounds, [(e.g. waxes and diterpenes (Adebesin et al. 2017)] instead, additional active mechanisms are needed to avoid over-accumulation in internal membranes. Possible contact sites for VOCs exchange are among endoplasmic reticulum (ER) and plasma membrane or through vesicular trafficking among Golgi, trans-Golgi network (TGN), and/or vacuole (Samuels and McFarlane 2012).

The translocation of lipophilic VOCs implies the presence of transporters as ATP binding cassette (ABC) on plasma membrane and Lipid transfer proteins (LTPs) to drive the passage through hydrophilic cell wall, aqueous stroma or cytosol. Lipophilic molecules are isolated in hydrophobic cavities on LTPs until release (Wong et al. 2019). In the case of trichomes, LTPs are likely to be exclusively localized on the side of excretion to direct VOCs export.

The overexpression of gene encoding LTP1 cause higher monoterpene emission in orange mint (*Mentha × piperita f. citrate*)(Hwang et al. 2020), while reduced ABC subfamily G member 1 (ABCG1) transcript level in *Petunia hybrida* flowers results in lower VOCs emission (methylbenzoate and benzyl alcohol) and their intracellular retention (Adebesin et al. 2017).

THE ROLE OF VOCs IN PLANTS

Plants are sessile organisms and the emission of VOCs has ecological meaning for reproduction, communication with the neighbourhood and defence against herbivores and pathogens (Loreto and Schnitzler 2010). During evolution, plants took advantage of the chemical properties of volatiles compounds, like volatility and solubility, to develop unique protective strategies. Despite VOCs release might appear as physiologically unavoidable, increasing evidences suggest that they might be involved in plant adaptation and acclimation to both mild and extreme environments (Holopainen and Gershenzon 2010, Loreto and Schnitzler 2010, Hartikainen et al. 2012, Rinnan et al. 2014).

This explains why plants invest high energy in VOCs production, regardless the unavoidable loss of carbon that could be invested otherwise (Dicke and Loreto 2010). As a matter of fact, during stress conditions, the carbon destined to secondary metabolites increase from 2% up to 67% in case of multiple stressors (Šimpraga et al. 2011).

VOCS IMPROVE PLANT GROWTH AND PRODUCTIVITY

VOCs represent a powerful weapon for plant's ecology and their emission, from both above- and below-grounded organs, allow the establishment of multiple networks among emitters and receivers. Potential receivers include neighbouring plants, insects, and microbes, both beneficial and pathogenic. The phenomenon of allelopathy occurs when the release of chemicals (allelochemicals) interferes with receiver's natural physiology or behaviour, with the final goal of defence and competition (Hickman et al. 2021). The so-called "phytoallelopathy" consists more specifically in affecting the growth or development of competitive plant species (Effah et al. 2019).

Some allelochemicals can interfere with seed germination or root growth of neighbours. For example, high concentrations of monoterpenes, precisely α-pinene, camphene, camphor, 1,8-

cineole, and β-pinene, produced by *Salvia leucophylla* inhibit root growth of *Brassica campestris,* while camphor, 1,8-cineole, and β-pinene inhibit seed germination (Nishida et al. 2005). These compounds seem to affect cell proliferation by inhibiting cell-nuclear and organelle DNA synthesis in the root apical meristem.

Maccioni et al. (2020) tested the phytotoxic effect of *Rosmarinus officinalis* L. essential oil in infected *Acacia saligna* seedlings. Authors concluded that high concentration (15.6 mL/L) of the essential oil, which contain abundant monoterpenes (α-pinene, limonene, 1,8-cineole, borneol and camphor), has effect on growth survival rate comparable with commercial herbicides.

Besides the allelopathic effects, VOCs have the potential to regulate plant senescence. Cell deterioration and death are caused when reactive oxygen (ROS) and nitrogen (RNS) species, the signalling molecules that trigger gene expression and defence responses in stressful conditions, exceed the tolerable threshold (Kapoor et al. 2019). The MEP pathway, located in chloroplast, is the major sources of antioxidants (e.g. carotenoids) necessary to quench the ROS species produced the by photosynthetic machinery. Because the same pathway produces hormones (e.g. cytokinins) and isoprenoids, it has been proposed that cytokinins, isoprenoids and carotenoids evolved functional synergism in delaying plant senescence by protecting chloroplast genomes from ROS activity (Dani et al. 2016). High isoprenoids emission is associated with high cytokinin levels because both depends on the availability of the same substrate (DMAPP). This trade-off is more evident during stressing conditions (e.g. drought), when both overexpression of cytokinins and sustained isoprenoids emissions restore photosynthesis (see "The role of VOCs in plant abiotic stress response" chapter).

VOCs also promote plant reproductive success when released from flowers and fruits, by attracting pollinators and seed dispersers (Rodríguez et al. 2013, Muhlemann et al. 2014).

Mono-, sesquiterpenes, ketones, benzenes, alcohols, aldehydes, esters and ethers are ubiquitous in floral scents, but the terpenes are predominant (Fernandes et al. 2019). Notably, VOCs released from flowers evolved as a response to both mutualists (true pollinators) and antagonists (florivores) (Schiestl et al. 2011). Thus, such compounds can also defend form pathogens that could damage floral structures (Muhlemann et al. 2014). Protective mechanisms are even more important for the delicate structure of flowers which, differently from leaves, lack of lignin, cuticle or other physical barriers.

The sesquiterpene (E)-β-caryophyllene emitted from the stigma of *Arabidopsis thaliana* confers resistance to *Pseudomonas syringae*. Indeed, the transgenic line with inhibited capacity to emit (E)-β-caryophyllene presents reduced seeds weight, demonstrating that this compound is important for plant fitness (Huang et al. 2012).

Differently from pathogens, the presence of florivores can be a physical deterrent for potential pollinators. Ants for examples are aggressive and occasionally feed on floral structures. Junker et al. (2011) demonstrated that the inhibition of terpene biosynthesis causes the loss of repellent power of *Phlox paniculate* flowers against *Lasius niger* ants. Intriguingly, the monoterpene linanool alone, which was particularly affected by specific biosynthetic inhibitors, is an effective deterrent for *L. niger*. Similarly to linanool, also the exogenous application of benzenoid compounds (benzaldehyde and 2-phenyl acetaldehyde) successfully acted as ant repellent.

Because fruits develop from flowers, they retain most of floral VOCs as terpenoids (e.g. mono- and sesquiterpenes and apocarotenoids), phenylpropanoids/benzenoids (e.g. eugenol, benzaldehyde), fatty acid derivatives (e.g. hexenal, hexenol) and amino acid derivatives (e.g. thiazole, 2- and 3-methylbutanal) (Rodríguez et al. 2013). Apart for the well-studied role as seed disperser attractors, fruit scents also serve as defence especially during the maturation process, when fruits are more attractive to antagonists. To give an example, ethylene has been proposed to be a modulator of defence response in *Olea europaea L*. fruits infested by Olive fly (*Bactrocera oleae R*.), the major olive pest (Alagna et al. 2016).

Indeed, the transcription of multiple defence-encoding genes were induced along with ethylene burst, as well as the production of JA-intermediates (e.g. 12-Oxo-phytodienoic acid). JA, together with SA, is a key modulator of plant defence responses to insect pests and pathogens (Cheong and Do Choi 2003).

THE ROLE OF VOCS IN PLANT ABIOTIC STRESS RESPONSE

Many processes involved in VOCs biosynthesis and release, as enzymatic activity, photosynthetic efficiency, stomata conductance, volatilization from water phase and tissue integrity are influenced by abiotic factors as temperature, drought, salt, oxidative stress, CO_2, ozone (O_3) and light exposure (Peñuelas and Staudt 2010).

Especially isoprenoids have been recognised for their potential to mitigate high temperature, water stress, and high light intensity. Increasing temperature is generally directly proportional to the quantity of isoprenoids released, especially monoterpenes (Lin and Chou 2006, Holopainen and Gershenzon 2010). In *Quercus ilex*, monoterpenes as α-pinene and limonene enhance thermotolerance when the photoprotective role of photorespiration is inhibited (Peñuelas and Llusià 2002).

However, the most relevant isoprenoid is isoprene (2-methyl-1,3-butadiene), at both atmospheric and physiological level. Isoprene alone accounts for the 70% of the global VOCs emission from plants, excluding methane, implies the loss of 2% of photosynthetic carbon and each molecule synthetized needs the consumption of 20 ATP and 14 NADPH molecules (Lantz et al. 2019). Such energy investment suggests that isoprene production might be advantageous for plants. The picture is complicated by the fact that not all but only the 20% of plants worldwide emit isoprene at significant amount (Loreto and Fineschi 2015). The capacity to emit isoprene is given by the presence of isoprene synthase gene (ISPS), which has been lost and gained multiple times during evolution. It has been hypothesized that the ISPS gene was gained during periods with high atmospheric CO_2, when photosynthesis operates more efficiently, and lost during low CO_2 periods, when the energy saving was advantageous (Sharkey et al. 2013).

Since isoprene synthesis is light and temperature-dependent (Sasaki et al. 2005) and takes place in chloroplasts, the link between isoprene production and environmental stresses affecting the photosynthetic apparatus has been extensively analysed.

The first studies were dedicated to naturally emitting species, as aspen (*Populus tremuloides*) and Kudzu (*Pueraria lobate*)(Monson and Fall 1989, Singsaas et al. 1997).

Under photodamaging light, isoprene increases thermotolerance of Kudzu leaves up to 10°C, while in dark conditions “only” up to 4°C. Also, isoprene increases the capacity of emitting plants to maintain photosynthetic CO_2 exchange at higher temperatures. The study also suggests that isoprene may represent a faster way to achieve thermotolerance, in respect of *de-novo* synthesis of heat-shock proteins, as its synthesis is almost immediate when stress occur (Singsaas et al. 1997).

However, the advent of new technologies allowed to confer the capacity to emit isoprene also to non-emitter species, as *Nicotiana tabacum* (tobacco) and *Arabidopsis thaliana*, by inserting the

ISPS gene. Because the MEP pathway is ubiquitous in plants and DMAPP is produced constitutively, the solely presence of the IspS enzyme allows the conversion of DMAPP to isoprene (Sharkey 2013). The ISPS genes used are typically obtained from *Populus x canescens* (Cinege et al. 2009), *Populus alba* (Sasaki et al. 2007) or *Eucaliptus globulus* (Zuo et al. 2019). Thus, transgenic lines were created also silencing or enhancing the ISPS gene expression in natural isoprene emitters as grey poplar and white poplar (Behnke et al. 2007). Gene transformation provided opportunities to study the physiological mechanism by which isoprene emission enhances thermotolerance in different plant families.

Pollastri et al. (2014) compared the photosystem II (PSII) efficiency of wild-type poplar, tobacco and *Arabidopsis* plants, both wild-type and transformed plants with ISPS gene. Under physiologically high temperatures (28–37 °C), the chloroplasts of isoprene-emitting leaves dissipate less energy as heat than chloroplasts of non-emitting leaves. Isoprene may allow better stability of photosynthetic membranes and a more efficient electron transfer through PSII at physiological temperatures. Similar results were obtained in transgenic poplar in which transient mild heat stress impaired the electron transport rate (ETR) (Behnke et al. 2007). Lower ETR indicates a decreased membrane stability or fluidity, which can be influenced by oxidative damage and lipid peroxidation (Murakami et al. 2000).

Compared with non-emitters, isoprene-emitting tobacco plants maintains PSII stability and high photosynthetic rate at high temperatures, exerting a function alternative to NPQ (Pollastri et al. 2019). Altogether, these facts imply that isoprene directly protects the photosynthetic apparatus and membrane stability.

Several studies have demonstrated that isoprene protects membranes against ROS production and lipid peroxidation under not only heat, but also ozone and high light (Loreto and Velikova 2001, Affek and Yakir 2002, Pollastri et al. 2021). It has been proposed that the capacity to deactivate reactive oxygen species (ROS) of isoprenoids is, at least partially, due to their conjugated double bounds (Peñuelas and Munné-Bosch 2005).

Zuo et al. (2019) demonstrated that the solely presence of isoprene, in both Arabidopsis and tobacco transgenic lines, can alter the expression of genes involved in growth, biotic and abiotic stress tolerance, intracellular transport and photosynthesis. The same study proved that isoprene also had a significant positive effect on leaf pigment production, seedling growth and

on both vegetative and reproductive growth under unstressed conditions. These facts, coupled with the up-regulation of genes belonging to signalling networks or associated with specific growth regulators (e.g., gibberellic acid, cytokinins, and jasmonic acid), suggest a possible role for isoprene as signalling molecule. Among abiotic stresses, drought is the most limiting environmental factor in crop productivity (Meza et al. 2020). Temperature fluctuations, light intensities and low rainfalls are all factors leading to water scarcity, which heavily affects plant morphology, physiology and biochemistry (Anjum et al. 2011). Due to climate change, plants are expected to cope more frequently with both mild and severe drought periods; maintaining yield stability of crops, under normal as well as drought stress conditions, is essential for the global population food security (Dai 2013).

Drought impacts growth, membrane integrity, pigment content, osmotic adjustment and photosynthesis. The ABA-mediated stomatal closure, which limit water and CO_2 absorbability, and chlorophylls reduction are considered primary causes of inactivation of photosynthesis during water stress. Chlorophyll degradation is a consequence of the oxidative stress, that also affects proteins, DNA and lipids (Anjum et al. 2011). Plants respond to water scarcity also accumulating specific compatible osmolytes as amino acids (e.g. proline and ectoine) or sugar alcohols (e.g. trehalose, mannitol) to maintain leaf turgor and enhance drought tolerance (Singh et al. 2015). The positive effects of isoprene emission on drought responses in wild-type and transgenic plants were demonstrated over the years. The isoprene-emitting tobacco plants did not experienced ROS burst or damage to membrane structures; thus, they maintained PSII efficiency and water use efficiency under mild drought (Ryan et al. 2014).

Intriguingly, the enhanced stomatal closure was uncoupled with ABA accumulation in isoprene-emitting plants. Possibly, because isoprene belongs to the same biosynthetic pathways of ABA, its cost-effective synthesis hijacks the available resources under prolonged stress (Ryan et al. 2014). Under severe water stress, isoprene-emitting tobacco plants were able to maintain the photochemistry of photosynthesis unaffected, consistently with the results obtained under mild drought (Tattini et al. 2014). Notably, both Ryan et al. (2014) and Tattini et al. (2014) found evidence that isoprene might protect photosynthesis most probably by improving the stabilization of photosynthetic membranes rather than acting as a sink for excess energy. Very recently, Xu et al. (2020) observed the up-regulation of genes encoding for proteins involved in

stabilization of chloroplast membrane and for key ABA-signalling genes in isoprene-emitting plants. The study concludes recognizing isoprene as a possible signalling molecule, able to shape the plant transcriptome.

Despite beneficial effect of isoprene has already been proven, studies focused on isoprene in drought conditions represent the minority and are limited to gene expression or metabolites analysis (Pollastri et al. 2021).

The effects of climate change are expected to induce extreme precipitation events causing destructions and unpredictable mild drought stress periods that, if prolonged, can cause yield losses to various degrees. Reduction of productivity is enhanced when mild drought occurs during the reproductive stage (Torres and Henry 2018).

Despite its potential importance for agriculture, the response of plants to mild drought stress is poorly understood compared with severe dehydration stress.

In Chapter two, we present evidence that in transgenic isoprene-emitting Arabidopsis plants grown in mild water stress conditions, isoprene largely affects the abundance of chloroplast proteins, confirming a strong antioxidant action, and modulates signalling and hormone pathways, especially controlling ABA synthesis. Unexpectedly, isoprene also alters membrane trafficking. It reshapes the proteome also in unstressed conditions, which suggests a priming action on several defensive metabolites.

THE ROLE OF VOCS IN PLANT BIOTIC STRESS RESPONSE

While VOCs emitted from reproductive organs primarily promote plant productivity, those released by leaves serve mainly for direct and indirect defence (Holopainen and Gershenzon 2010).

Direct defence consists of mechanisms that repel herbivores, kill or retard pathogen development or affect their reproductive success (War et al. 2012); indirect defence instead implies the attraction of the natural enemies of the attackers (Price et al. 1980).

Direct defence mechanisms are triggered by the mechanical wounding (chewing, sucking) or pathogen cell invasion and, in higher plants, are followed by the emission of Green Leaf Volatiles (GLVs), isoprenoids (monoterpenes, sesquiterpenes), phenylpropanoids, and sulphur- or nitrogen-containing compounds (Mumm and Dicke 2010, Meents and Mithöfer 2020).

The connection among herbivory, VOCs release and defence have been widely investigated; many studies proved that both single (e.g. E-β-Farnesene, indole) and combination (GLVs and terpene blend) of VOCs have direct repellent effect (Maurya 2020).

Thus, herbivore-induced plant volatiles (HIPVs) as indole, linanool, and MeJA can prime the defence responses in undamaged neighbours and attracts natural enemies (e.g. carnivorous) (Maurya 2020). Defensive functions have been attributed to terpenes also against root herbivores (Erb et al. 2012).

Plant VOCs can also provide resistance against microbial pathogens (bacteria, fungi); these microbe-induced plant volatiles (MIPVs) possess antimicrobial activity or induce internal defence mechanisms as ROS signalling cascade and SA/JA-dependent gene expression ((Sharifi et al. 2018).

The picture regarding pathogens is complicated by the different mode of nutrition, which can consist of living (biotrophy) or dead (necrotrophy) tissues. Also, some hemibiotrophic pathogens switch from biotrophy to necrotrophy at certain point of their life cycle (Imran and Yun 2020). Typically, solely the necrotrophic stage corresponds to the symptom's appearance as necrotic spots.

GLVs are particularly involved in protecting plants from bacterial infection: aldehydes (e.g. *trans*-2-hexanal), together with alcohols, act as growth inhibitors against phytopathogenic bacteria (e.g *Pseudomonas syringae)* (Croft et al. 1993). Other C_6 aroma compounds as (*Z*)-3-hexenal and (*E*)-3-hexenal show antibacterial activities against both gram-negative and gram-positive bacteria (Matsui 2006).

The establishment of airborne bacteria on leaves can be prevented by terpenoids, phenylpropanoid and benzenoid compounds from aromatic plants (e.g. *Salvia officinalis)* and by monoterpenes (limonene, β-pinene) and aldehydes from coniferous species (Junker and Tholl 2013). Similarly, plants emit VOCs after being challenged by fungal pathogens.

GLVs such as E-2-hexanal, s 2-nonenal, nonanal, Z-3- hexenal, and terpenes as limonene and linalool have antifungal/fungicidal activity (Maurya 2020). In recent years, the efficacy of VOCs has been tested against both hemibiotrophic (gen. *colletotrichum*) and necrotrophic (*Botrytis cinerea*, *Sclerotinia sclerotiorum*) pathogens on *Arabidopsis thaliana* and a wide variety of crops, as tobacco, lima bean, common bean, tea and wheat (Sharifi et al. 2018). It has been shown

that the GLVs (*E*)-2-Hexenal, (*Z*)-3-Hexenal and the monoterpene Allo-ocimene increased resistance to *Botrytis cinereal* in *Arabidopsis thaliana* (Kishimoto et al. 2006). Exogenous applications of (*E*)-nerolidol reduced the symptoms induced by *Colletotrichum fructicola* in tea plants (Chen et al. 2020b), while 3-methylbutanoic acid and 2-methylbutanoic acid, emitted by *Bacillus amyloliquefaciens*, were toxic to *C. lindemuthianum* in common bean (Martins et al. 2019).

Overall, the involvement of volatile secondary metabolites in plant defence has been confirmed. The activation of secondary metabolites is a well-known mechanism of defence, that usually complement ROS scavenge, stomatal closure, mitogen-activated protein kinase (MAPK) cascades, signalling modulated by phytohormones (JA, SA, ABA and ethylene) and the reinforcement of the cell wall (e.g. callose and lignin deposition) (Chen et al. 2020b). These events are activated prior recognition of the invader through their Molecular Associated Patterns (damage, DAMPs; herbivores, HAMPs; pathogen, PAMPs) and the activation of pattern-triggered immunity (PTI) and effector-triggered immunity (ETI) (Imran and Yun 2020).

However, the mechanisms that interconnect VOC's biosynthesis with other molecular responses are still unclear. For this reason, an increasing number of studies decided to couple physiological analysis with applied transcriptomics and metabolomics when investigating the VOCs-defence ratio.

The common bean-*Colletotrichum lindemuthianum* pathosystem is one of the most promising model systems for plant-pathogen interactions.

Common bean (*Phaseolus vulgaris* L.) is among the most relevant grain legumes for human consumption, with over 26 million hectares dedicated to its cultivation, especially in Latin America and Africa. (Morales 2003). Moreover, it plays an important role in sustainable agriculture as a result of the possibility of nitrogen fixation when associated with nitrogen-fixing bacteria (Schmutz et al. 2014).

Bean productivity is affected primarily by anthracnose disease, which can lead the yield losses up to 100 percent (Padder et al. 2017). Such disease is due to the hemibiotrophic fungus *C. lindemuthianum,* which overwinters in seed and crop residues and infects all the aerial parts. Fungus spores then spread to neighbours through wind or rain drops. When spores (also termed conidia) reach the plant tissue, the appressoria entry in the host cell and form the primary hypha.

The biotrophic-necrotrophic switch happened with the formation of the secondary hyphae that cause the cell death. New conidia are produced by the acervuli derived from the secondary hyphae (Quintana-Rodriguez et al. 2015, Padder et al. 2017).

Typical symptoms of necrotrophic stage include dark and shrunken lesions on hypocotyl, leaves and pods. The later stage of disease result in chlorotic and faded leaves, premature fall of pods and eventually in the death of the plant. Severely infected pods that reach the mature stage produce infected seed that are unmarketable to consumers. The control of the disease through the use of fungicides, crop rotation in field or the utilization of resistant genes is difficult to achieve due to the high number of *C. lindemuthianum* races, which continuously co-evolve with the host plants and render the majority of the cultivars susceptible (Padder et al. 2017).

Several publications were dedicated to *Phaseolus vulgaris* infected by *C. lindemuthianum* with rising interest in the genetic bases of anthracnose resistance.

Different loci involved in resistance have been identified through Quantitative resistance loci (QRL) mapping. Oblessuc et al. (2014) identified 11 QRL specific to three *C. lindemuthianum* races that might contain resistant (R) genes. Two of them (ANT02.1 and ANT07.2) were considered "major" QRL and contained putative genes with cellulose activity, genes related to the MYC TF family (involved in plant immune responses by activating the transcription of JA) and a SCD1 gene (Stomatal Cytokinesis Defective 1). The latter acts as a negative regulator of pathogen-associated molecular patterns (PAMP) signalling pathways through inhibition of SA-mediated responses. In addition, transcriptomic changes triggered by *C. lindemuthianum* infection have been widely investigated (Geffroy et al. 1999, Borges et al. 2012, Oblessuc et al. 2012, Fontenelle et al. 2017).

In common bean, transcriptome analysis indicated positive regulation of gene expression in response to *C. lindemuthianum* infection. Both Borges et al. (2012) and Fontanelle et al. (2017) observed a differential expression of marker genes at different time points of infection. All studies recorded an up-regulation of pathogen-related genes (PR genes) belonging to PR1 and PR2 families. In detail, 1,3-beta-D-glucanase (PR2 family) expression was higher during early stage of interaction, while PR1 were more expressed in later stage. In addition, Borges et al. (2012) recorded the activity of PR genes in all plant tissues (leaves, hypocotyl, and epicotyl), which demonstrate their primary role in plant-pathogen interaction. Also, the same study

observed high expression of the gene encoding for PAL enzyme (*PAL2*) specifically in leaves and during early infection stage. PAL is a key enzyme for SA biosynthesis, which is involved in Systemic Acquired Resistance (SAR), and its expression pattern suggests that it might act in early leaves defence.

Quintana-Rodriguez et al. (2015) first measured the VOCs emitted by common bean putatively involved in resistance to *C. lindemuthianum.* In detail, this study proved that VOCs emissions from an infected resistant bean cultivar (cv. Pinto Villa) induce resistance in a susceptible cultivar (cv. Negro St. Luis). The degree of resistance was assessed by measuring the expression of marker genes (PR genes) in the susceptible cv.; after the exposure, the expression of these genes was comparable to the resistant cv. Limonene, linalool, nonanal, MeSA and MeJa were identified as the main resistance inducers; in fact, susceptible plants fumigated with these compounds, once infected, presented lighter anthracnose symptoms (conidia germination) in respect of control plants. Similar effect was obtained on susceptible plants exposed to VOCs emitted by from resistant plants. Altogether, this study provided new evidence about the involvement of VOCs in the resistance of bean to fungal pathogens and about the potentiality of using resistant cultivars in the disease control.

Padder et al. (2016) provided additional information about the resistance mechanisms involved and the biotrophic-necrotrophic phase transition through the transcriptome analysis of susceptible and tolerant lines to *C. lindemuthianum*. Several defence-related genes encoding for sugar transporters, lipoxygenase and peroxidases were up-regulated during biotrophic phase (24 hours post inoculation), but mostly down-regulated within 72 hours. This switch has been proposed to be the development of necrotrophic phase, which likely starts 48 hours post inoculation. Thus, pathogen-related (PR) proteins, chitinase, peroxidases and lipoxygenases were found up-regulated in resistant line, whereas up-regulation of some of the genes, especially the sugar transporter, was specific of the susceptible line. This study suggests that the resistant line recognizes much faster the pathogen attack. Shams et al. (2020) observed that, differently from the resistant cv. (Naz). the susceptible cv. (Khomein) experienced an H_2O_2 burst in leaves infected by *C. lindemuthianum*. The generation of ROS is typically consequent to the activation of the hypersensitive response (HR), the programmed cell death activated to quarantine

biotrophic pathogens. It was hypothesized that the HR is triggered much faster in the susceptible plant.

Furthermore, O_2^- accumulated in apoplast in resistant plant, probably to confine fungal growth outside the cell. This study also confirmed the differential expression of marker genes in the two cultivars. PR1b showed higher expression during the biotrophic phase of the resistant cv., while PR1a gene was up regulated only during necrotrophy in the susceptible cv. PR2 gene was up-regulated in both biotrophic and necrotrophic stage in the resistant cultivar. PR1 and PR2 are SA-signature genes, which indicates the activation of SAR, a typical response to biotrophic pathogens (Ali et al. 2018).

Interestingly, the LOX gene, which is involved in the biosynthesis of JA, presents the same expression pattern of PR1b. JA-responsive genes are expressed in response to necrotrophic pathogens; this evidence demonstrates JA biosynthesis may occasionally synergize with SA pathway in a non-antagonistic manner.

To date, only one study provided proteomic data on this photosystem has been reported.

Borges et al. (2015) uses two-dimensional electrophoresis coupled with mass spectrometry to dissect the response of common bean to *C. lindemuthianum;* 17 differentially accumulated proteins were found in infected beans belonging to the following cellular processes: photosynthesis and carbon metabolism, antioxidant systems, genetic information processing, defence and stress response, protein folding, and phenylpropanoid and flavonoid biosynthesis. This study confirmed the findings of transcriptomic studies: the accumulation of antioxidant proteins and PR1 protein suggests that HR is activated in infected plants. Furthermore, chalcone isomerase, an enzyme involved in the production of cell-wall compounds, was over-accumulated at the beginning of necrotrophic stage (>48 h post inoculation). These results are in line with the findings at transcript level (Oblessuc et al. 2012).

The study reported in the Chapter three of this thesis fits into this area of analysis.

By comparing the volatilome and proteome profiles of two common bean genotypes displaying different levels of susceptibility against *C. lindemuthianum*, we collected evidence that two different strategies were activated by the bean genotypes studied and we provided novel insights into how this plant finely regulates its defence response to protect itself against the invading

fungal pathogen. This study contributes to a better understanding of the kinetics of reactions triggered by *C. lindemuthianum.*

IS IT POSSIBLE TO EXPLOIT VOCS TO IMPROVE SUSTAINABLE DEFENCE STRATEGIES AND PRODUCTIVITY OF CROPS?

The efficacy of VOCs in plant defence against stress in many controlled trials in the laboratory leads to the conclusion that natural and eco-friendly approaches based on VOCs can be developed to enhance both crop defence and production. As VOCs enhance plant defence from a wide range of factors, all equally likely to happened in field as pests, pathogens or drought, their use for agricultural purpose could be suitable (Brilli et al. 2019).

Facing the fact that the global population is expected to reach 10^9 billion in 2100 (Plesse 2020, van Dijk et al. 2021), in present days the 38% of the global land surface is already occupied by croplands (Zabel et al. 2019) and it is expected to be reduced up to 7% by rising temperature and up to 19% by drought (Zhao et al. 2017, Leng and Hall 2019), while the 50% of arid and semiarid areas are degraded by salt accumulation (Naeem et al. 2020).

Climate change is also expected to trigger the frequency of pests and disease from biotic agents as fungi, virus, bacteria and Oomycetes. Fungi alone account for the 70% of crop diseases (Patel et al. 2014) and 30% of global yield losses, which includes barley, wheat, rice, cotton and beans (Sharma et al. 2008, Patel et al. 2014, Bebber and Gurr 2015).

In absence of alternatives, the future scenario predict the expansion of croplands to compensate the yield losses, rising water use and plant protection products and progressive loss of biodiversity (Zabel et al. 2019). The annual use of pesticides and fertilizers, accounting for 65 tons and 2 tons respectively, put at risk human, food and environmental safety (Davydov et al. 2018). In this contest, it is urgent to provide sustainable technologies for agricultural purposes. On the other hand, the severe policies against chemical pesticides increases the demand for eco-friendly strategies. In light of these facts, it is not surprising that the interest in VOCs is rising.

However, the complex blend of VOCs is difficult to reproduce and their effects on receivers might be influenced by environmental ad physiological factors. Potential limitation for the use of VOCs in field is represented by their reactivity in atmosphere, that could nullify the VOCs released, even at high concentration (Brilli et al. 2019).

It is also necessary to avoid undesired-side phytotoxic effects; for example, the VOC Z-3-hexenyl acetate, which induce resistance against *F. graminearum* in wheat, trigger the production of the mycotoxin deoxynivalenol, dangerous for human health (Ameye et al. 2015).

Additional solutions, other than the use of synthetic VOCs, can be effective. An example is represented by the co-cultivation of companion crops that emit VOCs able to repel and attract insect pests away from the main crop, also known as the "push-and-pull" method (Khan et al. 2016). Recently, the oviposition deterrent effect of dimethyl disulfide (DMDS) was combined with the attractiveness of Z-3-hexenyl-acetate on chinese cabbage plants to hijack the *Delia radicum* L. (diptera) oviposition away from broccoli *B. oleracea* L.. The experiment was successful to reduce the oviposition on broccoli, without adverse effects on parasitism by the natural enemies of *D. radicum* L. (Lamy et al. 2018). Proper inter-cropping has potential also for priming against abiotic stresses as salinity (Landi et al. 2020).

Moreover, the genetic manipulation can confer the capacity to emit specific VOCs, enhancing resistance to pests or abiotic factors. For example, transgenic *Arabidopsis* plants able to emit the sesquiterpene (E)-β-farnesene, naturally emitted by aphid *Myzus persicae*, were more repellent to aphids and attractive to aphid predators in laboratory experiments (Beale et al. 2006).

METHODS

The main techniques used for the work presented in this thesis are HPLC-MS-MS for protein analysis and PTR-TOF- MS for VOCs measurements. Both techniques are briefly introduced in the following paragraphs.

Proteomics

Proteins are an essential part of all living organisms and participate in virtually every process within cells, including enzymatic reactions, transport, DNA replication, structural support, immune responses. The totality of proteins expressed by a genome in an organism at a certain time-point is defined as "proteome" and proteomics is the study of the proteome. Proteomics is challenging compared to genomics because of the numerous factors controlling protein content over time: gene expression, mRNA translation, post-translational modifications and environmental stimuli. Furthermore, the number of proteins largely exceeds the number of genes

and many technologies have limited capacity to manage large datasets (Domon and Aebersold 2006).

Protein identification can be achieved through non-quantitative techniques as wester blotting or chromatography (e.g. ion exchange chromatography (IEC), size exclusion chromatography (SEC)). These techniques are designed for the identification of few proteins. Protein microarray (e.g. analytical, functional) also manages small amount of proteins but allows expression analysis (Aslam et al. 2017).

The study of protein aggregates is possible through gel-based techniques [Sodium dodecyl sulphate (SDS)-PolyacrylAmide Gel Elecrophoresis (PAGE)], which separate proteins based on their size and charge on polyacrylamide gels. The use of appropriate staining is necessary for protein visualization and allows approximate quantification by measuring the size of the spots (Newton et al. 2004).

Quantitative analysis can be obtained combining in-gel (e.g. SDS-PAGE) or gel-free (labelled with isotopes or label-fee) samples with mass spectrometry (MS), which are considered "third generation" methodologies (Jorrin-Novo et al. 2019).

MS measures the mass-to-charge ratio (m/z) of ionized proteins ("top-down" approach) or relative peptides ("bottom-up" approach) (Gillet et al. 2016).

Commonly used ionization methods are MALDI (matrix-assisted laser desorption ionization), surface enhanced laser desorption/ionization (SELDI) and electrospray ionization (ESI) (Aslam et al. 2017). To date, mass spectrometry analysis coupled with the "bottom-up" approach is the most efficient methodology for large-scale proteome analysis. In the "bottom up" approach, proteins must be digested into small peptides using specific proteomic enzymes that cleave proteins in predictable sites (Gillet et al. 2016). Trypsin is the most commonly used enzyme and predominantly cleaves at the carboxyl side of the amino acids lysine and arginine (Elgendy and Abdelrasool).

Proteins or peptides are then separated through high performance liquid chromatography (HPLC) before being visualized and quantified by the mass spectrometer. Briefly, liquid chromatography consists in hydrophobicity-based separation strategy, in which the peptides are separated according to their hydrophobic properties. This is possible by pumping the protein mixture, which is the mobile phase, into a column filled with a hydrophobic solvent (i.e.

acetonitrile) which creates a gradient in the column. By mixing multiple solvents together in ratios changing in time (i.e. acetonitrile and water), a composition gradient in the mobile phase is created. Each peptide interacts slightly differently with the various solvent concentrations, causing different flow rates and leading to the separation of the ions as they flow out of the column. The HPLC instrument typically includes a degasser, a sampler, pumps and a detector. The sampler brings the sample mixture into the mobile phase stream which carries it into the column, while the pumps deliver the desired mobile phase flow through the column. The detector, connected to the HPLC instrument, generates a signal proportional to the amount of sample component emerging from the column, hence allowing quantitative analysis. This type of detector lead to protein identification by converting those in multiple ions using electrical energy; those ions are then separated and detected according to their specific mass-to-charge ratio (m/z). The relative abundance of each ion type is recorded and displayed graphically as a mass spectrum (see Fig. 3).

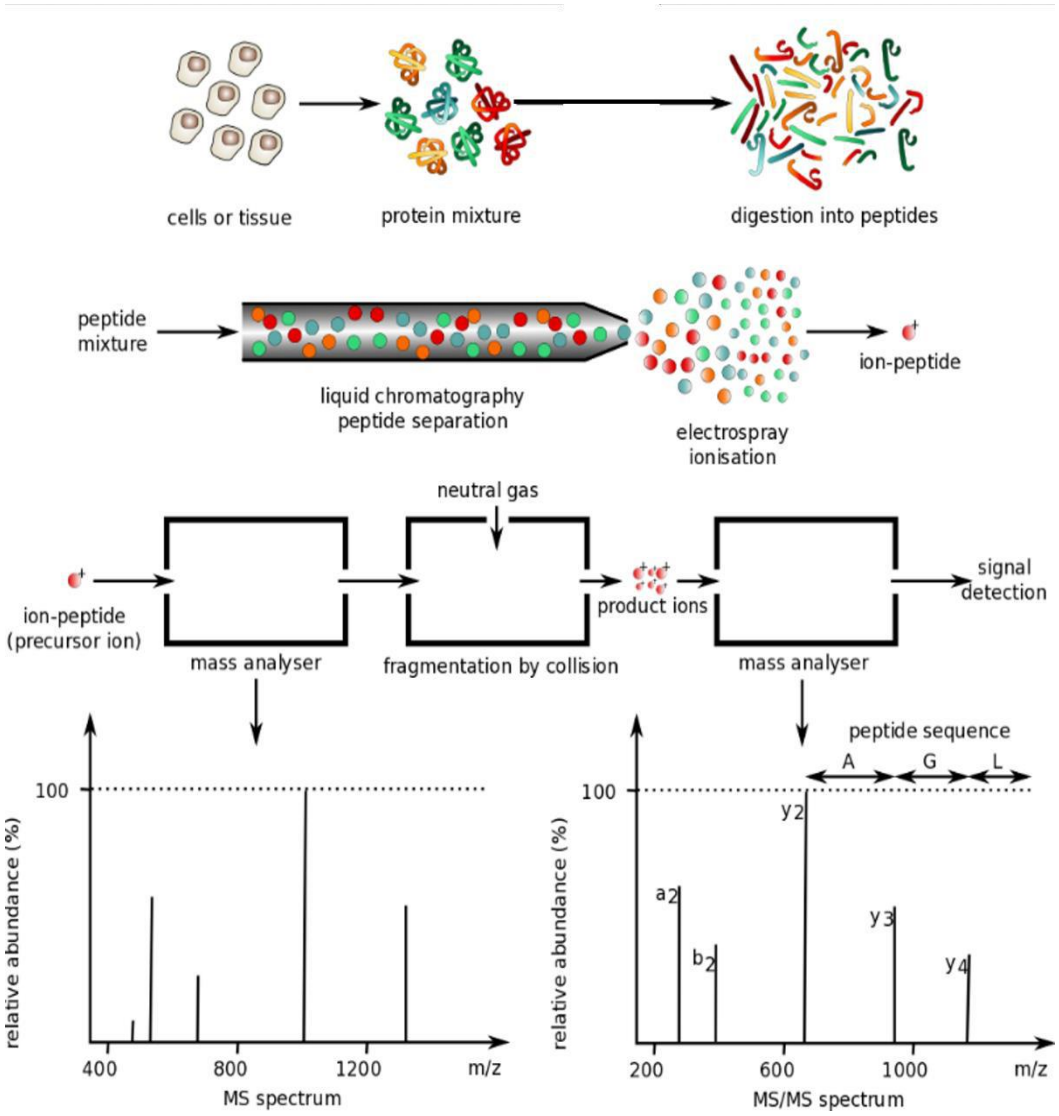

Fig. 3 HPLC-MS/MS schematic workflow from fresh cells/tissue to peptide sequence.

The overall spectra are interpreted by specific software [e.g. MaxQuant, (Cox and Mann 2008)] and the identified peptide sequences are re-assigned to the proteins they originate from, according to the chosen database. The identification of ions having identical m/z can be achieved by combining two mass spectrometers (in tandem MS-MS); this permits a more precise protein identification.

MS analysis implies protein isolation from other cell components as lipids, nucleic acids or other contaminants. The ideal extraction method must consider the protein biochemical properties (charge, size, hydrophobicity, susceptibility to proteolysis, post-translational modifications) and their variations among tissue type, species and developmental stage. Thus, there must be compatibility with downstream protein analysis and subsequent protein identification (Sheoran et al. 2009). Typical protein extraction methods involve phenol or trichloroacetic acid (TCA)–acetone to isolate and purify proteins (Wu et al. 2014). However, phenol-based extraction was preferred due to its suitability for mass spectrometry analysis (Paradiso et al. 2020).

Once the protein list corresponding to the target species has been obtained, the dataset can be analysed in various way. Several bioinformatic tools are available for functional categorization (MapMan, UNIPROT), subcellular localization (SUBA, WoLF PSORT), protein-protein interaction (STRING) or pathway collocation (KEGG). In case of incomplete database (e.g. non. model species), the sequence of unknown proteins can be searched in Protein Sequence Databases and matched the most similar one, belonging to a model species (Subba et al. 2019). Usually, fully sequenced species (e.g. *Arabidopsis thaliana*) present their own database (e.g. TAIR), containing all gene annotations and expression pattern.

Proton Transfer Reaction - Time of Flight - Mass Spectrometry

Proton-transfer-reaction time-of-flight mass spectrometry (PTR-TOF-MS) is a technique developed twenty years ago to measure VOCs in the air in real-time (Jordan et al. 2009). It has been successfully used in studies on plants (Brilli et al. 2011, Li et al. 2020), vertebrates ecology (Portillo-Estrada et al. 2021), human health (Huang et al. 2016), food quality (Deuscher et al. 2019).

This technique act as a hyper-sensitive ‘nose’, which monitors and records data in real-time at a high time resolution (up to 10 Hz) and with a low detection limit (usually a few ppbv, part per billion by volume) (Capozzi et al. 2017). Compared to gas chromatography-mass spectrometry (GC-MS), PTR-MS-TOF allows shorter time of analysis and requires neither sample preparation nor sample destruction (Blake et al. 2009). Also, the instrument size allows in-field measurements (Cappellin et al. 2013).

The principal PTR-TOF-MS components are: (1) the hallow cathode, (2) the drift tube, (3) the time-of-flight mass spectrometer (Fig. 4).

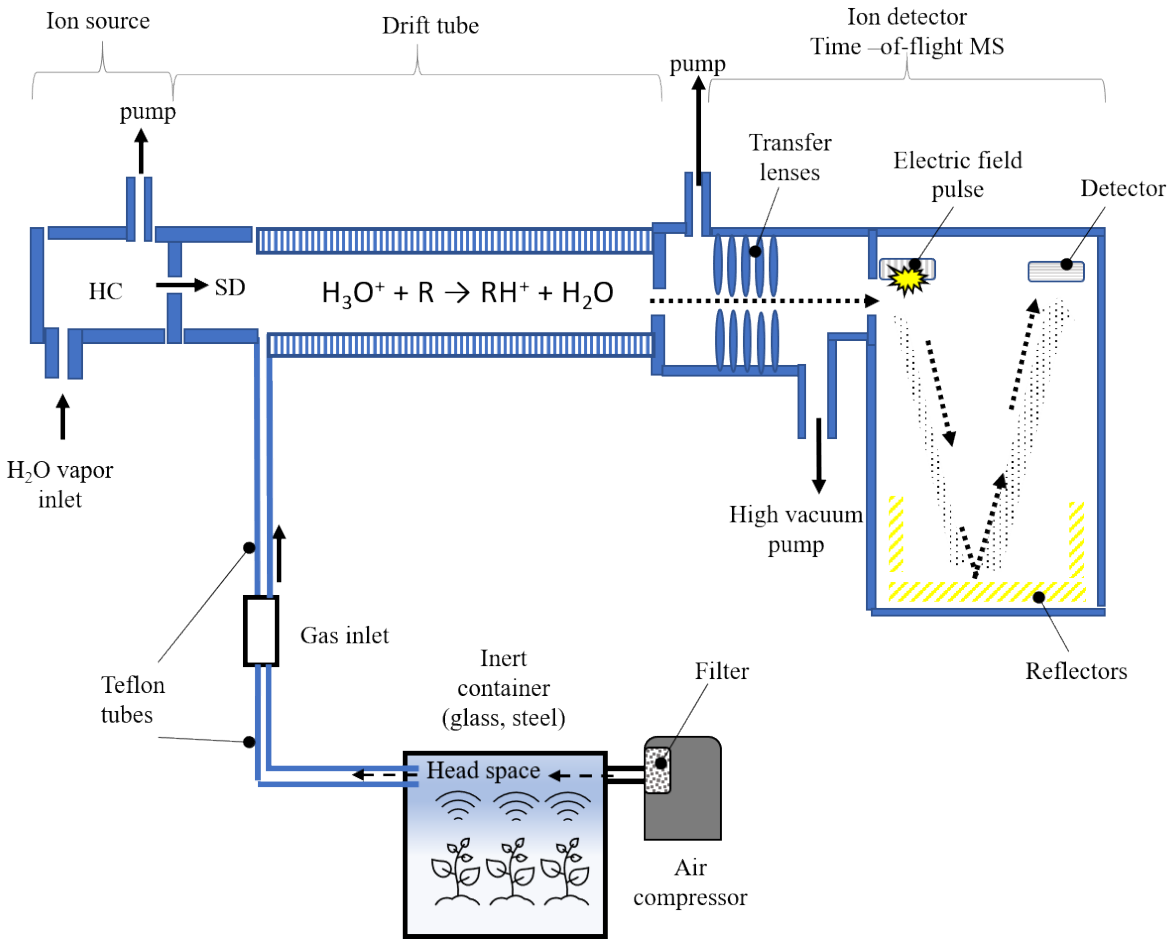

Fig. 4 Schematic illustration of a PTR-TOF-MS instrument. HC: external ion source with hollow cathode; SD: source drift. Pressurized and clean air flows from the air compressor to the sample container. Volatile compounds enter the drift tube through the gas inlet, where are ionized. Glass, steel and teflon are major inert materials.

In the hallow cathode, an electrical discharge generates hydronium ions (H_3O^+) from water vapor. Once formed, H_3O^+ ions pass a short "source drift region" and enter the drift tube, where react with the "neutral" volatilized compounds that must be analysed. More precisely, they undergo to the following ionization reaction: $H_3O^+ + R \rightarrow RH^+ + H_2O$, where R are the neutral

reactants (Kari et al. 2018). Such reaction typically transfers the proton without inducing fragmentation; for this reason, it is considered a "soft ionization"(Lindinger and Jordan 1998). H_3O^+ is the most used reactant ion because it does not react with any of the air components, as they all have proton affinities lower than H_2O molecules (Capozzi et al. 2017). In cases where dissociation does occur, they frequently follow a precise fragmentation pattern.

During the whole process, pressure and temperatures are set and kept stable. The pressure into the gas inlet (50-1000 cm^3/min) and then in the drift tube (2.2 -2.4 mbar) ensures continuous flow of ions. The temperature is adjustable between 40 and 150 °C in the gas inlet and between 40 and 120 °C in the drift tube (Jordan et al. 2009).

Once ionized, the compounds pass through transfer lenses and reach the electric field pulse that accelerates them repeatedly into the Time-Of-Flight section. The accelerated ions are reflected and then reach the detector, generating a complete mass spectrum that is processed by a fast data acquisition system. The flight times of ions determine the mass-to-charge (m/z) ratio (Jordan et al. 2009). The great advantages of TOF analysers, in respect of the quadrupole-based PTR-MS, is the capacity to separate isomeric compounds (Jordan et al. 2009).

In Figure 5 an example of the acquired average spectra during *Phaseolus Vulgaris* emissions monitoring. In every spectrum, more than 300 mass peaks in the m/z range can be identified. The broad range of masses (0-500 m/z) and the high mass accuracy (0.0001 m/z) make the PTR-TOF-MS a suitable tool for exploratory VOCs analysis. Thus, differently from GC-MS, there is no need to decide the targets beforehand (Portillo-Estrada et al. 2021).

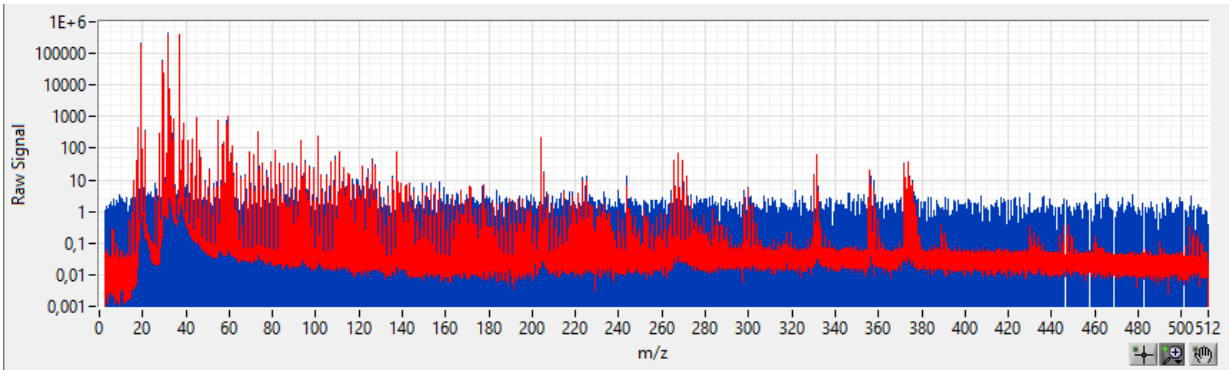

Fig. 5 Raw averaged spectrum of monitored VOCs from *P. Vulgaris* displayed through PTR-VIEWER v3.3 tool. The raw signal, also termed count per seconds (cps), of each nominal mass consists of the total ion recorded from the detector.

CHAPTER TWO

ISOPRENE EMISSION INFLUENCES THE PROTEOMIC PROFILE OF ARABIDOPSIS PLANTS UNDER WELL-WATERED AND WATER STRESS CONDITIONS[1]

Isoprene is a small lipophilic molecule synthetized in plastids and abundantly released into the atmosphere. Isoprene-emitting plants are believed to be better protected against abiotic stresses (i.e. temperature, oxidative stress, drought). The mechanism of action of isoprene is still under debate. In this study we compared the physiological responses and proteomic profile of isoprene-emitting (ISPS) and non-emitting *Arabidopsis thaliana* plants subjected to a moderate water stress and in control conditions. Our aim was to investigate if isoprene-emitting plants displayed a different proteomic profile, which may help explaining how isoprene protects plants from stresses, and the molecular mechanisms underlying isoprene emission. Only ISPS plants were able to maintain the same photosynthesis and fresh weight in well-watered and water-stress conditions. HPLC-MS-MS-based proteomic analysis revealed changes in protein abundance between non-emitting and ISPS plants both under control and moderate water stress conditions. Our data suggest that isoprene exerts its protective mechanism at different levels: under mild water stress, isoprene affects the abundance of chloroplast proteins, confirming a strong antioxidant action, and modulates signaling and hormone pathways, especially controlling ABA synthesis. Unexpectedly, it also alters membrane trafficking. Isoprene reshapes the proteome also in unstressed conditions, which suggests a priming action on several defensive metabolites.

---

[1] This chapter has been submitted as:

Mancini, I.; Domingo, G; Bracale, M; Loreto, F. and Pollastri, S. Isoprene emission influences the proteomic profile of Arabidopsis plants under well-watered and water stress conditions.

INTRODUCTON

Plants have developed many different defense systems and compounds to protect themselves against unfavorable environmental conditions (Loreto and Schnitzler 2010, He et al. 2018). Among these compounds, isoprenoids are a major class of volatile organic compound (VOCs). The most important isoprenoid, isoprene (C_5H_8), is synthesized at chloroplast level through the photosynthesis-dependent 2-C-methyl-D-erythritol 4-phosphate (MEP) pathway (Lichtenthaler 1997, Loreto and Schnitzler 2010) and is a costly compound in terms of carbon and energy. For example, it is estimated that 0.5-2% of photosynthetic carbon is re-emitted in the atmosphere as isoprene (Sharkey and Yeh 2001).

Not all plants are able to emit measurable rates of isoprene (around 20% worldwide according to Loreto and Fineschi (2015) but isoprene emitters are better protected against thermal, drought and oxidative stresses (Sharkey et al. 2001, Velikova and Loreto 2005, Loivamäki et al. 2007, Sasaki et al. 2007, Vickers et al. 2009, Tattini et al. 2015). The capacity to preserve high photosynthetic rates in adverse conditions is a desirable trait in a warming and drying world because of climate change influence. Many studies have been performed to understand how isoprene exerts its protective action, which seems to rely on a combination of effects. Thylakoid membranes of isoprene-emitting plants are more resistant to denaturation and maintain the same stiffness, fluidity and functionality at rising temperatures compared to non-emitting plants (Sasaki et al. 2007, Velikova et al. 2011). This effect may depend on the chemical and physical properties of isoprene. The lipophilic properties of isoprene may strengthen the lipidic layer of membranes (Sharkey and Singsaas 1995, Loreto and Schnitzler 2010, Pollastri et al. 2019). Isoprene conjugated double bounds allow this molecule to react and scavenge many reactive and dangerous chemical species (Vickers et al. 2009). The low evaporation temperature (34°C) may allow isoprene to remove heat from the membrane (Pollastri et al. 2014).

Vickers et al. (2009) claimed that isoprene effects may all converge toward a protective function of the photosynthetic apparatus from generalist stresses. However, this view is challenged by a possible too low concentration of isoprene to effectively carry out any antioxidant action or to have other membrane protection properties (Harvey and Sharkey 2016). Moreover, growing evidence of reprogramming of genes expression, proteomic and metabolomics profiles in isoprene-emitting plants, would imply a much wider action of isoprene (Behnke et al. 2010, Way

et al. 2013, Ghirardo et al. 2014, Tattini et al. 2014, Velikova et al. 2014, Harvey and Sharkey 2016, Vanzo et al. 2016, Zuo et al. 2019). Very recently, a role of isoprene as signaling and priming molecule is also emerging (Lantz et al. 2019, Zuo et al. 2019, Pollastri et al. 2021).

To further help gaining in-depth understanding of the molecular mechanisms underlying the effects of isoprene, we screened and identified changes in the proteomes of *Arabidopsis thaliana* plants that do not emit (wild type) or do emit isoprene after insertion of a *Eucalyptus globulus* isoprene synthase (ISPS), under control and mild water stress conditions. Transcriptomics analysis showed that many pathways are induced in these transgenic Arabidopsis isoprene-emitting lines (Zuo et al. 2019). However, due to post-transcriptional modification, translation regulation and protein degradations, mRNA expression levels could not fully predict the corresponding protein abundance, and research on proteomics can provide new and useful information complementing transcriptomics results. Here, proteome analysis indicates specific and distinct changes associated to isoprene presence and to metabolite distribution in well-watered and water-stressed plants. The results provide useful information for further research elucidating isoprene mechanism(s) of action defending plants against stresses.

MATERIALS AND METHODS

Plant material, growth conditions and water stress treatment

The study was performed using three different *Arabidopsis thaliana* (Col-0) genotypes: the non-emitting wild type (WT) and empty vector line EV-B3 (EV), and the isoprene-emitting line C4 where the isoprene synthase gene from *Eucalyptus globulus* was inserted (ISPS). Detailed description of the transgenic Arabidopsis lines, kindly provided by Prof Thomas Sharkey, may be found in Zuo et al. (2019). Seeds were sown in moistened peat pellets (Jiffy Products), kept at 4°C for 3 days and then transferred in a growth room with the following conditions: photoperiod of 12 h with a light intensity of 150 µmol photons m^{-2} s^{-1} and temperature of 22°C. During the night, the temperature was reduced to 20°C.

Six-week old plants were divided into two groups, one was subjected to mild water stress (WS) and the other was kept in well-watered condition (WW) and used as control. The WS group was maintained in controlled mild water stress by daily weighting the pellets and keeping the soil

moisture at 30% of field capacity. The mild water stress condition was reached after 5 days and plants were kept in this condition for 5 further days. At this point, plants were subjected to the following measurements and analysis.

Leaf gas-exchange and chlorophyll fluorescence measurements

A Li-Cor 6400-XT portable photosynthesis system (Licor, Inc., Lincoln, NE, USA) was used to measure photosynthesis (An, μmol $m^{-2}s^{-1}$), and stomatal conductance (gs, mmol $m^{-2}s^{-1}$) on five plants, for each genotype and treatment. Before measuring, leaves were allowed to reach steady state An and gs inside the 2 cm^2 cuvette, under 400 ppm of CO_2, 200 μmol $m^{-2}s^{-1}$ of light intensity and a leaf temperature of 22°C. Chlorophyll fluorescence parameters were also measured at this stage, namely the maximum quantum efficiency of photosystem II (PSII) by the ratio between variable and maximal fluorescence in darkened leaves (Fv/Fm); the PSII quantum yield (ΦPSII = Fm'- Fs /Fm') where Fm' is the maximal fluorescence and Fs is the steady-state fluorescence in light-adapted leaves; the non-photochemical quenching (NPQ = Fm−Fm′ /Fm) were Fm′ is the maximal fluorescence in light-adapted (1000 μmol m^{-2} s^{-1}) leaves (Genty et al. 1989).

Biomass and leaf relative water content and measurements

The rosette leaves of five Arabidopsis plants, for each genotype and treatment, were harvested and fresh weight recorded. The leaf relative water content (RWC, %) was estimated as described previously (Smart and Bingham 1974). In details, harvested leaves were placed in a jar with distilled water overnight after which the leaves were wiped, and the turgid weight was measured. Then the samples were dried in an oven at 60 °C until the dry weight (DW) was stable and could be measured.

Isoprene sampling and quantification

Isoprene sampling was performed on fully expanded leaves enclosed inside the cuvette. A total of 5 L of air was collected from the cuvette outflow using a mass flow pump set at 200 mL min^{-1} rate (AC Buck Inc. FL, USA) and a cartridge filled with absorbents (30 mg each of Carbosieve X and Carbosieve B, Supelco, USA). Isoprene from emitting lines was quantified using an

Agilent 5975 gas chromatograph-mass spectrometer (GC-MS) system fitted with an HP-INNOWax (50 m length, 0.2 mm ID, 0.4 µm film) column. Thermal desorption was executed by a Twister® multipurpose autosampler and TD unit (Gerstel Technologies, Germany) with an e-Trap cryofocussing system (Chromtech, Germany). The GC separation programme was 40 °C for 1 min, then ramping to 110 ˚C at 5 ˚C min^{-1}, remaining stable at 110 °C for 10 min, then increased to 260 °C at 30 °C min^{-1}, and maintained at the final temperature for 2 min.

Protein extraction

Proteins were extracted from 150 mg of leaf samples by SDS/phenol method (Wu et al. 2014). Briefly, leaves were ground in liquid nitrogen and homogenized with extraction buffer (0.15 M TRIS – HCl, pH 8.8, SDS 1%, 1 mM EDTA, 0.1 M DTT, 2 mM PMSF, 0.1 mg/mL Pefabloc, Protease Inhibitor 1:1000). After centrifugation, 1:1 volume of phenol saturated with 0.1 M TRIS-HCl was added to the supernatant phase. Phenolic phase was collected and overnight precipitated with four volumes of 0.1 M ammonium acetate in methanol at −20°C. Precipitate obtained by centrifugation at 15.000 g for 10 min at 4°C was washed twice with cold 0.1 M ammonium acetate and finally with cold 80% acetone. Pellet was dried and resuspended in 250 µL of SDS-lysis buffer (20% w/w SDS, 0.25 M Tris/HCl pH 7.5, 100 mM DTT). Protein concentrations were quantified using the 2-D Quant-kit (GE Healthcare). Four independent biological replicates were analyzed for each sample.

Trypsin digestion

Protein extracts were digested using the filter aided sample preparation (FASP) protocol (Wiśniewski et al. 2009). Briefly, protein extracts were heated for 5 min at 95°C, ten times diluted with UA buffer (8 M urea in 100 mM Tris-HCl, pH 8.0) and transferred to the YM-30 Microcon filter units (Millipore). The denaturation buffer was replaced by washing three times with UA buffer and proteins were alkylated using 50 mM iodoacetamide in UA for 15 min at room temperature in the dark. The excess of alkylation reagents was eliminated by washing four times with ABC buffer (50 mM NH_4HCO_3). Proteins were digested overnight at 37 °C with trypsin in ABC buffer at enzyme-to-substrate of 1:100 (w/w) ratio. The digested peptides were eluted by centrifugation. Peptide concentrations were measured spectrophotometrically,

assuming that a solution of proteins with a concentration of 1 mg mL^{-1} determines an absorbance of 1.1 at 280 nm. The peptides were finally desalted onto C18 Oasis-HLB cartridges and dried down for further analysis.

LC-MS-MS analysis and elaboration of raw data

The peptides were analysed in a Q-Exactive mass spectrometer as described in (Garcia-Seco et al. 2017). Raw data were searched against the *Arabidopsis thaliana* Uniprot protein database (version 2019-01, 76,141 entries) with MaxQuant program (v.1.5.3.3).

Protein identification was performed following these criteria: two missed cleavages, fixed modification of cysteine (carbamidomethylation), variable modifications of methionine (oxidation) and phosphorylation on serine, threonine and tyrosine, minimum peptide length of six amino acids, precursor mass tolerance 4.5 ppm for the main search. Label Free Quantification (LFQ), "match between runs" (time window of 0.7 min) and target-decoy search strategy (revert mode) options were enabled. A false discovery rate (FDR) of 1% was accepted for peptide and protein identification, respectively.

The raw data obtained as output from MaxQuant ("ProteinGroups" files) were initially processed using an in-house tool. Incorrect identifications ("Reverse", "One site", and "Contaminant" hits) and not consistent identifications were filtered out. Missing values were estimated from the dataset based on two criteria for each sample, depending on whether one or more missing values were observed for each entry: when two values were available, the imputation of the missing value was set to a random value within an interval of 1/4 of the entire sample standard deviation centred on the entry average.

The mass spectrometry proteomics data were deposited in the ProteomeXchange Consortium via the PRIDE partner repository (Perez-Riverol et al. 2019) with the dataset identifier PXD025069 using the following reviewer account details: Username: reviewer_pxd025069@ebi.ac.uk Password: ok3Yiae5.

For the quantitative proteome analyses the filtered data were processed with the Perseus software platform (http:// www.perseus-framework.org). Log_2 transformed LFQ intensities of protein groups intensities were centred by subtracting the median of the entire set of protein groups LFQ intensities per sample (column).

Quantification of free proline content

Free proline was extracted from lyophilized leaves (0.2 g FW per genotype per condition in four biological replicates), grounded and resuspended in 1 mL of 0.1% (v/v) formic acid (FA) in water/methanol (MeOH) (50:50). After 4h mixing in the dark, the mixture was centrifuged (15 min, 13.000 rpm) and the supernatant collected. Proline standard solution (1mM in 0.1% FA and 50% MeOH) was prepared from 10 mM stock solution in distilled water and used for the calibration (range 2–15 µM). The HPLC analyses was performed in a Finningan Surveyor MS plus HPLC system (Thermo Electron Corporation, CA, USA). For proline quantitation, separation was achieved using C18 column (ACQUITY UPLC Peptide BEH C18 Column, 300Å, 1.7 µm, 2.1 mm X 150 mm). The mobile phase was composed of (A) water with 0.1% (v/v) formic acid and (B) methanol/water (50:50) 0.1% (v/v) formic acid with flow rate 150 µL/min; gradient 0–3.0 min/2% (v/v) B, 3–16 min/2–50% (v/v) B. For the mass spectrometry quantification, a Finningan LXQ linear ion trap mass spectrometer, equipped with an ESI ion source (Thermo Electron Corporation, CA, USA), was used. The analyses were done in positive (spray voltage 4,5 kV, capillary temperature 270 °C) and in the multiple reaction monitoring (MRM) mode. The optimization of collision energy for each substance, the tuning parameters and the choice of fragments to confirm the identity of target compounds (proline) were done in continuous flow mode, by using standard solution at concentration of 5 µM. MRM acquisition was done monitoring the 116/70 transition.

Determination of ABA content

The Abscisic Acid (ABA) content was determined as described by Pan, Welti & Wang, (2010), with three biological repetitions. Briefly, 20 mg of freeze-dried leaf material was ground into powder in liquid nitrogen using a mortar and pestle and extracted by adding 800 µL of 2-propanol/H2O/concentrated HCl (2:1:0.002, vol/vol/vol). After shaking for 30 min at 4 °C, 1 mL dichloromethane was added to each sample. After a further shaking for 30 min at 4 °C, samples were centrifuged at 13,000 g for 5 min at 4°C and the lower phase was collected and concentrated (not completely dry) under nitrogen flow. Samples were then re-dissolved in 0.05 ml of methanol/H_2O/formic acid (2:1:0.1, vol/vol/vol). Separations were performed on an Acclaim

RSLC 120 C8 column (Thermo Scientific; 2.2 µm, 120 Å, 2.1x100mm) at 25°C on a gradient elution at the flow rate of 0.2 mL min^{-1}, using a Finningan Surveyor MS plus HPLC system (Thermo Electron Corporation, CA, USA). The mobile phase was composed of water with 0.1% (v/v) formic acid (solvent A), and methanol 0.1% (v/v) formic acid (solvent B). The gradient elution program was: 0–3.0 min/5% (v/v) B, 3–20 min/5–50% (v/v) B. A Finningan LXQ linear ion trap mass spectrometer, equipped with an ESI ion source (Thermo Electron Corporation, CA, USA) was used for ABA quantification. The analyses were done in negative (spray voltage 2,5 kV, capillary temperature 250 °C) and in the multiple reaction monitoring (MRM) mode. The optimization of collision energy for each substance, the tuning parameters and the choice of fragments to confirm the identity of target compounds (ABA) were done in continuous flow mode, by using standard solution at concentration of 0.01 mg mL^{-1}. MRM acquisition was done monitoring the 263/153 transition.

Trehalose determination

Lyophilized leaves (20 mg) in three biological replicates were grounded into powder, in liquid nitrogen using a mortar and pestle. Trehalose was extracted in 1 mL of water/ethanol (50:50) using a thermal mixer at 60°C and 250 rpm for one hour. After centrifugation at 13000×*g* for 5 min, the supernatant was collected and dried in a speedVac Vacuum evaporator at room temperature.

Monosaccharide permethylation was performed according to the procedure described by (Ciucanu and Kerek 1984) with minor modifications. Briefly, the dried samples were dissolved in 1000 µL of DMSO, introduced into a conical-glass vial and 50 µL of water were added, as suggested by Ciucanu & Costello (2003) After the addition of 40 mg of finely powdered NaOH, samples were stirred vigorously at room temperature and then 80 µL methyl iodide was added. The mixture was stirred at room temperature for 10 min. Permethylated monosaccharides were extracted two times using 1000 µL of dicloromethane.

The dicloromethane phases were then washed with 1000 µL of water for at least 2 times to remove any residual salts. The organic phases containing the permethylated monosaccharides were dried under nitrogen flow and reconstituted in 50 µL of 0.1% (v/v) formic acid (FA) in water/methanol (MeOH) (50:50).

Separations were performed on an Acclaim RSLC 120 C8 column (Thermo Scientific; 2.2 µm, 120 Å, 2.1x100mm) at 25°C on a gradient elution at the flow rate of 0.2 mL/min, using a Finningan Surveyor MS plus HPLC system (Thermo Electron Corporation, CA, USA). The mobile phase was composed of water with 0.1% (v/v) FA (solvent A), and methanol 0.1% (v/v) FA (solvent B). The gradient elution program was: 0–3.0 min/5% (v/v) B, 3–25 min/5–50% (v/v) B. A Finningan LXQ linear ion trap mass spectrometer, equipped with an ESI ion source (Thermo Electron Corporation, CA, USA) was used for trehalose quantification. The analyses were done in negative (spray voltage 2,5 kV, capillary temperature 250 °C) and in MRM mode. The optimization of collision energy for each substance, the tuning parameters and the choice of fragments to confirm the identity of permethylated trehalose were done in continuous flow mode, by using standard solution at concentration of 0.001 mg/ml. MRM acquisition was done monitoring the 477/259 transition.

Statistical analysis

Physiological data are shown as means ± standard errors (SEs). Data were analysed using Shapiro–Wilk test to determine normality distribution and one-way analysis of variance (ANOVA), with critical *p*-value set at 0.05. All analyses were performed using Sigma Plot Software (Systat Software Inc.).

In order to analyse the proteins changes in relative abundance between analytical groups we performed a statistical analysis on Perseus software (Max-Planck-Institute of Biochemistry, Martinsried, Germany; version 1.5.8.5). Transformed, centred, and normalized Log_2 LFQ data were subjected to one-way ANOVA, based on multiple-sample tests; an FDR cut-off of 0.01, based on the Benjamini-Hochberg correction, was used for truncation. One-way ANOVA was coupled with Tukey's test (FDR <0.01), to extrapolate statistically significant comparisons. Two-way ANOVA was then performed on significant data, to directly link the influence of genotype and treatment (mild water stress), or the interaction between them.

Protein fold change (FC) ratio, expressed as Log_2FC, was defined as the Log_2 of protein abundance in one biological conditions minus Log_2 protein abundance in another biological condition.

The Perseus software was also used for Principal Component Analysis (PCA) and plot scattering, to assess the quality of our datasets. To assess statistical significance of proline quantification, the Kruskal-Wallis test was applied and coupled with Dunn post-hoc comparisons method ($p < 0.05$).

Downstream bioinformatic analysis

Functional annotation and metabolic pathway analysis were performed with MapMan 3.6.0RC1 software (Thimm et al. 2004) using the *Arabidopsis thaliana* ISOFORM_TAIR10_2012 protein database as background.

Perseus software was used to build heatmaps and hierarchical clustering (Tyanova et al. 2016). Hierarchical clustering of significantly changing proteins was performed using the Z-score calculation on Log2 intensity values with the following settings: Row, Column distance calculated using the Euclidean algorithm; Row, Column linkage – Complete.

The potential subcellular localization of all the DAPs was analysed using the multiple marker abundance profiling method of the SUBA4 bioinformatic platform (https://suba.live/, (Hooper et al. 2017)).

ANOVA-one way of repeated measures followed the Tuckey's post-hoc test was used to verify ABA content differences between conditions ($p < 0.05$).

RESULTS

Physiological data

All plants showed the same photosynthesis (An) in WW conditions, whereas under WS An of the isoprene-emitting (ISPS) genotype was significantly less affected than in WT and EV plants (Fig. 1A). Stomatal conductance (gs) was similar among plants and treatments in ISPS and EV plants, whereas WT showed a reduction in stress conditions (Fig. S1A). Water-stressed WT showed the lowest gs values albeit differences were not statistically significant in this case (Fig. S1A). Chl fluorescence parameters revealed a similar pattern as An. ΦPSII and Fv/Fm were similar in the three WW lines and were significantly reduced only in non-emitting lines under WS (Fig. 1B, C). The NPQ of fluorescence was statistically similar in all the plants and

treatments, with the lowest values recorded on ISPS plants (Fig. S1B). Isoprene emission was only measurable in ISPS plants, where it was significantly lower in WS than in WW condition (Fig. 1D).

The fresh weight of the three genotypes was similarly significantly reduced in WS with respect to WW plants (Fig S1D). However, reduction of dry weight and RWC under WS conditions was not significant in any plant (Fig. S1E). Since, as expected, none of the measured parameters showed differences between WT and plants transformed with the empty vector (both unable to emit isoprene), the proteome of the EV plants was not further examined.

Overview of proteomic profiles.

To highlight the molecular mechanisms underlying the different responses of isoprene-emitting and non-emitting plants to water stress, we performed a quantitative proteomic analysis on WW and WS non-emitting (WT) and isoprene-emitting (ISPS) plants.

A total number of 2625 of proteins were identified and quantified. The detailed information of all proteins, including ID, intensity values and FASTA headers are provided in Table S1. The whole protein dataset was successfully mapped with UniProtKB ID. According to the one-way ANOVA consistency test (FDR < 0.01), 20% of the whole protein dataset (528 proteins) were differentially abundant proteins (DAPs; Table S2A). A post-hoc Tukey's test identified 275 DAPs (101 of which accumulated and 174 decreased) in WT WS vs. WT WW comparison; 271 DAPs (123 accumulated and 144 decreased) in ISPS WS vs. ISPS WW comparison, 284

DAPs (134 accumulated and 150 reduced) in the comparison between ISPS WW vs. WT WW, 273 DAPs (161 accumulated and 112 reduced) when comparing WW plants of ISPS and WT genotypes (Table S2B-E).

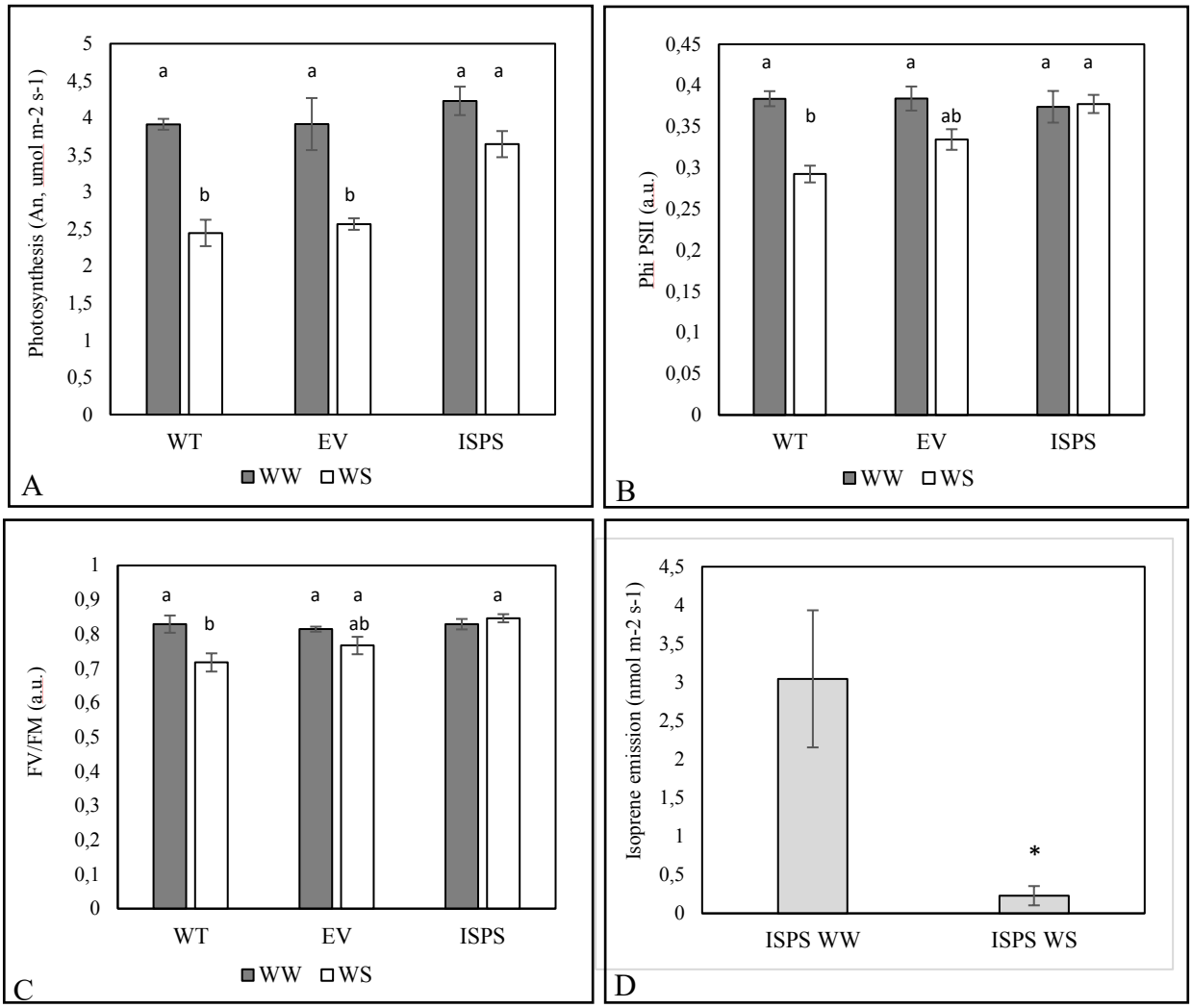

Fig. 1 Photosynthesis (An) (A), PSII quantum yield (ΦPSII) (B), maximum quantum efficiency of photosystem II (Fv/FM) (C) of wild-type (WT), empty vector (EV), and isoprene-emitting (ISPS) plants in well-watered (WW, grey bars) and water-stressed (WS, white bars) conditions. Isoprene emission (D) of ISPS plants measured in well-watered and water stressed conditions. Means + SE (n = 5) are shown. One-way ANOVA followed by Tukey's test was performed to statistically separate means (A, B, C). Means significantly different ($p < 0.05$) are represented by different letters (a, b, c). Student t test was applied to compare the isoprene emission in isoprene emitting plants in WW and WS conditions (*p <0.05).

The heatmap of the 528 DAPs revealed 14 distinct clusters of proteins changing on each condition (Fig. 2A, B). Clusters I and II were composed by proteins which accumulated and

decreased in ISPS plants with respect to WT plants, respectively, regardless of the growing condition. Cluster III and IV consisted of DAPs altered by WS, regardless of the genotype. The remaining clusters (V-XIV) consist of DAPs differently modulated by mild water-stress depending on the genetic background. For example, DAPs belonging to clusters V and VI, were affected by mild water-stress in ISPS mutant only; clusters VII and VIII, were DAPs affected by water-stress solely in WT plants.

Correlation coefficients of the 16 samples (four replicates × four groups) showed a high repeatability of the proteomic data. Indeed, the four experimental conditions were clearly separated by PCA score plot and replicates within each group plotted very closely (Fig. S2A). WS and WW plants were separated in PC1, while WT and ISPS plants were separated in PC2, accounting for 32.4% and 31.6% of the total variation, respectively. This indicates substantial and independent effects of both the capacity to emit isoprene and the stress treatment (Fig. S2B).

Analysis of proteomic differences. A two-way ANOVA analysis was performed on all 528 DAPs (FDR < 0.01) to assess any significant differences due to genotype (G), water stress treatment (T) or the interaction between these two factors (I) on protein abundance. Significant FDR values were selected for each variable (G, T or I) and separately grouped in three protein lists: G-dependent (Table S3A), T-dependent (Table S3B) and I-dependent DAPs (Table S3C).

The single factor (genotype or treatment) significantly influenced the abundance of 78 and 55 DAPs, respectively. The 78 G-dependent DAPs (39 of which accumulated more in ISPS than in WT) represent the basic response of the Arabidopsis proteome to the acquired capacity to emit isoprene, regardless of plant growing conditions. This trend is described by cluster I and II in Fig. 2B.

On the other hand, the 55 T-dependent DAPs (19 of which accumulated in both genotypes exposed to WS more than in WW plants) respond to water stress independently on the capacity to emit isoprene. Indeed, 67% of the T-dependent DAPS were reduced in their abundance, as expected for translation and protein synthesis under stress. T-dependent DAPs trend is displayed as Cluster III and IV (Fig. 2B).

The interaction G x T (I) affected the abundance of 396 DAPs (Table S3C). The interaction between G and T therefore influences the proteome more than G or T singularly. The expression profiles of the I-dependent DAPs are represented by Clusters V-XIV (Fig. 2B).

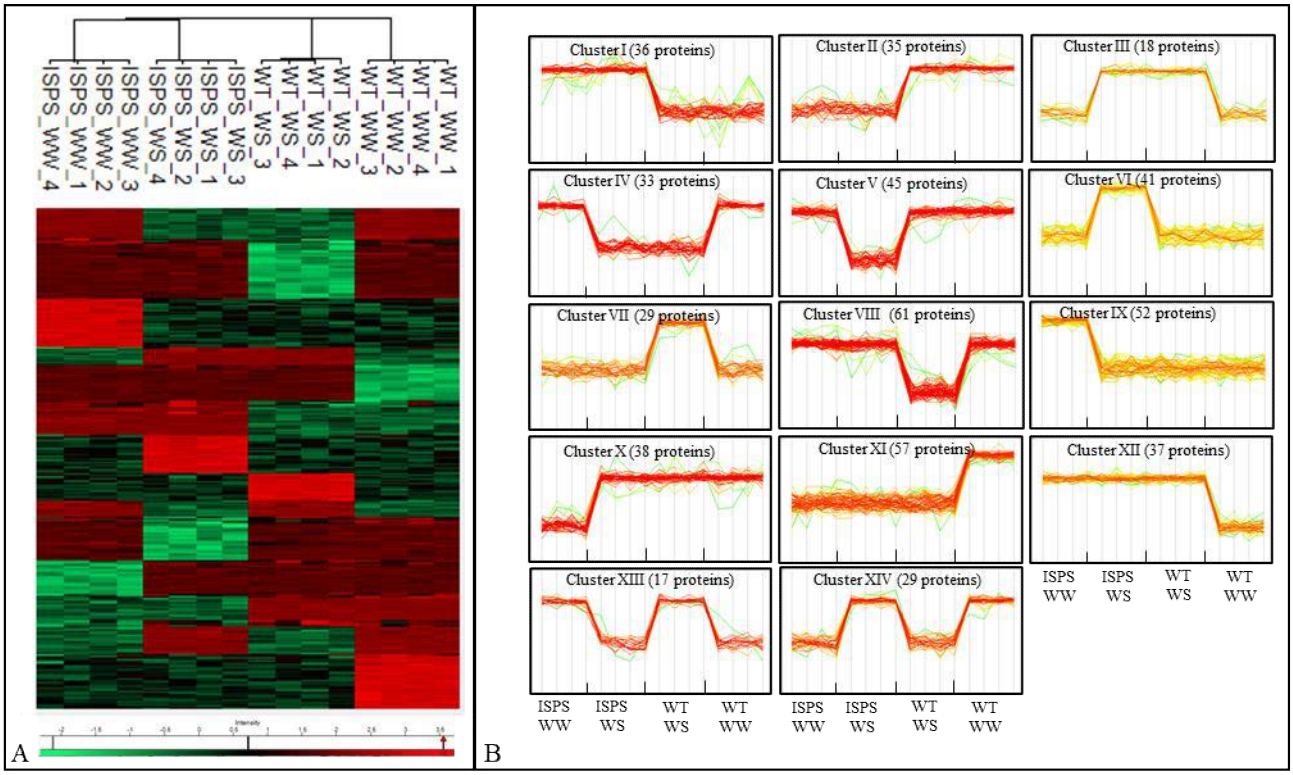

Fig. 2 Heatmap and hierarchical clustering of differentially abundant proteins (DAPs) according to one-way ANOVA analysis of wild-type (WT) and isoprene-emitting (ISPS) plants under well-watered (WW) and water stressed (WS) conditions. Heatmap colours are based on the combined Z-scored (log2) LFQ values. Green and red shades correspond to proteins that accumulated less and more, respectively.

The MapMan annotation revealed that proteins of 16 out of 36 pathways were influenced by G, indicating a large reshaping of the proteome associated to the capacity to emit isoprene (Fig. 3). For G- and I-list, functional classes included PROTEIN TRANSLATION, PROCESSING AND DEGRADATION (20% and 18% respectively), SIGNALLING (9% and 5%), TRANSPORT (4% and 4%), STRESS (6% and 3%) and HORMONE METABOLISM (6% and 2%). Functional classes in T-list were PROTEIN TRANSLATION, PROCESSING AND DEGRADATION (13%), CELL (10%), RNA (6 %) and STRESS (5%).

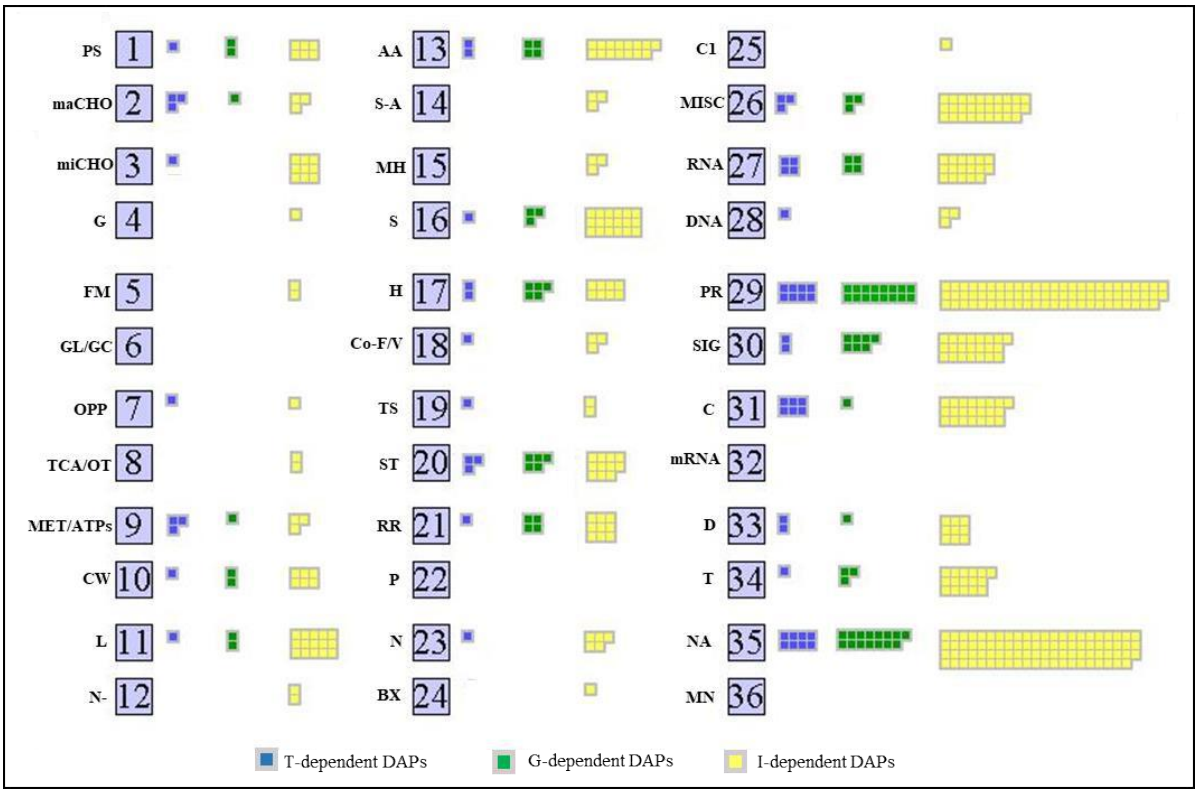

Fig. 3 Functional classification of genotype (green squares, G), treatment (blue squares, T) and interaction-dependent (yellow squares, I) differentially accumulated proteins (DAPs) by MapMan Overview map. Each square represents a protein; The 36 BINS abbreviations: PS, photosynthesis; maCHO, major carbohydrate metabolism; miCHO, minor carbohydrate metabolism; G, glycolysis; FM, fermentation; GL/GC, gluconeogenesis/glyoxylate cycle; OPP, oxidative pentose phosphate; TCA/OT, tricarboxylic acid/organic acid transformations; MET/ATPs, mitochondrial electron transport/adenosine triphosphate; CW, cell wall; L, lipid metabolism; N-, nitrogen metabolism; AA, amino acid metabolism; S-A, sulphur assimilation; MH, metal handling; S, secondary metabolism; H, hormone metabolism; Co-F/V, co-factor and vitamin metabolism; TS, tetrapyrrole synthesis; ST, stress; RR, redox regulation; P, polyamine metabolism; N, nucleotide metabolism; BioDX, biodegradation of xenobiotics; C1, C1-metabolism; MISC, miscellaneous; RNA, ribonucleic acid; DNA, deoxyribonucleic acid; PR, protein; SIG, signalling; C, cell; mRNA, messenger RNA; D, development; T, transport; NA, not assigned; MN, mineral nutrition.

The predicted subcellular localization was consistent for G, T and I lists, as proteins localized in "CHLOROPLAST" were the most affected, ranging from 29 to 30%, followed by those located in "CYTOSOL" (20-27% range). The genotype influenced a larger accumulation of proteins localized in GOLGI, ENDOPLASMIC RETICULUM, ENDOSOME AND PEROXISOME, with respect to those subjected only to stress or to the interaction of the two factors (Fig. 4), suggesting possible sites of action of isoprene at the level of cell organization.

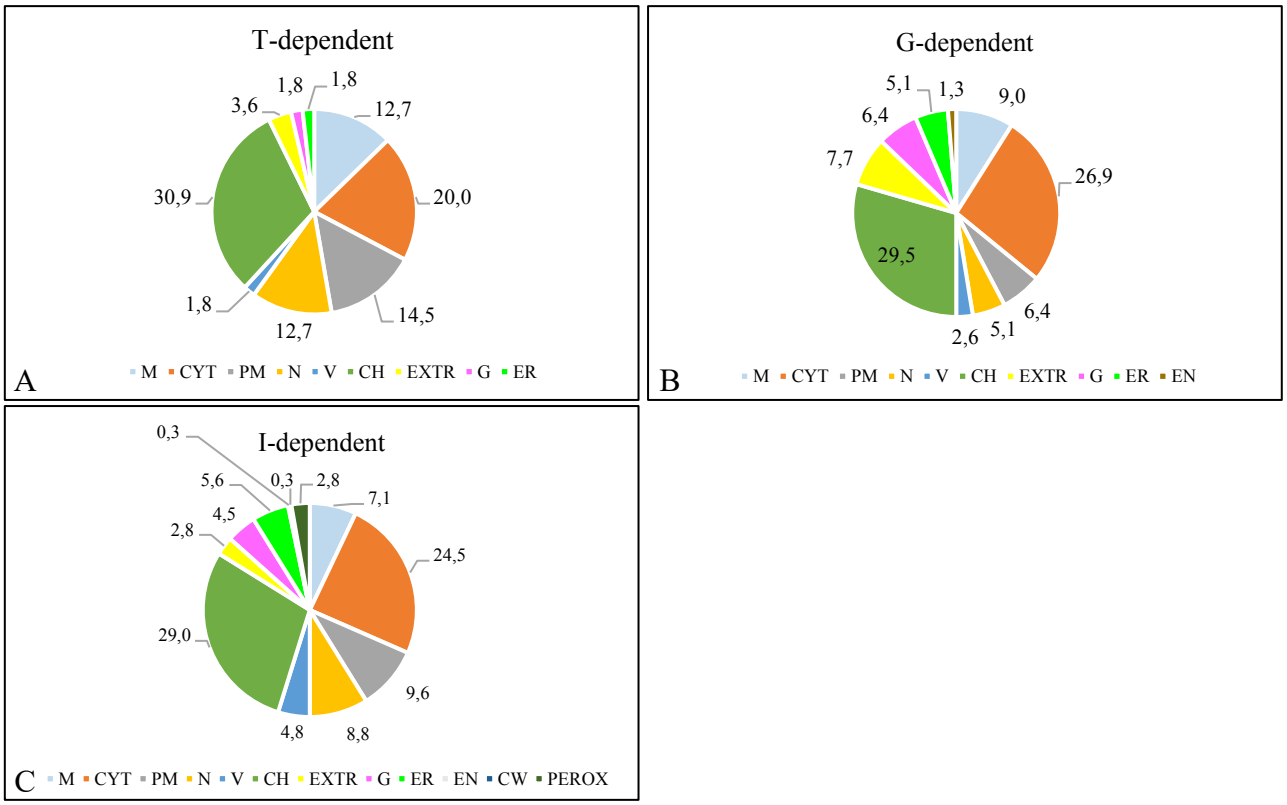

Fig. 4 Subcellular localization of (A) treatment-dependent DAPs (T); (B) genotype-dependent DAPs (G); (C) Interaction-dependent DAPs (I), using the multiple marker abundance profiling method of the SUBA4 bioinformatic platform. Abbreviations: M, mitochondria; CYT, cytoplasm; PM, plasma membrane; N, nucleus; V, vacuole; CH, chloroplast; EXTR, extracellular region; G, golgi; ER, endoplasmic reticulum; EN, endosome; CW, cell wall; PEROX, peroxisome. Numbers in the pie charts represent percentages of DAPs belonging to each subcellular compartment with respect to total DAPs.

Free proline, trehalose and ABA accumulation

We measured the levels of free proline, trehalose and ABA in WT and transgenic Arabidopsis under mild water stress conditions (Fig. 5). In WT plants, proline and trehalose did not accumulate significantly under water stress. In ISPS transgenic Arabidopsis, in the absence of drought stress, both proline and trehalose contents were similar to that observed in WT, but they became significantly higher than in WT under water stress conditions (Figure 5B, C). Similarly, there was no significant difference in ABA content between WT and ISPS plants under normal conditions. After the mild water stress treatment**,** significantly higher levels of ABA were recorded only in ISPS, while in WT WS samples ABA increase was not statistically significant (Figure 5A).

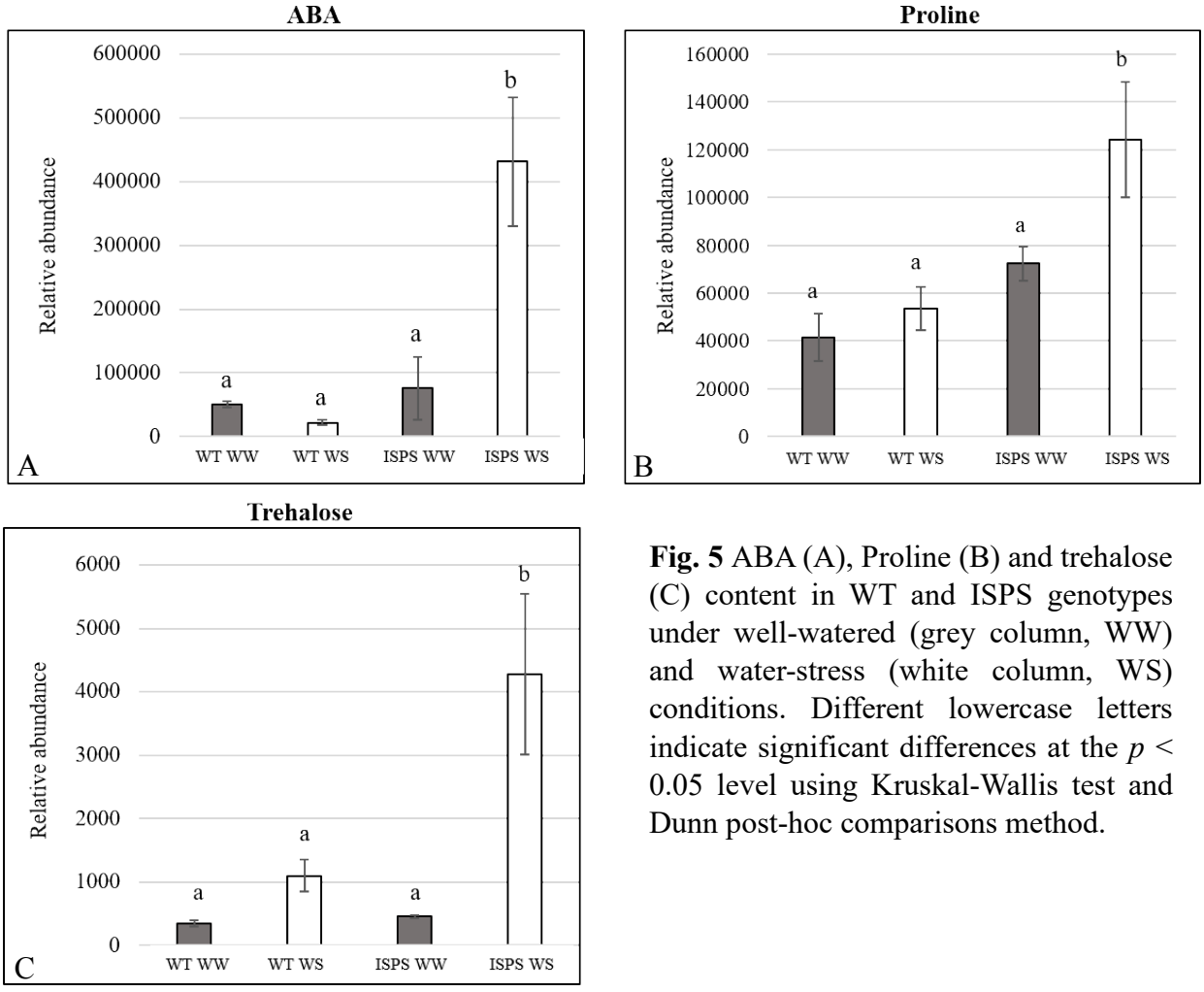

Fig. 5 ABA (A), Proline (B) and trehalose (C) content in WT and ISPS genotypes under well-watered (grey column, WW) and water-stress (white column, WS) conditions. Different lowercase letters indicate significant differences at the $p < 0.05$ level using Kruskal-Wallis test and Dunn post-hoc comparisons method.

DISCUSSION

Isoprene-emitting plants are able to maintain higher photosynthetic rates even when challenged by several abiotic stresses (Vickers et al. 2009, Pollastri et al. 2014). Our physiological measurements confirm such better protection in isoprene-emitting Arabidopsis facing a water stress. We tried to provide further information on the protective mechanism of action of isoprene by examining the proteomic profile of non-emitting and isoprene-emitting plants. We show that the induced capacity to emit isoprene causes a large reprogramming of the proteome, and, in the following discussion, we analyze the main biological processes (e.g. *chloroplast, membrane-trafficking, cell signaling, stress*) that were affected by the genotype (G), the water stress treatment (T) and the interaction between those two factors (I). The discussed DAPs are reported in Table 1.

Table 1 List of relevant differentially abundant proteins (DAPs) dependent on genotype (G), treatment (T) and interaction (I) divided according to their subcellular localization (Suba CC) and function (chloroplast-related function, endomembrane trafficking, cellular signalling, osmoprotection, redox homesotasis, defense,).

ID TAIR	Protein	WT WW	WT WS	ISPS WW	ISPS WS	Suba CC*
GENOTYPE-DEPENDENT DAPS						
CHLOROPLAST						
AT5G10470.1	KCA1	19,62	19,54	25,61	25,59	CYT
AT1G31800.1	CYP97A3, LUT5	18,78	19,09	25,05	25,12	CH
AT1G53520.1	Chalcone-flavanone isomerase	19,70	19,98	24,45	24,25	CH
AT4G25100.5	FSD1	20,16	20,09	24,25	25,95	CH
AT5G53170.1	FTSH11	19,76	19,72	24,15	23,97	CH
AT1G12270.1	Hop1	19,80	19,72	24,18	24,36	CYT
ATCG00190.1	RPOB	20,03	19,34	24,11	24,58	CH
AT2G28800.4	ALB3	25,28	25,36	25,97	26,11	CH
ATCG00820.1	RPS19	26,90	26,92	27,32	27,61	CH
ENDOMEMBRANE TRAFFICKING						
AT1G01910.4	GET3A	19,54	19,15	26,90	26,71	CYT
AT5G16300.3	COG1	19,25	19,92	22,56	22,38	CYT,G
AT4G29160.3	SNF7.1	19,55	18,71	24,84	25,19	ENDO
AT5G54440.1	CLUB/TRS130	19,57	19,70	24,21	23,93	G
AT5G58030.1	TRAPPC5	19,22	19,84	25,41	25,19	G

CELLULAR SIGNALLING						
AT5G07300.1	BON2	19,16	19,51	24,20	23,86	PM
AT1G70940.1	PIN3	19,57	18,75	24,56	24,12	PM
AT3G21220.1	MKK5	19,27	18,97	22,09	22,32	M
AT5G05590.1	PAI2	19,42	19,15	24,87	25,09	CH
AT5G09440.1	EXL4	25,24	25,02	19,79	19,67	EXTR
INTERACTION DEPENDENT DAPS						
ISOPRENE-SPECIFIC RESPONSE TO MILD WATER STRESS						
OSMOPROTECTANS AND REDOXHOMESOTASIS						
AT1G06410.1	trehalose-phosphatase/synthase 7	19,00	20,08	19,90	24,35	CYT
AT3G55610.1	P5CS2	19,19	19,71	19,17	23,63	CH
AT2G26230.1	urate oxidase	19,47	19,63	19,57	23,46	PEROX
AT1G75270.1	DHAR2	19,57	19,60	19,90	23,82	CYT
AT5G18100.2	copper/zinc superoxide dismutase 3	19,69	19,07	19,94	23,99	PEROX
AT2G22500.1	uncoupling protein 5	19,36	19,25	19,42	23,72	M
AT5G54430.1	PHOS32	18,73	19,19	19,15	24,90	CYT
AT3G13470.1	TCP-1/cpn60 chaperonin	19,50	19,53	19,74	24,61	CH
AT1G04980.1	PDIL2-2	19,73	19,67	19,70	23,81	ER
AT1G12010.1	ACO3	19,28	19,23	19,57	24,46	CYT
AT3G10130.1	| SOUL heme-binding	22,57	22,42	22,54	19,97	CH
AT1G21350.3	Thioredoxin	24,63	24,77	24,60	19,14	CH
DEFENSE						
AT1G02120.1	VAD1	19,43	19,27	20,15	23,46	ER
AT3G24550.1	PERK1	19,89	19,10	19,44	23,31	PM
AT2G44490.1	PEN2	25,43	25,46	25,24	19,17	PEROX
AT5G35620.1	Eukaryotic initiation factor 4E protein	22,71	22,42	22,83	19,45	N
AT1G55210.2	Disease resistance-responsive (dirigent-like protein)	26,56	27,01	26,22	19,19	EXTR
AT4G33500.1	Protein phosphatase 2C	23,74	24,36	19,39	19,44	CH
AT3G18165.1	MOS4	19,24	19,41	23,16	23,31	N
AT4G16990.2	RLM3	19,06	19,18	23,88	23,99	CYT
DAPS SIMILARLY ALTERED IN WT STRESSED AND ISOPRENE-EMITTING UNSTRESSED PLANTS						
CHLOROPLAST						
AT5G48790.1	low accumulation PSII protein	19,88	25,93	25,53	25,40	CH
AT1G32550.1	FdC2	19,46	24,59	25,10	25,43	CH
ATCG00150.1	ATPI	19,10	26,52	26,27	26,16	CH
ATCG00170.1	RPOC2	19,27	24,32	25,00	24,51	CH
CELLULAR SIGNALLING						
AT4G35860.1	RABB1B	19,36	25,16	24,88	25,04	CH
AT3G44340.2	CEF	18,58	23,89	24,11	23,62	CH

AT5G07340.1	Calreticulin	20,16	23,68	23,68	23,73	ER
AT4G29810.1	MKK2	19,86	24,85	24,85	25,01	PM
AT3G01090.3	KIN10	19,69	26,43	26,50	26,44	CYT
AT3G11660.1	NDR1/HIN1-like 1	19,53	25,04	24,85	24,76	PM
AT2G21600.1	RER1B	22,77	19,43	18,91	18,92	ER
AT5G65950.1	TRAPPC11	25,94	19,67	19,78	19,64	G
AT1G18210.2	Calcium-binding EF-hand family protein	25,17	19,71	18,87	19,17	CYT+
AT3G22370.1	alternative oxidase 1°	24,47	19,15	19,94	19,35	M
AT4G23150.1	CRK7	24,64	19,33	19,78	18,95	PM
AT1G49340.2	ATPI4K ALPHA	24,57	18,74	19,42	19,07	PM
AT1G76040.2	CPK29	23,33	19,21	19,06	19,52	CYT
DAPS ALTERED BY MILD DROUGHT STRESS IN WT BUT NOT IN TRANSGENIC ARABIDOPSIS						
CHLOROPLAST						
ATCG00520.1	YCF4	25,09	19,69	25,14	25,42	CH
AT3G48870.1	CLPC	23,60	19,54	23,88	24,02	CH
AT2G32480.1	ARASP	24,52	19,38	24,64	24,58	CH
AT1G06820.1	CCR2 carotenoid isomerase	23,56	19,14	23,45	23,59	CH
AT2G26540.1	UROS uroporphyrinogen-III synthase	24,52	19,72	24,65	24,39	CH
AT1G09940.1	HEMA2	19,63	27,04	19,62	19,30	CH
AT1G17050.1	SPS2 solanesyl diphosphate synthase 2	19,32	24,70	19,08	19,42	CH
ATCG00360.1	YCF3	19,06	26,08	19,62	19,70	CH
CELLULAR TRAFFICKING						
AT1G09210.1	CRT1b	19,79	25,33	19,33	19,02	ER
AT5G54750.1	Transport protein particle (TRAPP)	19,50	25,27	19,55	19,55	G
AT1G15130.1	Endosomal targeting BRO1-like domain-containing protein	24,95	19,48	25,02	24,90	ENDO
AT3G25220.1	FKBP15-1	25,23	19,64	25,56	25,56	ER
AT1G31730.1	Adaptin family protein	25,04	19,58	25,06	25,36	CYT,G
AT1G67930.1	Golgi transport complex protein-related	23,63	19,63	23,65	23,15	G
AT4G02350.1	SEC15B	23,32	19,59	23,63	23,13	CYT
AT3G46830.1	ATRABA2C	24,42	18,84	24,28	24,25	G-ENDO
AT5G35160.1	Endomembrane protein 70 protein	23,84	19,14	24,01	24,02	G
AT5G15970.1	KIN2	22,75	19,86	22,74	22,99	CYT
AT3G48170.1	ALDH10A9	24,82	19,46	25,68	25,71	PEROX
AT4G01850.2	SAM2	24,22	19,18	24,56	24,85	CYT
AT1G35670.1	CDPK2 calcium-dependent protein kinase 2	31,09	19,36	31,15	31,10	CYT
AT5G13710.2	SMT1	24,61	18,72	24,94	24,74	V
AT1G20050.1	HYD1	25,48	19,54	25,70	25,22	PM
AT1G71270.1	POK Vps52 / Sac2 family	19,78	26,21	19,59	18,87	G

***Suba CC legends**: CH, chloroplast; PEROX, peroxisome; PM, plasmatic membrane; G, golgi; CYT, cytosol; V, vacuole; M, mithocondria; ENDO, endosome; ER, endoplasmic reticulum; N, nucleus; EXTR: extracellular.

1. Genotype-dependent DAPS

Genotype-specific responses were shown in 78 DAPs (Table S3A). Differential accumulation of these proteins was exclusively caused by the acquired capacity to emit isoprene.

1.a Chloroplast-related proteins.

A large number of DAPs differently abundant in the isoprene-emitting and the non-emitting genotype were chloroplast-based and involved in chloroplast processes, primarily photosynthesis. Proteins accumulating in the ISPS genotype included one regulator of chloroplast movement (KCA1, AT5G10470.1); two enzymes respectively involved in the biosynthesis of xanthophylls (CYP97A3, AT1G31800.1) and flavonoids (Chalcone-flavanone isomerase, AT1G53520.1); Fe superoxide dismutase 1 (AT4G25100.5) which destroys superoxide anion radicals, toxic to biological systems (Dvořák et al. 2020). ALB3 (AT2G28800.4) which is involved in PSII assembly, by interacting with several PSII subunits as D1, D2 and CP43 (Schneider et al. 2014); the ATP-dependent zinc metalloprotease FtsH11 (AT5G53170.1). The latter is a zinc-containing metallo-endopeptidases essential for plant growth, with both chaperone and proteolytic functions, which, along DEG serine proteases, participates to photodamage repair cycle by accelerating the turnover of PSII reaction center protein D1 and cytochrome b_6f complex (Nishimura et al. 2017).

Other chloroplast genotype-dependent DAPs accumulating in ISPS plants are related to chloroplast import and synthesis processes, as co-chaperone HOP1 (AT1G12270.1), a HSP70-HSP90 organizing protein, which has a fundamental role in maintain the correct folding of the proteins transported to the chloroplast (Toribio et al. 2020), the ribosomal protein S19 (ATCG00820.1) and RPOB (ATCG00190.1), a plastid-encoded core subunits of a RNA polymerase active in green and non-green plastids at all stages of development and whose

transcriptional activity is affected by both endogenous and exogenous factors (Börner et al. 2015).

Overall, these results may indicate a modified composition of the photosynthetic antenna in isoprene-emitting plants and confirm positive correlation between isoprene emission and photosynthetic pigments (Behnke et al. 2007, Harris et al. 2016, Harvey and Sharkey 2016, Zuo et al. 2019), allowing better light capture and better photoprotection of photosynthesis. This could explain the stability of PSII quantum yield and of NPQ under stress conditions, observed here and often reported earlier (Pollastri et al. 2019).

It should be observed that the proteins found as differentially abundant in our study are not coded by the genes reported by Zuo et al. (2019) for ISPS-transgenic Arabidopsis plants. This indicate an even more complex impact of isoprene than hitherto evident.

1.b Membrane trafficking proteins.

In eukaryotic cells, endomembrane trafficking is vital for the physiological processes and, in plants, it is tightly related to stress tolerance, to meet the cell request of rapid molecular changes and to ensure the rapid delivery of stress-related cargo molecules (Wang et al. 2020b).

The results of the proteomic analysis highlighted that in the isoprene-emitting plants, pivotal proteins involved in different steps of membrane trafficking accumulated. This is the case of GET3A (AT1G01910.4) required for to the delivery to the ER; COG1 (AT5G16300.3), which mediates retrograde vesicular trafficking at the level of the Golgi apparatus, ensuring protein correct glycosylation, localization, and stability (Ungar et al. 2006, Blackburn et al. 2019, Linders et al. 2020); SNF7.1 (AT4G29160.3), a component of the ESCRT-III complex which is required for multivesicular bodies formation; CLUB/TRS130 (AT5G54440.1) and TRAPPC5 (AT5G58030.1), which are tether regulators of intracellular trafficking. Mutations in TRS130 cause very strong defects resulting in seedling lethality (Thellmann et al. 2010, Qi et al. 2011). The gene coding for GET3A was found to be over-expressed in the same Arabidopsis line by Zuo et al. (2019) (Supplementary Material).

1.c Cell signaling proteins.

Recent evidence indicates an important role of isoprene as a cellular signaling molecule (Zuo et al. 2019); our proteomic results confirm this role and reveal new implications.

BON2 (AT5G07300.1) over-accumulated in all ISPS samples. BON2 physically interacts with calcium pumps ACA8 and ACA10 in Arabidopsis and it has overlapping functions with BON1 and BON3 in regulating both the upstream osmotic stress responses (including Ca^{2+} signaling, and ABA accumulation), and the induction of downstream stress responsive genes (Chen et al. 2020a). Isoprene also induced changes in proteins involved in plant hormone signaling, namely: accumulation of the PIN3 protein (AT1G70940.1), an auxin transporter contributing to asymmetric auxin distribution for phototropic hypocotyl bending (Ding et al. 2011, Rakusová et al. 2016) and of the mitogen-activated protein kinase 5 (MKK5, AT3G21220.1) which regulates ABA in a MAPKKK20-MKK5-MPK6 cascade involved in stomatal response (Li et al. 2017); reduction of the EXORDIUM-like 4 protein (AT5G09440.1), with a role in a brassinosteroid-dependent regulation of plant growth and development (Schröder et al. 2011). Finally, phosphoribosyl anthranilate isomerase (AT5G05590.1) accumulated in ISPS-genotype. This enzyme catalyzes the third step in the biosynthetic pathway of tryptophan which is thought to play an important role as an inductive signal for osmotic adjustment, stomatal regulation and ROS scavenging under stress condition (You et al. 2019).

2. Treatment-dependent DAPS

In plants, the inhibition of metabolic processes is one of the primary detrimental effects of stresses. Accordingly, about 2/3 of the DAPs belonging to the T-list were less abundant under mild water stress with respect to normal growth conditions in both isoprene-emitting and non-emitting genotypes (Table S3B).

2.a Chloroplast-related proteins.

Chlorophyll biosynthesis is controlled by NADPH: protochlorophyllide oxidoreductase (POR) which expression under water stress is significantly down-regulated (Dalal and Tripathy 2012, Gabruk et al. 2015). Interestingly, the chaperone-like protein (CPP1, AT5g23040), required for POR stabilization (Lee et al. 2013) was less abundant under mild water stress. Moreover, we

observed a down-accumulation of K^+ efflux antiporter 3 (AT4G04850.2), which is localized in the thylakoid membrane and is involved in PSII quantum efficiency (Armbruster et al. 2016). On the other end, we observed enhanced accumulation of several chloroplast proteins known to be responsive to osmotic stress, among which HEMA1 (AT1G58290.1); or involved in the tetrapyrrole synthesis required for the chlorophyll biosynthesis (Turan and Tripathy 2015). Tetratricopeptide repeat (TPR)-like superfamily protein (AT3G53560.1) (Rosado et al. 2006, Haider et al. 2017) and Inositol monophosphatase (AT4G05090.1), acting in inositol signaling plays a crucial role in various aspects of plant stress adaptation (Jia et al. 2019).

2.b Stress proteins.

Besides acting on chloroplast proteins, mild water stress induced the accumulation of CML20 (AT3G50360.1) and 26S proteasome non-ATPase regulatory subunit 2 homolog B (AT4G28470.1) proteins. CML20 has been shown to be a fine regulator of Ca^{2+} and ROS signal pathways to regulate stomatal closure in Arabidopsis either exposed to exogenous ABA treatments or subjected to drought stress (Wu et al. 2017). The 26S proteasome is an ATP-dependent, multi-subunit protease complex that controls protein turnover and plays an essential role in responses to environmental stresses which generally induce an increase of misfolded or orphaned proteins. In particular, 26S proteasome non-ATPase regulatory subunit 2 homolog B seems to be important during abiotic stress responses (Wang et al. 2009).

ROF2 (AT5G48570.1) was the most reduced DAP in this list. ROF2 is a negative regulator for HSFA2 transcriptional activity (Meiri et al. 2010). Plant HSFs are key components of signal transduction which mediates the expression of genes responsive to various abiotic stresses (Guo et al. 2016).

2.c *Cell signaling proteins.*

Starch is a key molecule in mediating plant responses to abiotic stresses. Starch mobilization provides energy and carbon and the released sugars and other derived metabolites function as osmoprotectants and signaling molecules able to activate downstream components in the stress response cascade (Thalmann and Santelia 2017). Notably, we observed a lower accumulation of glucose-1-phosphate adenylyl transferase (AT4G39210.1), heteroglycan glucosidase 1

(AT3G23640.2) and plant neutral invertase (AT1G56560.1) and over-accumulation of beta-glucosidase 40 (AT1G26560.1) in both genotypes under WS conditions with respect to WW conditions.

Proteomic evidences seem also to indicate that mild water stress induced an hormonal remodulation which involves the downregulation of both 3-oxo-5-alpha-steroid 4-dehydrogenase (AT5G16010.1), acting in the early C-22 oxidation branch of brassinosteroid (BR) biosynthesis (Fujioka et al. 2002) and auxin transport protein (AT3G02260.1), required for auxin efflux and polar auxin transport.

Compelling evidence indicates that BRs play a prominent role in controlling the balance between normal and drought-adapted growth, but, although an antagonistic role has been shown between ABA and BR, the complexity of BR-mediated responses to water stress has not yet been fully understood (Planas-Riverola et al. 2019, Wang et al. 2020a). The interdependent and often synergistic action of auxin and BRs pathways has been reported, occurring through both transcriptional regulation of common target genes and upstream connection involving calcium-calmodulin and phosphoinositide signaling (Halliday 2004, Hardtke et al. 2007).

3. DAPS dependent on genotype–treatment interaction

3.1 Several I-dependent DAPs represent the isoprene-specific response to mild water stress

In the I-list, 81 proteins were found to accumulate or be reduced in ISPS WS plants with respect to all the other condition tested (ISPS WW, WT WS and WT WW). These proteins represent the specific impact of isoprene-water stress interaction (Table S3C).

3.1.a Stress proteins.

Osmotic stress triggers the accumulation of osmo-protectants that stabilize and protect biological structures from damage and may function as potent signaling molecules and ROS scavengers. Proteins known to be involved in the synthesis of these osmo-related metabolites accumulated in this subset of the I-list. Among them, two ABA-dependent proteins, trehalose-phosphatase/synthase 7 (AT1G06410.1) which catalyzes the synthesis of trehalose 6-phosphate (Li et al. 2011) and Δ1-pyrroline-5-carboxylate synthetase 2 (AT3G55610.1), the rate-limiting

enzyme in proline biosynthesis (Qamar et al. 2015). Consistently, the levels of free proline and trehalose increased significantly in ISPS WS plants with respect to the other treatments (Fig. 5). Proline and trehalose accumulations are well-known plant physiological responses to water stress (Nathalie and Christian 2008, Redillas et al. 2012). Proline act as a stabilizer for cellular structures reducing damage to photosynthetic apparatus (Matysik et al. 2002, Rontein et al. 2002). The simultaneous increase of proline and ABA content found in isoprene-emitting plants under mild drought stress confirm the observed link between these molecules (Strizhov et al. 1997, Abrahám et al. 2003). Trehalose is a compatible solute that plays its protectant role mainly stabilizing dehydrated enzymes and lipid (Li et al. 2011, Shafiq et al. 2015). Moreover, in addition to its osmoprotective roles, proline and trehalose are free-radical scavengers able to buffer cellular redox potential altered by stress (Türkan and Demiral 2009, Fernandez et al. 2010, Trouvelot et al. 2014).

These findings support the hypothesis that isoprene-emitting plants have a prompter response to drought stress with respect to non-emitting plants. This confirms that isoprene can prime defensive secondary metabolism also inducing synthesis of osmoprotective compounds that protect plants under stress condition(Pollastri et al. 2021).

Also, urate oxidase (AT2G26230.1) followed the same trend as the two previous enzymes. Urate oxidase catalyzes the oxidation of uric acid to 5-hydroxyisourate and is further processed to form allantoin, which has been reported to activate ABA production (Watanabe et al. 2014, Kaur et al. 2021). We found that ISPS plants under stress conditions produced significantly more ABA than all other plants. The observed interaction of isoprene with ABA signaling is very interesting, as ABA is formed by oxidative cleavage of xanthophylls formed in the MEP pathway that also produce isoprene. Indeed, a correlation between ABA and isoprene has been reported (Barta and Loreto 2006) and isoprene has been hypothesized to interact with several hormones made by MEP thus regulating leaf senescence (Dani et al. 2016). Isoprene may simply proxy ABA, but it may also compete for substrates with ABA, as both compounds are formed by the same methylerythritol phosphate (MEP) pathway in chloroplasts. This explains further results indicating that ABA increases when isoprene is reduced by severe water stress (Tattini et al. 2014). In any case, our results strengthen the idea that isoprene is an important mediator of stress hormones, perhaps even deploying a hormonal action by itself (Pollastri et al. 2021).

It is an established notion that increasing ABA content in leaves induces stomatal closure thereby reducing water loss in water-stressed leaves (Jones and Mansfield 1970, Wilkinson and Davies 2002). This is however not the case with our plants where gs was never statistically different across specimens and treatments, irrespective of ABA level. ABA conjugates (e.g. ABA-GE) are unable to affect stomata (Dietz et al. 2000) and plants able to maintain unchanged their apoplastic pH are also poorly affected by ABA (Schurr and Schulze 1995). Causes that might uncouple ABA increase and gs reduction have been reviewed by Wilkinson and Davies (2002). Perhaps isoprene emission only proxies ABA foliar content but this is not in the active form for stomatal closure to occur or is not located at the guard cell where actively controls stomatal closure. ABA induces NO and H_2O_2 synthesis and all three cooperate to induce stomatal closure (Bright et al. 2006). However, isoprene removes NO and ROS [reviewed by Pollastri et al. (2021) and further discussed below and this might also have lessened stomatal response to increasing ABA in water stressed ISPS plants. Finally, ABA is not the only factor involved in stomal closure. Stomata may also close passively in response to reduction of the vapor pressure difference between the leaf and air (Merilo et al. 2018). As we have maintained the vpd constant along foliar gas-exchange measurements, this might have also temporarily counteracted stomatal closure otherwise occurring in water-stressed plants.

Water stress induces the production of ROS resulting from impaired efficient use of light energy by electron transport. The antioxidant action of isoprene was shown by early work (Loreto and Velikova 2001), and direct reaction between isoprene and singlet oxygen was in particular demonstrated (Velikova et al. 2004). Our proteomic characterization confirmed that isoprene modulates the oxidative load under mild water stress. In fact, specific to ISPS WS condition, eight proteins involved in redox homeostasis significantly changed. DHAR2 (AT1G75270.1), copper/zinc superoxide dismutase 3 (AT5G18100.2), uncoupling protein 5 (AT2G22500.1), PHOS32 (AT5G54430.1), TCP-1/cpn60 chaperonin (AT3G13470.1) accumulated, while PDIL2-2 (AT1G04980.1), SOUL heme-binding (AT3G10130.1) and thioredoxin (AT1G21350.3) were reduced. It is known that ethylene mediates hormone and redox signaling processes under abiotic stress conditions (Dietz et al. 2010). Data indicate the accumulation of 1-aminocyclopropane-1-carboxylate oxidase 3 (ACO3, AT1G12010.1), which controls ethylene production in ISPS plants (Houben and Van de Poel 2019).

3.1.b Defense.

Plants must cope simultaneously with multiple stresses and elaborate stress responsive networks with frequent cross-talks between metabolites improving abiotic stress tolerance and disease resistance. Five defense-responsive proteins known to increase their expression under pathogen attack were found to be altered (more or less accumulated) in ISPS plants.

VAD1 (AT1G02120.1), involved in ethylene-dependent cell death control (Khafif et al. 2017), and proline-rich extensin-like receptor kinase 1 (PERK1, AT3G24550.1), which is induced by wounding (Silva and Goring 2002), accumulated exclusively in ISPS WS plants. Other proteins like the Eukaryotic translation initiation factor isoform 4E (AT5G35620.1), essential for the resistance against some viruses (Schmitt-Keichinger 2019), the dirigent-like protein 20 (AT1G55210.2) involved in pathogen response in various plant species (Paniagua et al. 2017) and PENETRATION 2 (PEN2, AT2G44490.1), essential for callose deposition and glucosinolate activation during pathogen-triggered resistance (Clay et al. 2009), were less accumulated in ISPS WS plants.

Finally, it should be observed that, in ISPS plants, the protein phosphatase 2C (AT4G33500.1), which negatively correlates with immunity to bacterial pathogens, was reduced, while MOS4 (AT3G18165.1), essential for plant innate immunity, and disease resistance protein (RLM3, AT4G16990.2), important for the defense against necrotrophic fungi, accumulated with respect to WT. The activation of a large group of disease-protection related proteins seems indicate that, when elicited by an abiotic stress, isoprene-emitting plants can also be primed against possible incoming biotic stresses (Pollastri et al. 2021), as further discussed below.

3.2 Several I-dependent DAPs are similarly altered in WT stressed plants and in isoprene-emitting unstressed plants

This subset of the I-dependent DAPs includes drought-specific proteins whose abundance is affected by isoprene even under unstressed conditions. Isoprene seems able to prime the defense system of plants, activating, under yet unstressed growing conditions, signaling pathways which help making plants more and better responsive to mild drought stress and, unexpectedly, to biotic stresses.

3.2.a Chloroplast proteins.

In this subset we found chloroplast-related proteins that accumulated in WT plants after mild stress and in all isoprene-emitting plants. Among these: Low PSII Accumulation protein (AT5G48790.1), FdC2 (AT1G32550.1) which regulates the Iron Stress Induced protein in turn protecting PSI (Kroh and Pilon 2020); ATPase complex CF0 (ATPI, ATCG00150.1), which plays a direct role in the translocation of protons across the thylakoid membrane; and the RNA polymerase subunits RPOC2 (ATCG00170.1) which is involved in chloroplast DNA replication and protein synthesis.

3.2.b Membrane trafficking proteins.

Cellular trafficking is another biological process affected at the same degree in stressed WT and in isoprene-emitting unstressed plants. In this I-dependent subgroup we found pivotal proteins involved in all the different steps of the membrane trafficking: Ras-related protein RABB1b (AT4G35860.1), CEF (AT3G44340.2), Calreticulin family protein (AT5G07340.1) and MAP kinase kinase 2 (MKK2, AT4G29810.1) that regulates MPK6 and MPK4 in response to cold and salt stresses, were over-accumulated in respect of unstressed WT; endoplasmic reticulum retrieval protein 1B (RER1B, AT2G21600.1), a cis-Golgi protein responsible for retrieving a subset of ER membrane proteins from the Golgi to the ER (Sato et al. 1999), TRAPPIII complex protein (TRAPPC11, AT5G65950.1) involved in regulation of endosomal function (Rosquete et al. 2019), calcium-binding protein (AT1G18210.2), RECEPTOR-like protein kinase 7 (CRK7, AT4G23150.1) and ATPI4K ALPHA (AT1G49340.2) were instead down-accumulated.

3.2.c Cell signaling proteins.

Fluctuations in sugar levels are specific signals for metabolic responses, although the exact mechanisms of how different sugar levels are perceived are not yet completely understood. KIN10 (AT3G01090.3), one of the three glucose-modulated master regulators, belong to this subset of I-dependent proteins. KIN10 (whose activity is repressed by glucose) and TOR kinase (which on the contrary is activated by glucose) govern the transcriptional networks related to metabolite signaling tightly connected with glycolysis and mitochondrial bioenergetics. KIN10

controls the expression of thousands of genes involved in a wide spectrum of cellular functions as signaling, transcription, anabolism, catabolism, transport, development, and stress adaptation (Baena-González et al. 2007).

The reduced accumulation of two proteins whose gene expression is ABA-repressed, mitochondrial alternative oxidase 1A (AOX, AT3G22370.1) and leucine-rich repeat proteins CPK29 (AT1G76040.2) whose gene is ABA-repressed in guard cells (Giraud et al. 2009, Wang et al. 2011), and the accumulation of NDR1/HIN1-like 1 (AT3G11660.1) which plays an important role in the abiotic stresses-induced ABA signaling and biosynthesis (Bao et al. 2016) indicate that isoprene influences ABA metabolism and action even in unstressed conditions, ABA is indeed slightly (but not significantly, at least with the low number of replicates used in our experiment) higher in well-watered ISPS with respect to well-watered WT, again confirming the proposed direct control of isoprene on ABA proposed earlier in this paper and experimentally reported by Barta and Loreto (2006).

3.3 Several I-dependent DAPs are altered by mild water stress in WT but not in ISPS Arabidopsis

These I-dependent DAPs include proteins which are affected by the stress but not in water-stressed isoprene-emitting plants.

3.3.a Chloroplast-related proteins.

Following the mild water stress, several chloroplast proteins were less abundant in WT, but not ISPS Arabidopsis. Among them: YCF4 (ATCG00520.1) which controls the assembly of the PSI subunits and is a major mediator of the PSI–LHCI assembly process (Nellaepalli et al. 2018); the chaperone protein CLPC (AT3G48870.1); ARASP protease (AT2G32480.1) essential for chloroplast development (Bölter et al. 2006); carotenoid isomerase (CCR2, AT1G06820.1); Uroporphyrinogen-III synthase (UROS, AT2G26540.1) which catalyzes cyclization of the linear tetrapyrroles to uroporphyrinogen III, a precursor of tetrapyrroles such as chlorophyll, heme and phycobilins (Tan et al. 2008). Other chloroplast proteins showed an opposite trend: Glutamyl-tRNA reductase family protein (HEMA2, AT1G09940.1) involved in supply of heme for extraplastidic factors associated with defensive functions (Nagai et al. 2007), solanesyl

diphosphate synthase 2 (SPS2, AT1G17050.1) which contributes to the production of plastoquinone and plastochromanol that act as protectant against photooxidative stress (Block et al. 2013); YCF3 (ATCG00360.1) which is involved in PSI assembly and is present in protein complexes that are associated with the thylakoid membrane (Krech et al. 2012). Overall, this pattern again can be interpreted as a consequence of isoprene a) mitigating stress occurrence and b) priming a mild increase of defenses that may help readily respond to upcoming stresses.

3.3.b Membrane trafficking proteins.

In this group, several proteins involved in cellular trafficking and accumulated in WT plants grown in stress conditions, while their abundance remained unaffected in the ISPS genotype, both grown in control and in water stress conditions. Belonging to this group are: calreticulin 1b (CRT1b, AT1G09210.1), a chaperone promoting folding, oligomeric assembly and quality control in the ER and mitigating biotic and abiotic stresses in plants (Joshi et al. 2019); Transport Protein Particle component (TRAPPC3, AT5G54750.1); BRO1 (AT1G15130.1) participating to pre-vacuolar compartment/multivesicular body biogenesis and maturation in plant cells (Hu et al. 2020); FKBP15-1 (AT3G25220.1). Moreover, proteins involved in the antero- and retro-grade targeting from TGN to endosomal-lysosomal system show the same behavior: the AP-4 complex subunit epsilon (AT1G31730.1), a subunit of a novel type of clathrin- or non-clathrin-associated protein coat; Vacuolar protein sorting-associated protein 52 A (AT1G71270.1) which facilitate tethering as well as SNARE complex assembly at the Golgi (Vukašinović and Žárský 2016), Golgi transport complex protein (AT1G67930.1), Sec15b (AT4G02350.1), ATRAB2C (AT3G46830.1) and Endomembrane protein 70 (AT5G35160.1), whose function in the endosomal pathway has not yet clarified (Heard et al. 2015).

3.3.c Stress proteins.

In this I-dependent subset, two enzymes involved in earlier steps of phytosterol biosynthesis and precursors of BRs showed reduced accumulation in WT WS plants but not in ISPS plants, regardless of the presence of stress: the sterol methyltransferase 1 (SMT1; AT5G13710.2) a major rate-limiting step in the sterol biosynthetic pathway (Shi et al. 2012) and the HYDRA1 (HYD1; AT1G20050.1) which encodes a Δ^8-Δ^7sterol isomerase, responsible for converting 4α-

methylfecosterol to 24-methylenelophenol; *hydra* mutants of Arabidopsis are defective in sterol profiles (Schrick et al. 2002, Souter et al. 2002).

BRs are known to regulate and maintain the photosynthetic activity by counteracting the oxidative stress generated by abiotic environmental stresses (Hasan et al. 2011, Li et al. 2015, Shu et al. 2016). Isoprene priming of BRs is a novel result that could also help explain better photosynthetic efficiency in ISPS plants, especially after mild water stress.

CONCLUSIONS

It is confirmed that isoprene exerts a protective action against stresses, reducing the impact of water stress on photosynthesis. The extensive proteomic analysis performed on ISPS-transgenic Arabidopsis under both normal and mild water stress conditions narrows down the candidate proteins responsible for the observed phenotypic changes, and overall confirms recent findings that isoprene is a molecule that perturb plant metabolism at multiple scale (Harvey and Sharkey 2016, Zuo et al. 2019), rather than having a single action as antioxidant or membrane protector (Loreto and Velikova 2001). This also goes beyond the "single biochemical mechanism for multiple physiological stresses" proposed by Vickers et al. (2009).

More in detail, the analysis highlights some major trends related to the expression of the ISPS gene in *Arabidopsis*. The first trend is a large reshaping of chloroplast proteome in isoprene-emitting plants, further amplified under water stress, and possibly inferring a priming action on defensive metabolism, beside the well-acknowledged direct antioxidant action. The second trend encompasses processes related to cell signaling, which strengthens current perception that isoprene largely interacts with hormones, and especially with those synthesized in the MEP pathway (cytokinins, beside ABA) (Dani et al. 2016). Proteomic analysis identified new molecular players in this scenario. The third trend reveals a so far overlooked link between isoprene and cellular trafficking. Perhaps this is a consequence of isoprene large positioning into membranes, where it improves membrane properties under physiological and stressful conditions (Pollastri et al. 2019), and perhaps also regulates movement of molecules and solutes.

SUPPLEMENTARY INFORMATION

Supplementary Figures

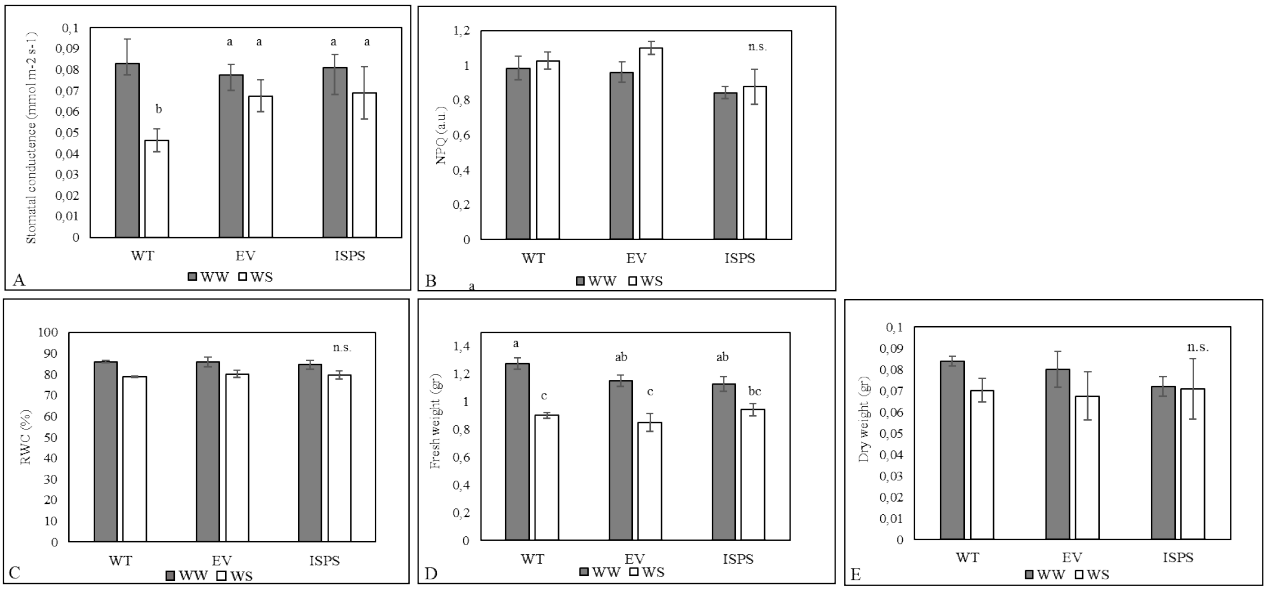

Fig. S1. Stomatal conductance (A), Non-photochemical quenching of chlorophyll fluorescence (NPQ) (B), Relative Water Content (RWC) (C), Fresh weight (D) and dry weight (E) of wild-type (WT), empty vector (EV), and isoprene-emitting (ISPS) plants in well-watered (WW, grey bars) and water-stressed (WS, white bars) conditions. Means $\pm$ SE (n = 5) are shown. One-way ANOVA followed by Tukey's test was performed to statistically separate means. Means significantly different ($p < 0.05$) are represented by different letters.

A

	WTww1	WTww2	WTww3	WTww4	WTws1	WTws2	WTws3	WTws4	ISPSww1	ISPSww2	ISPSww3	ISPSww4	ISPSws1	ISPSws2	ISPSws3	ISPSws4
WTww1	1	0,98926	0,987225	0,987536	0,841699	0,841275	0,836453	0,842681	0,833486	0,837898	0,831827	0,833956	0,841291	0,835514	0,835751	0,838278
WTww2	0,98926	1	0,986509	0,985923	0,83925	0,838262	0,831866	0,83839	0,830249	0,834154	0,828391	0,8303	0,837904	0,829894	0,833231	0,834166
WTww3	0,987225	0,986508	1	0,983479	0,836778	0,836962	0,832246	0,837308	0,828362	0,833692	0,828463	0,830537	0,834085	0,826768	0,831462	0,832531
WTww4	0,987536	0,985923	0,983479	1	0,840183	0,838749	0,837509	0,843437	0,830551	0,837465	0,831695	0,832859	0,837188	0,835147	0,833056	0,839363
WTws1	0,841699	0,83925	0,836778	0,84018	1	0,984725	0,98794	0,988646	0,836958	0,841134	0,838028	0,840342	0,849665	0,848737	0,850348	0,850883
WTws2	0,846453	0,831866	0,832246	0,837509	0,98794	1	0,987268	0,987268	0,838061	0,843234	0,841531	0,84323	0,846133	0,850286	0,848894	0,851268
WTws3	0,842681	0,83839	0,837308	0,843437	0,988646	0,983683	1	0,986126	0,839148	0,844437	0,838672	0,842118	0,850729	0,848547	0,850501	0,853522
WTws4	0,841275	0,838262	0,836962	0,838749	0,984725	0,986126	0,983683	1	0,831522	0,835046	0,829468	0,834704	0,84445	0,840961	0,846518	0,847283
ISPSww1	0,831827	0,828391	0,828463	0,831695	0,838028	0,829468	0,841531	0,838672	1	0,988718	0,988718	0,987187	0,845814	0,847327	0,844893	0,843919
ISPSww2	0,837898	0,834154	0,833695	0,837465	0,841134	0,835046	0,843234	0,844437	0,986895	1	0,987187	0,987432	0,852256	0,849304	0,847924	0,846953
ISPSww3	0,833956	0,8303	0,830537	0,832859	0,840342	0,834704	0,84323	0,842118	0,987742	0,987432	1	0,988378	0,848507	0,848256	0,846944	0,845039
ISPSww4	0,833486	0,830249	0,828362	0,830551	0,836958	0,831522	0,838061	0,839148	0,988378	0,987742	0,986895	1	0,853471	0,849837	0,848862	0,848545
ISPSws1	0,838278	0,834166	0,832531	0,839363	0,850883	0,847283	0,851268	0,853522	0,848545	0,846953	0,843919	0,845039	1	0,985703	0,985858	0,985858
ISPSws2	0,835751	0,833231	0,831462	0,833056	0,850348	0,846518	0,848894	0,850501	0,848862	0,847924	0,844893	0,846944	0,986936	1	0,986579	0,986936
ISPSws3	0,831291	0,837904	0,834085	0,837188	0,849665	0,84445	0,846133	0,850729	0,853471	0,852256	0,845814	0,848507	0,986579	0,985939	1	0,985703
ISPSws4	0,835514	0,829836	0,826768	0,835147	0,848737	0,840961	0,850286	0,848547	0,849837	0,849304	0,847327	0,848256	0,983037	0,983037	0.9859387	1

B

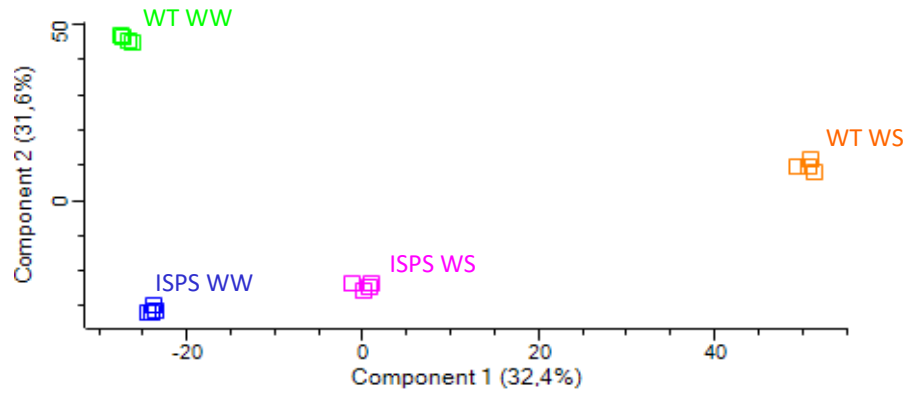

Fig. S2 Validation of HPLC-MS/MS data. (A) Pearson's correlation of proteomes from different sample groups. (B) Principal component analysis of the proteomic data. Numbers in parentheses represent the percentage of total variance explained by the first and second principal component.

Supplementary data[2]

Table S1 Total proteins identified by LC-MS-MS in isoprene-emitting (ISPS) and non-emitting (wild-type, WT) *Arabidopsis thaliana* plants subjected to a water stress (WS) and well-watered (WW) conditions.

Table S2 List of Differentially Abundant proteins (DAPs) divided in significant comparisons emerged from one-way ANOVA and Tukey test (FDR <0.01). Log_2 Fold-change (Log_2 FC) and imputation values are also listed.

[2] Supplementary tables are available in the "Supplementary data_Chapter two" folder

Table S3 Lists of genotype-dependent (G), treatment-dependent (T) and genotype-treatment interaction (I)-dependent Differentially Abundant Proteins (DAPs). Log_2 Fold-change (Log2 FC) values, MapMan Bins, Subcellular localization, and clusters are also listed.

CHAPTER THREE

VOLATILOME AND PROTEOME RESPONSES TO *COLLETOTRICHUM LINDEMUTHIANUM* INFECTION IN MODERATELY RESISTANT AND SUSCEPTIBLE BEAN GENOTYPE[1]

Plants respond to stress with changes in the blend of volatile organic compounds (VOCs) they emit into the atmosphere. The main functions of this 'volatilome' are signalling and defence, with targets of signalling comprising distal parts of the same plant, other plants, and beneficial arthropods and microorganisms, while defence is achieved via VOCs with repellent, insecticidal, antibacterial or antifungal effects. Here we focus on the putative roles of VOCs in the resistance to a hemibiotrophic fungal pathogen. We analysed the changes in the volatilome and proteome of a susceptible and a moderately resistant genotype of common bean, *Phaseoulus vulgaris L*., challenged with *Colletotrichum lindemuthianum*, the causal agent of fungal anthracnose. Our results indicate differences at both proteome and volatilome levels between the two genotypes, before and after the infection, and possibly different strategies of defence. The moderately resistant genotype contrasted pathogen infection, invasion and replication mainly by maintaining epidermal and cell wall structure, and probably also by reducing stomatal gas-exchanges. The susceptible genotype did not limit early stages of pathogen infection. Rather, this genotype activated a wide range of defensive biochemical responses, involving release of VOCs and induction of hypersensitivity, as indicated by enhanced synthesis of Green Leaf Volatiles (GLVs) and salicylic acid (SA). Proteomic investigation provided a general framework for these evidences, whereas observed changes in the volatilome suggested that VOCs may principally represent stress markers rather than defensive compounds *per se*.

[1] This chapter has been submitted as:

Mancini I, Maurilia M.M., Gualtieri L., Domingo D., Beccaccioli M., Heil M., Bracale M., Loreto F., Ruocco M. Volatilome and proteome responses to *Colletotrichum lindemuthianum* infection in moderately resistant and susceptible bean genotype

INTRODUCTION

Common bean (*Phaseolus vulgaris* L.) is an important staple crop all over the world, with high nutritional value in terms of proteins, minerals and fibers. Beans are the primary source of protein for humans in many developing countries (Castro-Guerrero et al. 2016, Myers and Kmiecik 2017, Rendón-Anaya et al. 2017). The production, yield and quality of beans are affected by many pathogens, among which fungal anthracnose is one of the most destructive, causing up to 90% potential yield losses, especially under cool and humid environmental conditions (Sharma et al. 2008, Bardas et al. 2009). The causal agent of anthracnose is the fungus *Colletotrichum lindemuthianum* (Sacc. & Magnus), a hemibiotrophic pathogen which can be transmitted *via* infested seeds or soil. *C. lindemuthianum* conidia can be dispersed by wind and rainfall and can also germinate on leaf surface to directly infect the aerial parts of the plant. Upon entering the plant, first *C. lindemuthianum* establishes a biotrophic infection and subsequently switches to the necrotrophic phase. Induced cell death generates phenotypically visible disease symptoms in the form of necrotic lesions on stems, leaves, pods and seeds (Mohammed 2013).

During bean-*C. lindemuthianum* coevolution, the pathogen evolves a great pathogenic variability making most of the cultivated varieties susceptible, though with intraspecific variability. To date, more than 182 races of the pathogen have been identified worldwide (Padder et al. 2017) and it has been verified that the resistance of most bean cultivars follows the gene-for-gene (R/Avr) model, also known as race-specific resistance (Flor 1955). Most recently, Mungalu et al. (2020) identified 14 quantitative trait loci (QTL) for resistance to nine races of *C. lindemuthianum*.

Plant-pathogen interactions are driven by an intense molecular "dialogue" between the two organisms, aiming at each one survival. Besides r-gene mediated race-specific resistance, plants possess an innate immune system that senses herbivore- or pathogen-associated molecular patterns (HAMPs/PAMPs), in turn activating secondary signals and generating pattern-triggered immunity (PTI) (Jones and Dangl 2006). In addition, upon damage, plants recognize endogenous molecules like self-DNA as damage-associated molecular patterns (DAMPs) (recently reviewed by Tanaka and Hel (2021b). During the initial phase of PTI, DAMPs, HAMPs and PAMPs trigger conserved early secondary signals, such as reactive oxygen species (ROS) and mitogen-activated protein kinases (MAPKs) (Boller and Felix 2009, Hou et al. 2019, Albert et al. 2020, Fichman and Mittler 2020). Subsequently, enemy-specific responses are orchestrated by hormones such as ethylene (ET), jasmonic acid (JA) and salicylic acid (SA). In most cases, chewing herbivores and necrotrophic pathogens trigger a JA-dependent 'wound response', while

sap-sucking insects and biotrophic pathogens trigger a SA-dependent 'systemic acquired resistance' (SAR), which usually is characterized by the induction of a hypersensitive reaction (HR) and of pathogenesis-related (PR) proteins with direct antimicrobial activities such as chitinases and glucanases (Pieterse et al. 2012, Campos et al. 2014, Klessig et al. 2018, Ding and Ding 2020). The two pathways that are controlled by SA and JA are frequently subjected to a negative trade-off, with the consequence that hemibiotrophic pathogens represent notoriously difficult cases for plants to control. An analysis of the transcriptomic response of common bean to *C. lindemuthianum* infection reported an upregulation of cytokinin and ET responses, while JA, gibberellin, and abscisic acid responses were down-regulated (Oblessuc et al. 2012). However, several studies reported that treatments with PAMP-mimic compounds such as chitosan, or with benzothiadiazole (BTH), a chemical analogue of SA, or with SA itself, induced resistance in common bean to pathogens, including *C. lindemuthianum* (De Meyer et al. 1999, Siegrist et al. 2000, Bigirimana and Höfte 2002, Iriti and Faoro 2003, Di Piero and Garda 2008, Quintana-Rodriguez et al. 2015).

Plants respond to abiotic and biotic stress with significant changes in the blend of volatile organic compounds (VOCs) that are emitted from the vegetative aerial parts and roots into the atmosphere and rhizosphere, respectively. Since the first reports on talking trees and the plants ´'cry for help' (Baldwin and Schultz 1983, Rhoades 1983, Dicke and Sabelis 1988), signalling and resistance induction have been confirmed as the main functions of stress-induced plant VOCs. Their biological targets of stress-induced VOCs range from the distal parts of the same plant, neighbouring plants, as well as beneficial and detrimental arthropods and microorganisms, with effects that range from the induction of transcriptional or behavioural changes to insecticidal, antibacterial or antifungal effects (Heil 2014, Ameye et al. 2018b, Turlings and Erb 2018, Hammerbacher et al. 2019) (Fig. 1).

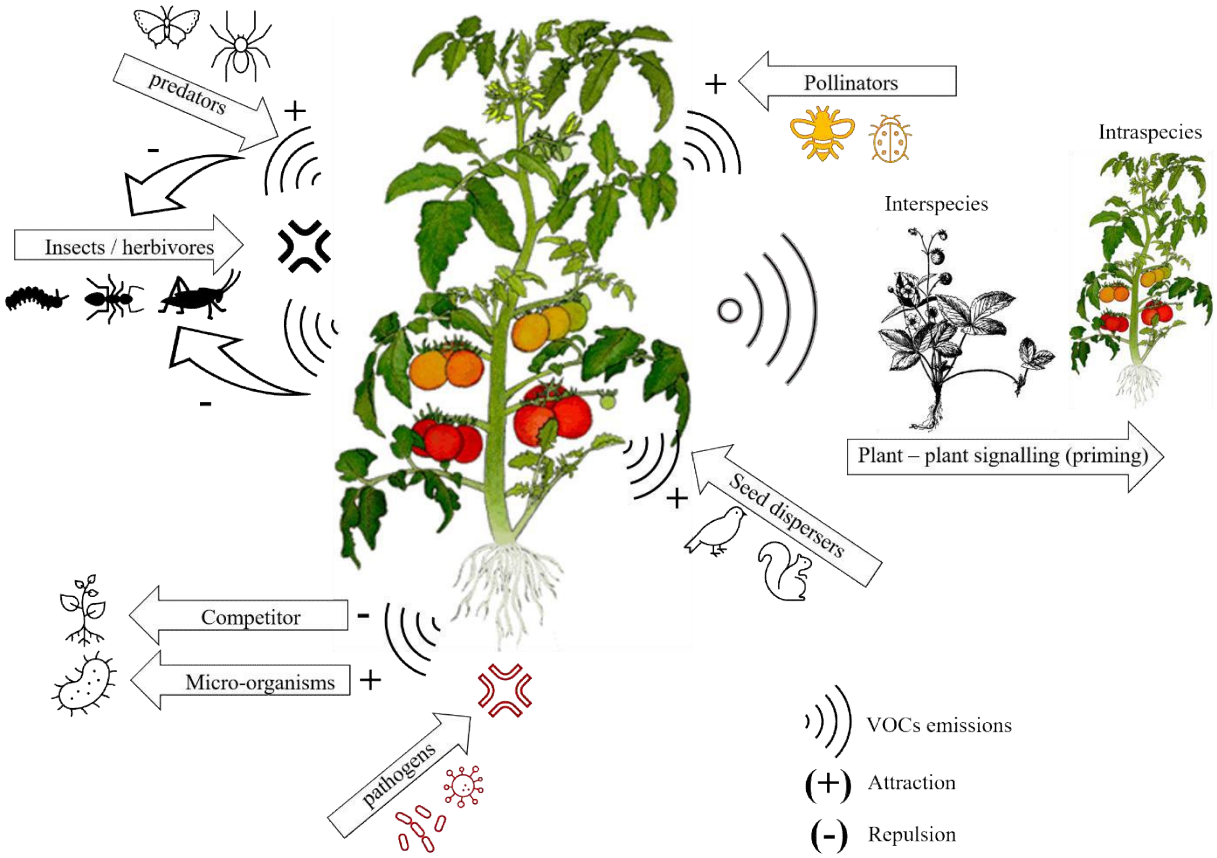

Fig. 1 Scheme for the effects of VOCs emitted in response to biotic factors.

The complete blend of VOCs – the so-called 'volatilome' - can be composed of hundreds of compounds from diverse structural classes, although they are predominantly derived from four major biosynthetic pathways: the shikimate/phenylalanine, the mevalonic acid (MVA), the methylerythritol phosphate (MEP) and the lipoxygenase (LOX) /oxylipin pathway (Dudareva et al. 2004, Dudareva et al. 2013, Scala et al. 2013, Ameye et al. 2018b). Interestingly, the same compound can play multiple roles.

For example, indole, a common herbivore-induced benzoxazinoid in the Gramineae, primes the expression of defence genes in maize but also exerts toxic effects on herbivores (Veyrat et al. 2016). The antioxidant effects of isoprene (C_5H_8), a small lipophilic product of the 2-C-methyl-D-erythritol 4-phosphate (MEP) pathway, have been attributed to direct reactions with reactive oxygen species as well as the strengthening of membranes, but isoprene also acts as a signal that

primes plants genes involved in the protection of oxidative stress (Pollastri et al. 2021). Finally, cis-2-hexen-1-ol, trans-2-hexen-1-al and *cis*-3-hexenyl acetate and other C6-alcohols, aldehydes and esters (so-called green leaf volatiles, GLVs), the C_9 aldehyde nonanal and methyl jasmonate (MeJA), are generated in wounded plant tissue via oxylipin pathway, i.e. by the oxygenation of fatty acids and well known for their role as signals that trigger resistance gene expression (Kishimoto et al. 2005, Matsui 2006, Shiojiri et al. 2006, Scala et al. 2013, Ameye et al. 2018b, Wasternack and Feussner 2018), but the same compounds also inhibit the growth of plant pathogenic fungi (Scala et al. 2013, Ameye et al. 2018a, Quintana Rodríguez et al. 2018).

However, as compared to the intensive research into the synthesis and functions of herbivore-induced VOCs, relatively little research efforts focused on the role of VOCs in the resistance of plants to microbial pathogens (Hammerbacher et al. 2019). Moreover, classical approaches focused on individual compounds that exhibit a significant increase in their emission rate in response to a defined challenging event; an approach that is likely less suitable for plant-pathogen interactions (Ameye et al. 2018b). First, volatilomes are composed of complex blends of numerous molecules with different sizes, structures and properties and synergistic interactions have been reported in particular for their antimicrobial effects (Bisignano et al. 2001). Second, bacteria and fungi emit complex volatilomes themselves, basically to achieve the same functions and partly comprising the same individual compounds (Lemfack et al. 2014, Schmidt et al. 2016, Quintana Rodríguez et al. 2018, Garbeva and Weisskopf 2019). For example, the 'biocontrol' properties of the endophytic bacterium *Pseudomonas chlororaphis* strain PA23 and of various strains of the fungal genus *Trichoderma* could be attributed to antifungal effects of nonanal emitted by these microorganisms (Athukorala et al. 2010, Lee et al. 2016). Likewise, several C6 alcohols and aldehydes, monoterpenes, sesquiterpenes and even the volatile ester of salicylic acid (methyl salicylate, MeSA, - a hormone that controls plant resistance to biotrophic pathogens - has been reported as fungal VOCs (Lee et al. 2016, Li et al. 2016). Therefore, a certain compound emitted from an infected plant could be a part of the plant´s defence response as well as a microbial weapon (Lee et al. 2016). Third, co-called 'compatible' interactions between a pathogen and a susceptible plant host are frequently leading to a systemic infection, which means that the pathogen once it has entered its host continuously grows into the newly formed organs; a biological system in which the time point of challenge does not allow to define a clear time 'point' of infection.

In all cases, VOCs seem to help plant self-defense through a range of molecular and physiological mechanisms that are not fully elucidated. Interest in using VOCs as a sustainable defense strategy with applications in agro-ecology is rising (Brilli et al. 2019). Production and roles of plant VOCs in response to mechanical wounding by herbivores have been extensively investigated for many cultivated species (Bricchi et al. 2010, Coppola et al. 2017, Portillo-Estrada et al. 2021). Hundreds of examples of direct interactions between plants and their host insects have been described, where VOCs act either as repellents or as attractive cues (Holopainen and Gershenzon 2010). VOCs may also contribute to plant-pathogen dialogues. However, knowledge about VOC induction and modulation during a plant-pathogen interaction is limited (Steindel et al. 2005), and studies of bean-*Colletotrichum* interaction are scarce. Studies reported that common bean and lima bean (*Phaseolus lunatus*) plants exhibit primed resistance to pathogens ,including *C. lindemuthianum*, after the exposure to VOCs that had been emitted by infected conspecific plants (Yi et al. 2009, Girón-Calva et al. 2012, Quintana-Rodriguez et al. 2015), similarly as it had been reported earlier for the induction of JA-dependent resistance responses in bean by diverse VOCs (Heil and Bueno 2007, Jewell and Tanaka 2019). In particular, two individual VOCs, nonanal and MeSA, primed the expression of PR proteins.

The induction of JA-dependent resistance responses in bean by diverse VOCs was also reported (Heil and Kost 2006, KOST and Heil 2006, Heil and Bueno 2007, Jewell and Tanaka 2019, Tanaka and Heil 2021a). Moreover, many VOCs that are emitted from resistant plants exert direct antifungal effects and their absorbance to plant surfaces has been discussed as an additional mechanism of VOC-mediated phenotypic resistance (Quintana-Rodriguez et al. 2018, Camacho-Coronel et al. 2020). Very recently, the terpenoid volatile (E)-nerolidol has been recognized as inducer of defenses both against insects (*Empoasca onukii*) and the pathogen *Colletotrichum fructicola* in tea plants (Chen et al. 2020b).

To date few proteomic data on bean-*Colletotrichum* pathosystem have been reported. Borges *et al.* (2015) detected, by using two-dimensional electrophoresis coupled with Mass Spectrometry, differentially accumulated proteins (DAPs) in inoculated leaves of *Colletotrichum*-resistant bean plants related to photosynthesis, carbon metabolism, antioxidant systems, defense and stress response, chaperones and folding catalysts, and phenylpropanoid or flavonoid biosynthesis.

All available evidence indicates that JA- and SA-dependent components of classical PTI could contribute significantly to the resistance of bean to *C. lindemuthianum*. Nevertheless, most of the researches on this topic have been performed by using targeted approaches, i.e. they focused

on molecules and genes that *a priori* were likely to play a role in this context (Sicard et al. 1997, Kelly and Vallejo 2004, Campa et al. 2009, Campa et al. 2017).

The aim of our present study was to employ a non-targeted comparative approach to improve our understanding of the role of VOCs in fungus-plant interaction and identify proteins involved in plant resistance. We used a Proton Transfer Reaction-Quadrupole ion guide (Qi) -Time of Flight - Mass Spectrometry (PTR-QiTOF-MS) to explore the volatilomes and HPLC-MS-MS to explore the proteomes in two cultivars of common bean plants with different levels of resistance against *Colletotrichum lindemuthianum* isolate 1088.

MATERIALS AND METHODS

Plant material and treatments

We selected two genotypes of bean (*Phaseolus vulgaris* L.) with different levels of resistance to anthracnose, and for which earlier studies reported an inducible phenotypic response. Seeds of the commercial cultivar Flor de Junio Marcela (FJM) and of the landrace Negro San Luis (NSL), as well as *C. lindemuthianum* isolate 1088 spore stock, were obtained from the Departemento de Ingenieria Genética CINVESTAV – Unidad Irapuato, GTO Mexico. While FJM exhibits moderate level of resistance to *C. lindemuthianum*, the NSL landrace is highly susceptible to the fungal infection (Castellanos-Ramos et al. 2003, Quintana-Rodriguez et al. 2015). Hereinafter, we use (R) to refer to the moderately resistant FJM and (S) to refer to the susceptible NSL genotype.

The conidial suspension of *C. lindemuthianum* was prepared as described by Quintana Rodriguez et al. (2015) and suspended in distilled water with 0.1% Tween (Sigma, St. Luis, MO, USA), adjusting concentration to 1×10^7 conidia mL^{-1} by using a Burker counting chamber.

Seeds were sterilized in 1% bleach solution for 20 min, washed five times with sterile distilled water and stored on a sterile wet paper sheet at room temperature in the dark until primary root emersion (3 days). Once germinated, seeds were immerged in *C. lindemuthianum* conidial suspension for 5 min and then sowed in non-sterile commercial soil. Four seeds were sown in each pot, for a total of 20 plants *per* each of the four conditions tested: susceptible not infected (S-), susceptible infected (S+), resistant not infected (R-) and resistant infected (R+). To avoid any possible airborne interaction, plants of the four treatments were grown in separate rooms of the greenhouse, at 25 ± 2 °C and under 16 h light/8 h dark photoperiod for 21 days after sowing

(das). At that time, disease severity was assessed by counting necrotic lesions; statistical differences among R+ and S+ were evaluated by Student's t-test ($p < 0.05$).

PTR-QiTOF-MS parameters

All the measurements of VOCs were performed by using a commercial PTR-QiTOF-MS instrument (PTR - ToF 8000, Ionicon Analytik GmbH, Innsbruck, Austria) with H_3O^+ as reagent ion for the proton transfer reaction (O_2^+ signal intensity was ca. 0.5% of the H_3O^+). The instrument was set to a drift-tube pressure of 2.30 mbar, drift temperature of 80 °C, and drift voltage of 480 V, which resulted in electric field strength to number density ratio E/N of 111 Townsend (Td, 1Td = 10−17 V cm^{-2}).

Plants VOC measurements

VOC measurements were performed on plants at 21 das. The experimental station for VOC collection consisted of two chambers, 60 cm^3 each, made of inert materials (glass and steel) and directly connected to the PTR-QiTOF-MS entry port. A flow of clean air (11 L min^{-1}) was generated from a pump (ABAC Silent LN HP2, ABAC Torino, Italia) connected to a hydrocarbon trap (Supelco Supelpure HC, Sigma Aldrich). The clean air flux stabilized the air background (blank) in the empty chamber. Blank measurements were performed after 30 min of continuous air flux. Then, the chambers were quickly opened, and five pots per each tested condition (S-; S+; R-; R+) were moved in and measured in each recording session separately. Measurements were performed in Head Space condition, after 30 min of VOC accumulation within the sealed chamber. Each session consisted of three 600 s-long VOC measurements. Three technical and three independent biological replicates were carried out for each condition.

PTR-QiTOF-MS data analysis

The raw data were acquired by the TOFDAQ Viewer® software (Tofwerk AG, Thun, Switzerland) and evaluated with the PTR-MS Viewer 3.3.8. For peak quantifications, ion count rate was directly converted into a concentration unit (ppb) by using the transmission tool of the PTR-VIEWER v3.3 tool. To guarantee high mass accuracy, the calibration of PTR spectra was performed on three points calibration using m/z =21.022 (H_3O^+), m/z 330.848 (internal gas standard 1,3-diiodobenzene) and m/z =203.943 (a fragment of 1,3-diiodobenzene). Peaks below

5 cps threshold (count per second signal from the ion detector, raw signal) were discarded as noise background.

The peaks associated with the PTR-QiTOF-MS ion source including those ascribed to water chemistry or other interfering ions e.g., m/z = 32 (O_2^+), m/z=31.022 (NO^+), m/z= 37 and m/z= 39.033 (corresponding to $H_3{}^{18}O^+$ and water cluster ions H_2O-$H_3{}^{18}O^+$, respectively) were removed. Blank measurements on the empty system were run before every experiment and used for background subtraction. After blank subtraction, concentration values (ppb, 10^{-9}) were normalized on fresh plant weights (FW). After filtering, 69 mass peaks were obtained and subjected to statistical analysis.

VOC statistical analysis

Samples normalization and all statistical analyses were carried out on Metaboanalyst online platform (Chong et al. 2018). Before statistical analysis, data were transformed with Log_{10} function and auto scaled. Principal component analysis (PCA) was carried out for the initial exploration of the data set ensuring an objective and unsupervised analysis. Subsequently, two-way analysis of variance (ANOVA) followed by Tukey's test for multiple comparisons was performed on VOC data to identify significant differences (p <0.05) and to examine the influence of the two different categorical independent variables (genotype G, and *Colletotrichum* infection C) and their interaction (I) on VOC emission. We additionally performed the hierarchical clustering of statistically significant VOCs to better visualize the data (Euclidean distance, Ward D clustering algorithm).

Extraction and analysis of fatty acids, salicylic acid and of 13-LOX derived oxylipins

Analysis of SA, oxylipins and fatty acids (FA) was performed as reported previously (Beccaccioli et al. 2021), grinding 20 mg of lyophilized bean leaves in presence of liquid nitrogen and extracting with 750 µL of methanol–water–acetic acid (90:9:1, v/v/v) in presence of the internal standard 1-naphthaleneacetic acid (NAA MW 186.21 g mol^{-1}) at final concentration of 5 µM. Extraction was repeated and the supernatant was collected and dried by nitrogen flow. Extract was resuspended in 100 µL of water–acetonitrile (85:15, v/v) and 0.05% of acetic acid. Analysis was conducted by HPLC-MS-MS Agilent 6420 (Agilent Technologies, Santa Clara, CA, USA) and chromatographic separation was performed with a Zorbax ECLIPSE XDB-C18 rapid resolution HT 4.6 × 50 mm 1.8 µm p.s. column (Agilent Technologies, Santa Clara, CA,

USA) at room temperature;10 µL of extract were analysed. The chromatographic separation was performed in presence of the mobile phases (A: water/acetonitrile 97:3 v/v containing 0.1% formic acid; B: acetonitrile/isopropyl alcohol 90:10 v/v).

For SA, the elution gradient was: 0–3 min 15% B, 3–5 min 100% B, 5–6 min 100% B, 6–7 min 15% B, and 7–8 min 15% B. The gradient was followed by 5 min (15% B) for re-equilibration. The constant flow-rate was 0.6 mL min^{-1}. The column temperature was set at 25°C.

For oxylipins (13-hydroperoxy-9,11-octadecadienoic acid - 13-HpODE –, 13-hydroxy-9,11,15-octadecatrienoic acid - 13-HOTrE- and 13-hydroxyoctadecadienoic acid - 13-HODE) and fatty acids (linoleic acid - C18:2- and gamma linolenic acid - C18:3) the elution gradient was: 0–2 min 80% A and 20% B, 2–4 min 65% A 35% B, 4–6 min 60% A and 40% B, 6–7 min 58% A and 42%, 7–9 min 52% A and 48% B, 9–15 min 35% A and 65% B, 15–17 min 25% A and 75% B, 17–18.50 min 15%A and 85% B, 18.50–19.50 min 5% A and 95% B, 19.50–24 min 5% A and 95% B, 24–26 min 1% A and 99% B, 26–30 min 1% A and 99% B, 30–34 min 80% A and 20% B. The flow rate was: 0–24 min at 0.6 mL min^{-1}, 24–30 min at 1 mL min^{-1}, 30–34 min at 0.6 mL min^{-1}. The column temperature was set at 50°C. Metabolites were analysed by negative ion mode electrospray ionization (ESI); SA and oxylipins by multiple reaction monitoring (MRM), while the FA by single ion monitoring (SIM). Characteristic SIM parameters and MRM transition are reported in Supplementary Table S1.

Protein extraction

Proteins were extracted from 0.5 g (FW) of 21-days old leaves by SDS/phenol method (Wu et al. 2014). Briefly, leaves were ground in liquid nitrogen and homogenized with extraction buffer (0.15 M Tris – HCl pH 8.8, 1% SDS, 1 mM EDTA, 0.1 M DTT, 2 mM PMSF, 0.1 mg/ml Pefabloc, 1:1000 Protease Inhibitor). After centrifugation, 1:1 volume of phenol saturated with 0.1 M Tris-HCl was added to the supernatant phase. Phenolic phase was collected and overnight precipitated with four volumes of 0.1 M ammonium acetate in methanol at −20°C. The precipitate obtained by centrifugation at 15.000 *g* for 10 min at 4°C was washed twice with cold 0.1 M ammonium acetate and finally with cold 80% acetone. Pellet was dried and resuspended in 100 µL of SDS-lysis buffer (20% SDS w/w, 0.25 M Tris-HCl pH 7.5, 100 mM DTT).

The proteins were quantified by the 2- D Quant-kit (GE Healthcare). All chemicals were purchased by SIGMA. Five independent biological replicates were performed for each sample.

Trypsin digestion

Samples (150 μg of proteins) were trypsin-digested by using FASP (Filter Aided Sample Preparation) method (Wiśniewski 2016). Briefly, protein extracts were heated for 5 min at 95°C, ten times diluted with UA buffer (8 M urea in 100 mM Tris-HCl, pH 8.0) and transferred to the Amicon Ultra-0.5 Centrifugal Filter Unit.

The denaturation buffer was replaced by washing three times with UA buffer and proteins were alkylated using 50 mM iodoacetamide in UA for 15 min at room temperature and in the dark. The excess of alkylation reagents was eliminated by washing four times with ABC buffer (50 mM NH4HCO3). Proteins were digested with trypsin in ABC buffer (enzyme-to-substrate of 1:100 w/w ratio) overnight, at 37 °C. The digested peptides were eluted by centrifugation. Peptide concentrations were spectrophotometrically measured, assuming that solution of proteins with a concentration of 1 mg/mL determines an absorbance of 1.1 at 280 nm.

The peptides were finally desalted onto C18 Oasis-HLB cartridges and dried down for further analysis.

HPLC-MS-MS analysis and elaboration of raw data

The tryptic peptides were analysed by Liquid Chromatography with tandem mass spectrometry (HPLC-MS-MS) in a Q-Exactive mass spectrometer as described in (Garcia-Seco et al. 2017). Mass spectrometer raw files were processed by using MaxQuant V1.5.3.3, (http://www.coxdocs.org/doku.php?id=maxquant:start); annotation of proteins was obtained by searching MS/MS spectra against *Phaseolus vulgaris* L. (30554 entries (Uniprot database, downloaded December 2020). The raw data obtained as output from MaxQuant ("ProteinGroups" files) were processed for identification as described in (Paradiso et al. 2020). Protein annotation was performed using default MaxQuant parameters. A false discovery rate (FDR) of 1% was accepted for both peptide and protein identification. The mass spectrometry proteomics data were deposited in the ProteomeXchange Consortium via the PRIDE (Perez-Riverol et al. 2019) partner repository with the dataset identifier PXD025070 using the following reviewer account details: Username, reviewer_pxd025070@ebi.ac.uk Password: RR9cX8Om.

Quantitative proteome analyses of the filtered data were carried out on the Perseus software platform (V1.5.8.5, ttp:// www.perseus-framework.org). Log_2 transformed Label Free Quantitation (LFQ) intensities of protein groups were centred by subtracting the median of the entire set of protein groups LFQ intensities per sample (column).

Statistical and bioinformatic analyses of proteome changes

In order to analyse the proteins changes in relative abundance among treatments, fold changes ratio expressed as Log_2 FC were assessed on Perseus platform. Transformed, centred, and normalized Log_2 LFQ data were subjected to both one-way and two-way ANOVA, based on multiple-sample tests with an FDR cut-off of 0.05 and on the Benjamini-Hochberg correction. Two-way ANOVA was performed to directly link the influence of genotype (G), treatment (*Colletotrichum* infection, C), or the interaction between them (I) on the *P. vulgaris* proteome. Perseus software platform was also used for Principal Component Analysis (PCA) in order to assess the quality of our datasets.

For the annotation of the uncharacterised proteins in *P. vulgaris* and the bioinformatic analysis, a BLAST search was made against *Arabidopsis thaliana* TAIR10 (The Arabidopsis Information Resource) protein database using the online BLAST search tool in Phytozome V12.1 (https://phytozome.jgi.doe.gov/pz/portal.html) taking as valid the hits with the highest sequence similarity (expressed in percentage) and lowest e-value with respect to the target sequence.

The AGI (Arabidopsis Gene Identifiers) codes relative to each protein and percentage of similarity were included in two-way ANOVA results. Functional classification and subcellular localization were assigned using MapMan and SUBA4 tools (https://suba.live/) (Hooper et al. 2017), respectively.

Protein–protein interactions Network and identification of hub Proteins

Using STRING (http://string-db.org/) (Szklarczyk et al. 2015), a biological database and web resource for known and predicted protein–protein interactions (PPIs), we developed networks of DAPs from G-, C- and I- lists. Parameters used included a minimum required interaction score > 0.4 (medium confidence) and only connected proteins being displayed. Cytoscape software (Doncheva et al. 2018) was applied to visualize the protein interaction relationship network and identify those proteins, hereafter defined as hub proteins, with many interaction partners. After importing the data into Cytoscape and running the CytoHubba application, the top 20 proteins were evaluated by the five calculation methods (Degree, EPC, EcCentricity, MCC and MNC). The intersecting proteins obtained using Venn plot (http://www.interactivenn.net), represent key candidate with important biological regulatory functions.

RESULTS

Disease symptoms

The first disease symptoms were observed on the hypocotyls at 7 das (days after sowing); prior to that time, we did not observe any differences between treatments. At 21 das, the phenotypic disease levels of S+ plants (quantified as number of necrotic lesions/plant) were significantly higher in respect of R+ plants (Fig. 2). Furthermore, S+ plants exhibited higher incidence of symptoms on hypocotyls and leaves than R+ plants (Fig. 3).

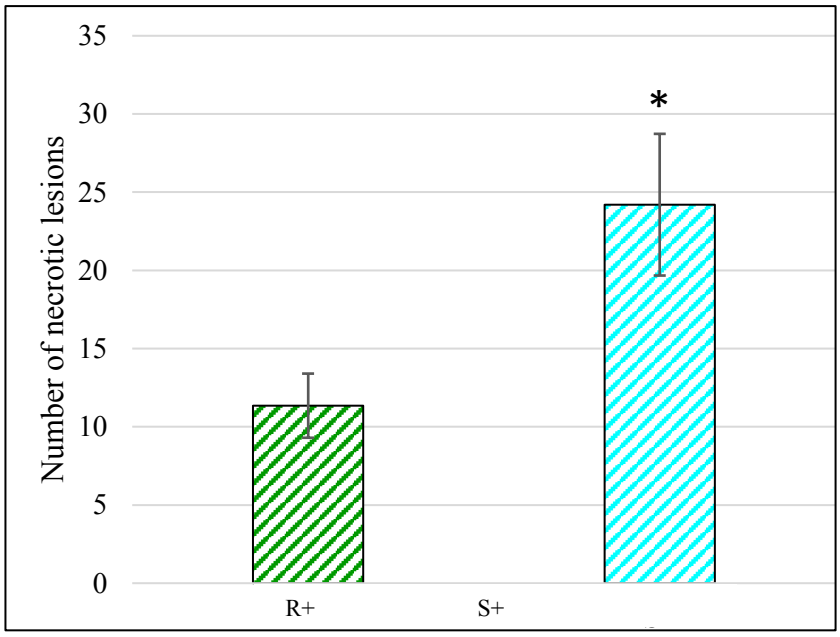

Fig. 2 Number of necrotic lesions at 21 das on Flor de Junio Marcela (moderately resistant, R+) and Negro St. Luis (susceptible, S+) plants challenged with *C. lindemuthianum*. Asterisk above the S+ bar indicates significant difference with R+ (Student's t-test, $p < 0.05$).

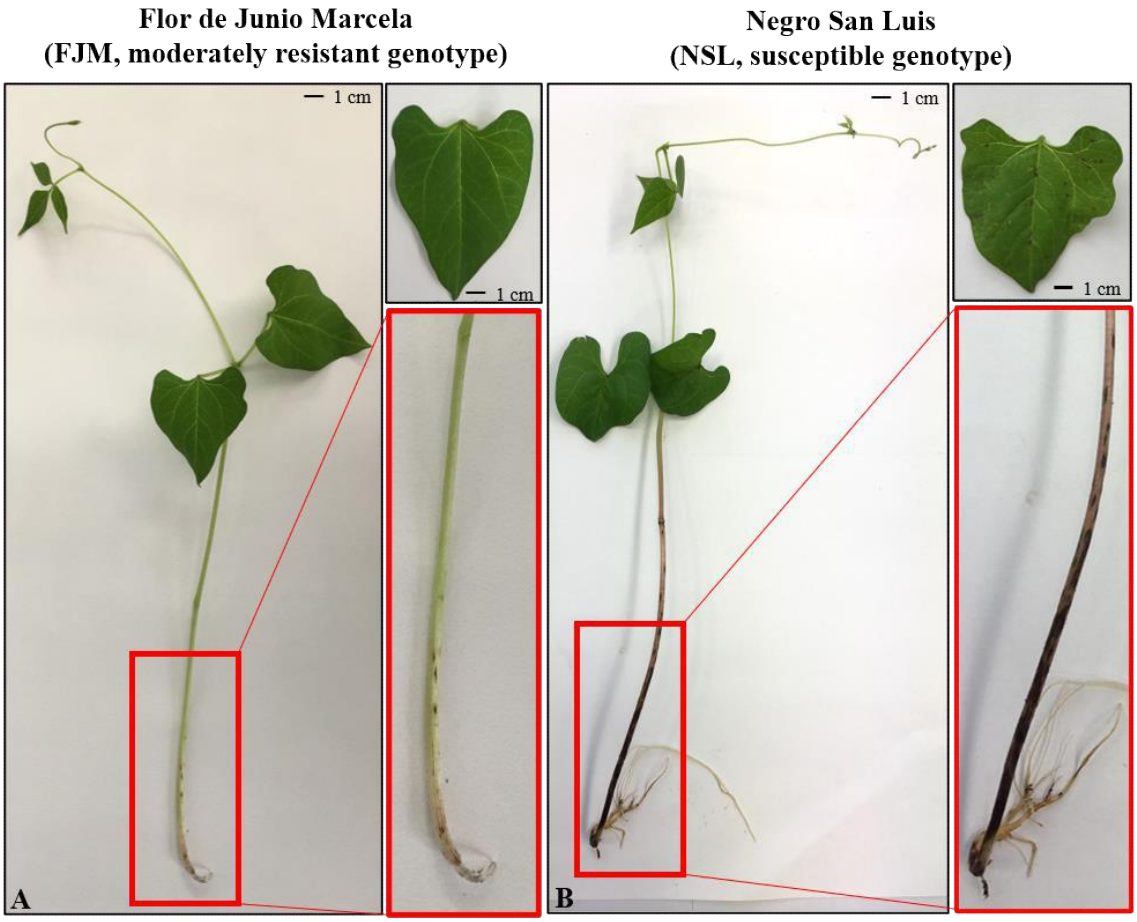

Fig. 3 Anthracnose symptoms on stems and leaves of (A) Flor de Junio Marcela (moderately resistant, R) and (B) Negro St. Luis (susceptible, S) plants at 21 das.

Volatilome analysis

In terms of overall fluxes, R- plants emitted a significant higher amount of VOCs (5.13 ppb g^{-1}fw) than R+ (3,65 ppb g^{-1}fw). S- (3,97 ppb g^{-1}fw) and S+ (3,98 ppb g^{-1}fw) VOC emissions were similar to R+. After threshold filtering and blank subtraction, 69 mass peaks were obtained (Supplementary Dataset 1), on which statistical analysis was performed. These peaks putatively identified according to available data in literature and/or with genuine standards.

In order to estimate the degree to which the common bean volatilome is determined by genotype and treatment, we applied a PCA which revealed a clear separation of the four conditions and, in particular, a separation of the volatilome emitted from control (-) versus infected (+) S plants

(Fig 4). The first three principal components (PC1, PC2 and PC3) explained the 85.5% of the total variance (Fig.4A, B). The genotype effect was described by PC2 (13.1% of total variance, Fig. 4A), while the PC1 and PC3 described the treatment effect on both genotypes (Fig. 4B). Two-way ANOVA analysis identified 10, 24 and 6 VOCs dependent on genotype (G), treatment (*Colletotrichum* infection, C) and interaction (I), respectively (Supplementary Table S2). The larger number of C-dependent VOCs suggests that the pathogen influences VOCs more than the genotype, while the I factor seems to have a limited additional effect on the volatilome (Fig. 5).

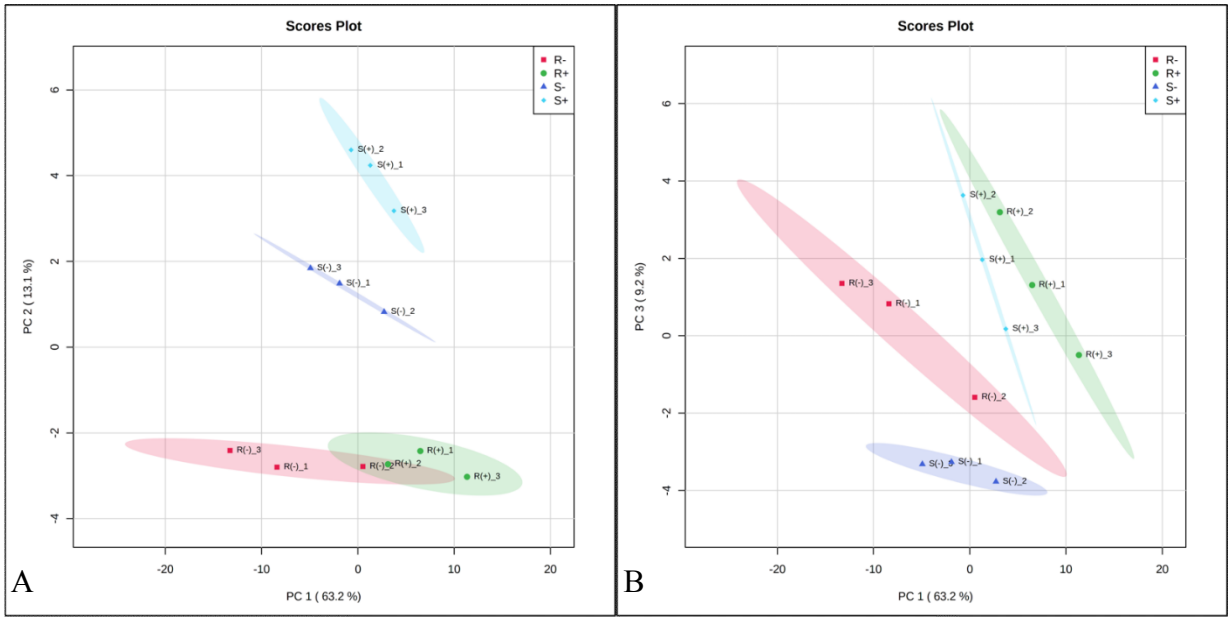

Fig. 4 Principal component analysis (PCA; Metaboanalyst V5.0) of PTR-MS TOF data about volatile organic compound (VOC) blends. Samples were collected from three biological replicas of moderately resistant controls (R-, red), moderately resistant infected plants (R+, green), susceptible controls (S-, blue) and susceptible infected plants (S+, light blue). The percentage of variance explained by each component is reported in brackets.

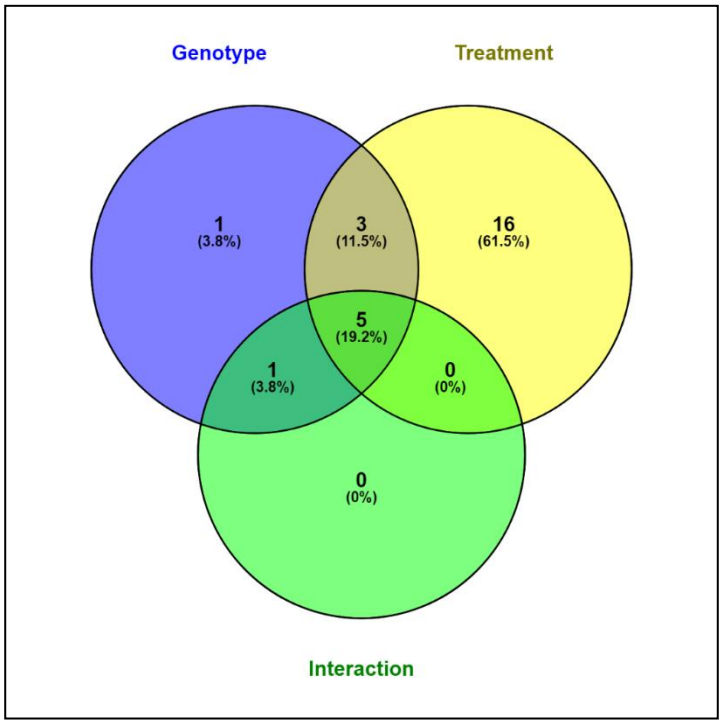

Fig. 5 Venn diagram (from VENNY V2.1) highlighting the distribution of the identified VOCs, in genotype, treatment (*Colletotrichum* infection), or interaction-dependent groups, based on a two-way ANOVA test ($p < 0.05$; Metaboanalyst V5.0).

The differential effect of genotype and treatment on the abundance of VOCs emitted was displayed as heatmap (Fig. 6), which shows that among the I-dependent VOCs hexanal (m/z 101.089) was released by S- in higher amounts in respect of R- plants. However, the differential emission of hexanal is more evident once the two genotypes were infected with *C. lindemuthianum* (Fig. 7E).

Allene or 1,2-propadiene (m/z 41.039), also an I-dependent VOC, was emitted only by R- plants.

Among the G-dependent VOCs, 2-Cyclopenten-1-one (m/z 83.048) showed a trend similar to hexanal, by increasing from S- to S+ and decreasing from R- to R+ plants (Fig. 7F).

Finally, among the C-dependent VOCs, ethanol (m/z 47.049) decreased in both R and S when challenged with *C. lindemuthianum*.

As displayed in the heatmap, five VOCs were over-emitted and 14 less-emitted in S+ in respect of S- plants; comparing R+ and R-, we identified four over-emitted and 19 less-emitted VOCs in R+ plants (Fig. 6). In particular, 2-butanone (MEK, m/z 73,064), benzaldehyde (m/z 79.053) and p-cymene fragment (m/z 93,067) showed similar expression pattern in R and S samples, as their emission was stimulated upon infection. The alkyl fragment instead, also termed butene, (m/z 57.069) was more emitted only in S+ vs S- while dimethyl trisulphide (m/z 126.968) was more emitted only in R+ vs R-. Among the VOCs inhibited by the infection, the butane-2.3-dione emission (m/z 87.0434) was particularly affected in both S+ and R+ plants.

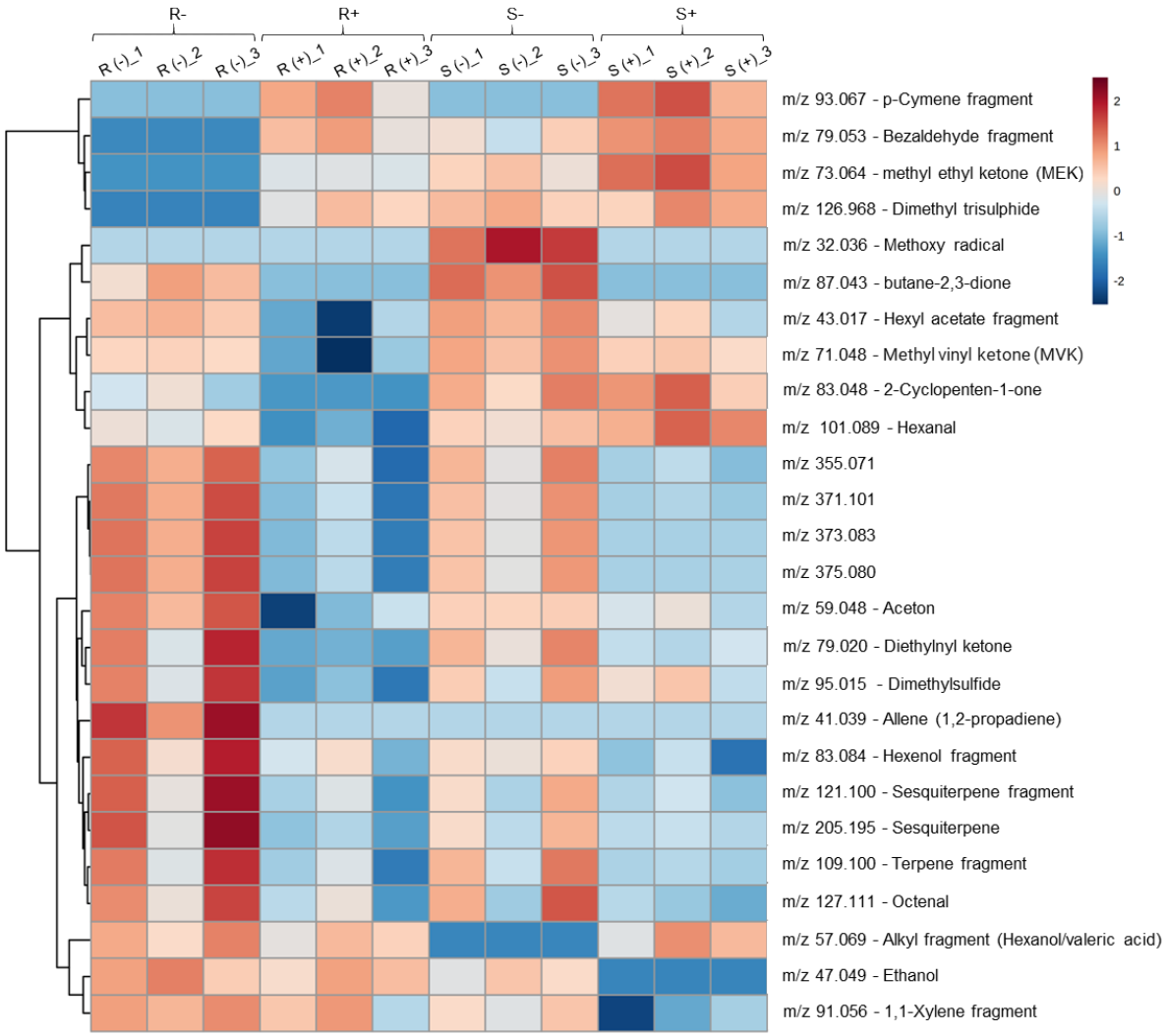

Fig. 6 Heatmap of significantly abundant VOCs ($p < 0.05$; Metaboanalyst V5.0) emitted by moderately resistant (R) and susceptible (S) genotypes in control (-) and infected (+) conditions. VOCs are grouped according to abundance similarity due to both genotype and treatment effects; the abundance of VOCs emitted is described by the colorimetric scale, shading from blue (less abundant VOCs) to red (more abundant VOCs).

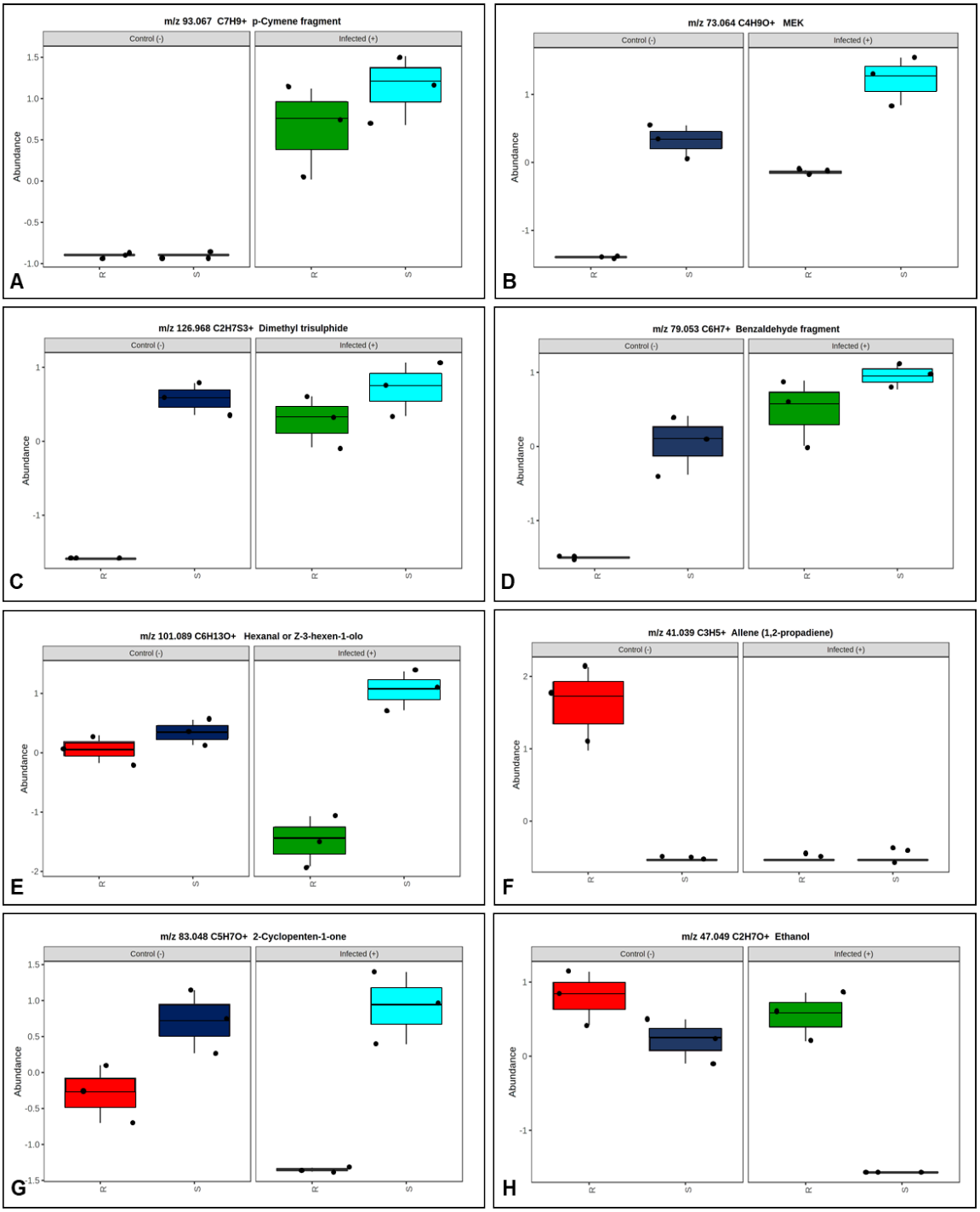

Fig. 7 Graphical representation of abundance of some statistically significant VOCs, identified by two-way ANOVA, emitted by moderately resistant (R) and susceptible (S) genotypes in control (-) (coloured in red and blue, respectively) and infected (+) (coloured in green and light blue, respectively) conditions. p-Cymene (A), methyl-ethyl-ketone (MEK) (B), dimethyl trisulphide (C), benzaldehyde fragment (D), hexanal or Z-3 hexen-1-ol (E), allene (1,2-propadiene) (F), 2-cyclopenten-1-one (G) and ethanol (H) (False discovery rate adjusted value $p< 0.05$). Abundance values refers to Log_{10} transformed and auto-scaled ppb g^{-1} fw values (Metaboanalyst V 5.0).

SA and JA precursors analyses

Results of the HPLC assays are reported in Fig. 8. SA was significantly more abundant in S+ than in all other treatments (Fig. 8A), whereas 13-LOX derived oxylipins (C18:3, C18:2) and octadecenoics polyunsaturated fatty acids were triggered in R+ only (Fig. 8B, C). Intriguingly, no trivial oxylipin precursor (e.g., 13-HpOTrE) nor even JA itself were found in our samples. Intriguingly, linolenic acid as well as some oxylipins formed by 13-LOX activity [e.g., 13-HpODE and the 13-HpOTrE reduced form 13-HOTrE (peroxidised forms of PUFA can be either spontaneously or enzymatically reduced in the cascade HpOTrE→HOTrE→oxoTrE (Beccaccioli et al. 2019)] were differently abundant in R+ and S+ (Figs. 8 D-E).

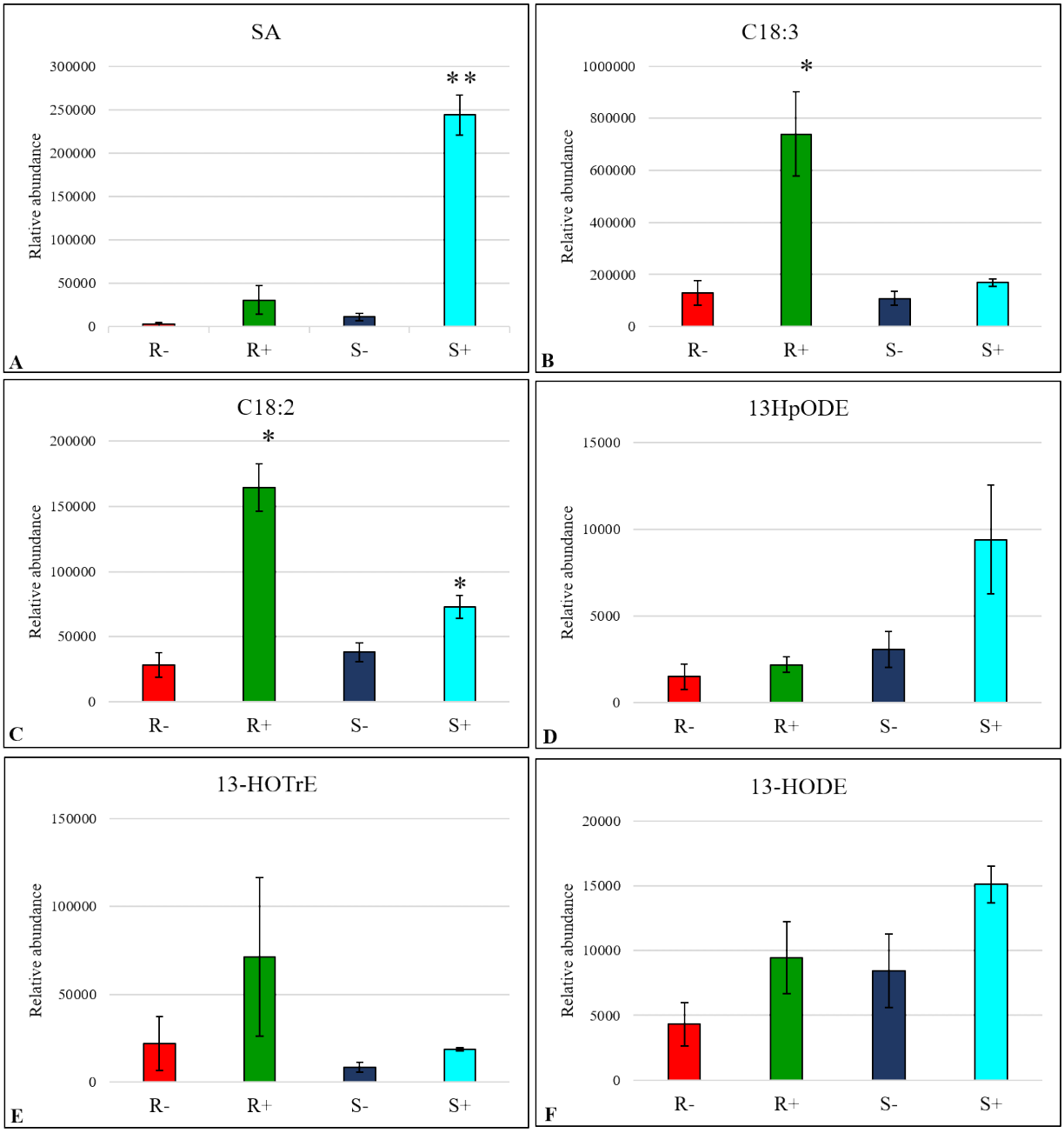

Fig. 8 HPLC-MS-MS measurements of SA (A), α-linolenic acid (B), Linoleic acid (C), 13-Hydroperoxy-9,11-octadecadienoic acid (D), 13-Hydroxy-9,11,15-octadecatrienoic acid (E), 13-Hydroxyoctadecadienoic acid (F). Measurements were carried out in susceptible (S) and moderately resistant (R) genotypes in control (-) and infected (+) conditions. Bars represent the means ± standard error of three biological replicates technically repeated two times. Asterisks above the bars indicate significant differences between the (-) and (+) treatments (Two-way ANOVA, based on multiple-sample tests FDR adjusted value * $p < 0.05$; ** $p < 0.01$).

Proteome quality control and overview of quantitative proteomics analysis

Quantitative proteomic analysis using HPLC-MS-MS was performed to study the molecular differences, at protein level, between moderately resistant and susceptible genotypes after *C. lindemuthianum* infection occurred. The proteomic study identified a total of 2721 proteins assigned to *P. vulgaris* (Supplementary Dataset S2). The total proteins of the four experimental conditions plotted closely in the PCA (Supplementary Fig. S1); the two genotypes were well-separated on PC2, which accounts for 18.6 % of the total variation. PCA also showed a distinct separation between infected and non-infected S plants, as obtained by comparing volatilomes (Fig. 4).

DAPs obtained from the one-way ANOVA consistency test (FDR < 0.05) and statistically significant in at least one comparison represented the 9% of the whole protein dataset (250 proteins) (Supplementary Dataset S3).

The *P. vulgaris* proteome genotype-, treatment-, and interaction-dependent differences

A two-factorial ANOVA on the 250 DAPs confirmed a significant genotype effect on 64 proteins (G-DAPs), while the infection treatment had significant effect on 25 proteins (C-DAPs) and a significant interaction was confirmed for 174 proteins (I-DAPs) (Supplementary Table S3A-C). The majority of the I-DAPs (110) were more abundant in S+ than in R+ plants, indicating stronger changes of the proteome of the susceptible genotype after infection (Supplementary Table S3C, "R+_S+" column).

Results of functional classification of DAPs are reported in Supplementary Fig. S3. The 64 G-DAPs were involved in "protein-related" processing (20%), "signalling" and "stress" (6%), "transport" (5%), "cell wall", "RNA" and "amino acid metabolism" (3%), "secondary metabolism" and "hormone metabolism" (1.5%) processes. The 25 C-DAPs were equally distributed among "stress", "RNA", "cell wall" and "amino acid metabolism" categories (8%), with exception made for "protein-related" group (about 12% for each category). The 174 I- DAPs mostly belonged to the functional classification of "protein-related" processing (12%), "RNA-related" (7%), "cell organization" (6%), "stress" (5%), "signalling" (4%) processes.

Identification of hub proteins

Neither G-DAPs nor C-DAPs showed proteins biologically connected. On the contrary, among the I-DAPs, a Protein-Protein Interaction (PPI) network containing 172 nodes (proteins) and 113 edges (interactions) was constructed using the STRING online database. The PPI enrichment *p*-value was 0.00794 indicating that I-DAPs are biologically connected (Supplementary Fig. S4), The 9 significant interactome members that serve as central hubs were: Imidazole glycerol-phosphate dehydratase (IGPD;V7BCG1), Pyrroline-5-carboxylate reductase (P5CR; V7CV89), Matrin-type domain-containing protein (V7BXY; AT2G32600), DNA-directed RNA polymerase subunit (NRPB1;V7CLS7), DUF1716 domain-containing protein (V7BPH9; AT3G02710), Aspartokinase (AK-LYS1; V7C2X5), Ribosomal_S13_N domain-containing protein (V7CE67), RNA helicase (V7CGX3), RRM domain-containing protein (U1-70K; V7CI13).

DISCUSSION

When challenged with *C. lindemuthianum*, the two bean genotypes exhibit very different behaviours. As expected, the susceptible genotype showed more severe symptoms, with diffuse necrosis on stems and leaves. We now analyse the responses of volatilome and proteome of the two genotypes, especially aiming to identify changes that might be important in terms of resistance to the pathogen infection.

***C. lindemuthianum* induces emission of few VOCs, mainly in susceptible beans**

The PCA of the two bean genotypes volatilomes, infected and non-infected, clearly discriminated among the conditions; the volatilome of S+ and R- plotted much closer than S- and R- volatilomes (Fig. 4B), demonstrating an existing genotype-based difference between R- and S- volatile emissions.

As a first general observation, R+ plants emitted about 30% less volatiles than R-, S- and S+ plants. Comparable results were obtained at proteomic level, as many DAPs were significantly less abundant in R+ in respect of R- and S+ plants (Supplementary Fig. S3).

The lower emission of volatiles in R+ could be due to a stomatal closure in response to pathogen invasion, reducing diffusion of VOCs outside leaves. This hypothesis was corroborated by proteomic evidences, as two proteins of the I-DAPs list, which play fundamental roles in stomatal opening, accumulated more in S+ than in R+ plants: Munc-13-like protein

(AT5G06970.1) and phototropin 1 (AT3G45780.1) (Hashimoto-Sugimoto et al. 2013, Takemiya et al. 2013).

Furthermore, none of the VOCs was exclusively elicited in R+ plants, which suggest at a glance no association between resistance to *C. lindemuthianum* infection and VOC emission. However, the following observations can also be made when comparing volatilome and proteome of the two bean genotypes.

Among the C-dependent VOCs, emission of the monoterpene p-cymene [(retrieved as a fragment m/z 93.067, which usually represents 70-100% of the molecular ion, (Maleknia et al. 2007)] was stimulated in both genotypes when infected by *C. lindemuthianum* (Fig. 7A). p-cymene is a constituent of essential oils, characterizing the scent of many aromatic plants such as basil and thyme (Bagamboula et al. 2004). When accumulated in specialized plant structures, p-cymene is known for its antibacterial, antiviral and antifungal activities (Singh and Pandey 2021) and its stimulation in both R+ and S+ (Fig. 7A) might indicate that the biosynthetic pathway of monoterpenes, the MEP pathway (Lichtenthaler 1999), is induced by *C. lindemuthianum* . *De novo* synthesis of isoprenoids in response to pathogen infection has been reported in numerous plants. For example, isoprenoids are induced in poplars susceptible to the rust fungus *Melampsora laricipopulina* (Eberl et al. 2018). To the best of our knowledge, this is the first time that p-cymene has the same pattern of Pathogen Induced Plant Volatile (PIPV), at least in *P. vulgaris*. However, we were unable to assess at which extent this VOC is able to exert antifungal activity in beans. In fact, other monoterpenes that are generally co-synthesized with p-cymene were not statistically differentially emitted, suggesting that p-cymene might cover a specific role in the bean-*colletotrichum* pathosystem.

Methyl ethyl ketone (MEK, m/z 73.064; also known as 2-butanone, butanone, methyl acetone, butan-2-one, methyl propanone and ethyl methyl ketone) is an oxygenated volatile organic compound (OVOC) produced by plants (Bracho-Nunez et al. 2013, Brilli et al. 2014), fungi (Wheatley et al. 1997) and bacteria (Wilkins 1996, Song and Ryu 2013). Yáñez-Serrano *et al.* (2016), conducting an extensive study in-field, demonstrated that MEK is emitted by vegetation and also by other biogenic sources, like dead and decaying plant matter. Biosynthetic pathways for MEK production in plants are not completely elucidated. Fall (2003) suggested that MEK is a bioproduct of a cyanohydrin lyase reaction during cyanogenesis, but MEK is emitted also in non-cyanogenic species (Yáñez-Serrano et al. 2016). Cappellin et al. (2019) showed that MEK can derive from in-planta transformation of methyl vinyl ketone (MVK), a bioproduct of

isoprene. In our analysis, isoprene was not emitted at statistically different rate but MEK was G- and C-dependent. Also, MEK was stimulated in both infected genotypes (Fig. 7B). To date, the biological significance of MEK emissions by plants is unclear. When exogenously applied, MEK confer plant protection against aphids and bacterial pathogen (biotrophic *P. syringae*) (Song and Ryu 2013). Overall, the possibility that MEK could be produced by plants in response to *C. lindemuthianum* and/or by the pathogen itself during its necrotrophic growth cannot be *a priori* excluded.

Similarly to MEK, two G-dependent VOCs corresponding to m/z 126.968 and m/z 79.053 were also constitutively emitted by S- plants but not by R- plants. *C. lindemuthianum* infection clearly further elicited emission of these two VOCs both in S and R plants (Fig. 7C, D). The m/z 126.968 peak was putatively identified as dimethyl trisulphide (Fig. 7C). Sulphur-containing VOCs, as glucosinolates and/or their breakdown products, are known for their fungicidal, bactericidal, nematocidal and allelopathic properties (Fahey et al. 2001). However, glucosinolate production has not been reported in *Phaseolus vulgaris*, although our proteomic analysis supports the idea that glucosinolate production might be elicited during the *C. lindemuthianum* infection. Both R+ and S+ plants presented an accumulation of tryptophan synthase beta type 2 (V7BZU9) protein (see C-DAPs list, Supplementary Table S3B), an enzyme producing tryptophan, which is a precursor of secondary metabolites as camalexin and glucosinolates (Barth and Jander 2006, Bednarek et al. 2009).

The m/z 79.053 peak was putatively identified as a fragment of benzaldehyde, which was more emitted in both infected genotypes (Fig. 7D). Benzaldehyde can be produced through the shikimic pathway, the same biosynthetic pathway of phenylpropanoids and SA. Two core phenylpropanoid pathway enzymes are I-dependent (Supplementary Table S3): the cinnamate 4-hydroxylase (AT2G30490.1) and the chorismate mutase (V7CUM8) showed differential accumulation before and after fungal infection. The proteome and volatilome results were supported by the presence of SA in the leaves of S+ plants compared to the other samples (Fig. 8A). Higher emission of benzaldehyde by S+ plants could indicate a shift of the metabolic pathways towards the production of SA confirmed by direct measurements of high amount of SA in S+ while in R+ plants benzaldehyde could be directed towards different metabolic pathways.

Hexanal is part of the important group of plant GLVs. These six carbons (C6) compounds including alcohols, aldehydes and esters (Dudareva et al. 2006) are generated through the

oxylipin pathway from C18-polyunsaturated fatty acids (α-linolenic acid and linoleic acid) through the membrane lipids hydrolysis (Matsui et al. 2006). GLVs are usually synthesized and emitted by leaves exposed to abiotic stresses (Brilli et al. 2011). However, they are also produced after fungal infection, and seem to act as aerial messengers to prime neighbouring plants (ul Hassan et al. 2015). Ameye et al. (2018a) showed enhanced GLV emission in response to fungal treatments, followed by wounding and herbivory. In maize, GLVs were recently shown to be related to susceptibility to *Colletorichum graminicola* (Gorman et al. 2020). Perhaps GLVs are a marker of the cellular oxidative damage that is likely to happen during necrotrophic fungi infections. Furthermore, in our study, the emission of hexanal was stimulated by the pathogen in the susceptible genotype, while was significantly less emitted in the moderately resistant one both in control (R-) and infected (R+) conditions (Fig. 7E). We can hypothesize a different genotypic response to the pathogen leading to GLVs release (Verhage et al. 2010, Ameye et al. 2018a) (see below, proteomic discussion).

The oxylipin pathway is also involved in JA production, an important defensive hormone (Castillo et al. 2004, Pinfield-Wells et al. 2005, Schilmiller et al. 2007). We have identified at least two VOCs produced in this same pathway: allene or 1,2-propadiene (m/z 41.039) and 2-cyclopenten-1-one (m/z 83.048) (Fig. 7F, G). Both VOCs are suppressed in R+ plants, confirming a general down-regulation of the oxylipin pathway in the moderately resistant genotype after infection. We speculate that the emission of these VOCs was inhibited due to a different allocation of intermediates or by-products of the oxylipin pathway in the infection phase. Interestingly, the allene oxide cyclase (AOC, V7B379) accumulated R+ plants.

2-Cyclopenten-1-one, besides being a by-product of the oxylipin pathway, can be involved in plant protection: the Arabidopsis mutant (*opr3*) is defective in the isoform of 12-oxo-phytodienoate (OPDA) reductase, which is required for JA biosynthesis, still produces 2-Cyclopenten-1-one and is resistant to the necrotrophic pathogen *Alternaria brassiciola* and to the insect *Bradysia impatiens* (Kourtchenko et al. 2007).

These evidences are mirrored at proteomic level. Among the I-DAPs, LOX protein (V7ASA9), peroxisomal 3-ketoacyl-CoA thiolase 3 (AT2G33150.1) and RNA helicase (V7CGX3) accumulated in S+ plants. It should be observed that the latter is a hub protein (Supplementary Fig. S4), involved in JA mediated signalling pathways. Interestingly, RNA helicase Arabidopsis mutants showed altered levels of LOX2 (Shi et al. 2012, Sakr et al. 2018) .

Plant defence against pathogens usually operates through a complex network of "defence hormones" such as SA, JA and ethylene (ET). Their relative fine-tuning switches on/off appropriate responses to pathogens with different lifestyle. Typically, the SA signalling pathway is active in plant challenged with biotrophic pathogen, whereas the JA/ET signalling pathway is stimulated in response to necrotrophic pathogens. Nevertheless, a "contamination" among these pathways may occur (Robert-Seilaniantz et al. 2011). Moreover, pathogens can overcome plant defences manipulating these pathways. Other pathosystems involving the *Colletotrichum* genus (namely, *Fragaria* × *ananassa* Duch. and *C. acutatum*), present impaired SA and JA pathways resulting in some advantage for fungal spreading (Amil-Ruiz et al. 2016). In our system, SA was elicited in S+ while the JA-precursor linolenic acid was triggered in R+ alongside with 13-LOX derived oxylipin, 13-HOTrE (Fig. 7). We might speculate that the pathogen trigger SA response in S+ plants. By provoking cell death, the pathogen accelerates its necrotrophic growth in S plants, whilst the moderately resistant genotype succeeds to limit pathogen contamination by enhancing JA pathway. We did not find neither JA nor jasmonoyl isoleucine (JA-Ile), its active conjugate, in S+ as well as in R+. Instead, we found linolenic acid (JA precursor) was more abundant in R+ plants (Howe 2001). We suggest that even if the R+ plants are moderately resistant to the pathogen, *C. lindemuthianum* succeeds in harnessing JA "maturation" and JA-related pathways, thus limiting plant defences. Indeed, both allene oxide synthase (AOS) and allene oxide cyclase (AOC), which are key enzymes in the oxylipin pathway, are slightly more abundant in R+ than in S+ (Supplementary Table S3).

Among short chain oxygenated VOCs, also ethanol emission pattern deserves to be highlighted. Ethanol was constitutively emitted by S- and R- plants but its emission only dropped in the susceptible plants after *C. lindemuthianum* infection (Fig. 7H). Ethanol is generally produced by anaerobic fermentations of plants (cotyledonal leaves, stems, flowers, or even necrotic tissues) under hypoxia or anoxia conditions (Ventura et al. 2020). In our experiments, the reduced emission of ethanol could reveal reduced respiration rate induced by the stress in the susceptible genotype, that enhances the availability of precursors (e.g. pyruvate) for competing fermentation processes. Alternatively, we may speculate that ethanol precursors (acetaldehyde or pyruvate) are used to supply more energy to other competing pathways activated by the infection, e.g. to produce intermediates of the lipoxygenase pathway producing GLVs.

Proteomic analysis provides a general molecular framework of genotypic differences and of mechanisms of defense activated by the pathogen

Among C-DAPs that accumulated after *C. lindemuthianum* infection in both genotypes, we identified several proteins that could be involved in plant defence response. Among them, phosphatase 2A regulatory subunit TAP46 (V7AWB1) plays multifaceted roles in biotic stress perception, signalling and response, and in plant immunity; DEAD-box ATP-dependent RNA helicase 37 (V7BIK6) is involved in mRNA quality control, in turn fine-tuning transcript levels to reduce fitness costs and achieve effective immunity (Jung et al. 2020, Sulkowska et al. 2020); arginosuccinate synthase (V7CBE7) is involved in the synthesis of L-arginine, an important amino acid for nitrogen storage and to fine-tune the production of NO (Winter et al. 2015). In *Arabidopsis thaliana*, a reduction in arginine levels promotes the growth of *Pseudomonas syringae* (Anwar et al. 2019). On the contrary, the abundance of dihydrofolate reductase (V7CUJ1) and basic endochitinase B (V7CG25) were strongly decreased in both genotypes. Dihydrofolate reductase regulates the folate pathway, that participates in fine-tuning NADPH production, cellular reducing power, and ROS levels (Gorelova et al. 2017). In *Arabidopsis thaliana*, the disruption of the folate pathway has been shown to enhance the resistance against *Pseudomonas syringae* pv. *tomato* DC3000 via the activation of a primed immune state, whereas the stimulation of folate results in an enhanced susceptibility (González and Vera 2019). Basic endochitinase B is involved in ET- and JA-mediated signalling pathways during the systemic acquired resistance. The *Capsicum annuum* homolog of basic endochitinase B (CaChiIII7) is transcriptionally stimulated by *Colletotrichum acutatum* infection. Knockdown of *CaChiIII7* reduced the expression of several defence response related genes in pepper leaves upon *C. acutatum* infection, whereas the transient expression of *CaChiIII7* increased their expression, resulting in the induction of a hypersensitive response (HR) and of the biosynthesis of hydrogen peroxide (Ali et al. 2020). The picture emerging from the analysis of the I-DAPs is more complex and informative. In particular, cell wall stability, the first line of defence against pathogen, seems to explain a better resistance to *C. lindemuthianum* colonization in R than in S genotype. Not only, as previously discussed, proteomic results show an alteration of the proteins involved in stomatal opening, but also R+ accumulated several proteins specifically involved in cell wall reinforcement and protein delivery to plasma membrane. These included proteins associated with cell wall tensile strength and integrity [e.g. Syntaxin/t-SNARE family protein (V7CWZ1), Novel Plant Snare 13 (V7C8E7), and the Trichome Birefringence-Like 39 protein (AT2G42570.1)],

extracellular medium alkalization and accumulation of phenolic compounds [e.g. flavin mononucleotide hydrolase 1 (V7B1G5) and farnesyltransferase A (V7BWN0)] (Escamilla-Treviño et al. 2006, Hochholdinger et al. 2008, Zhang et al. 2009, Liu et al. 2010, Taheri and Tarighi 2011, Gille and Pauly 2012, Boubakri et al. 2013, Jalakas et al. 2017). It should be observed that differences in cell wall composition characterize R and S genotypes. Indeed, in the G-DAPs list, several enzymes involved in the biosynthesis of cuticular wax and cutin (AMP-dependent synthetase and ligase family protein, V7BJB3), hemicellulose (cellulose synthase like E1, V7B9B7), xyloglucan (glycosyl hydrolase family protein, V7B6Y9), and alpha/beta-hydrolase superfamily protein (V7BLY4), accumulated more in R than in S.

Notably, also the level of MLO protein (V7BGV6), a negative regulator of plant defence (Zheng et al. 2013, Acevedo-Garcia et al. 2014), was lower in R+ than in S+ plants in the I-list. In the same list, Aspartokinase (V7C2X5) accumulated in R- more than in S- and to levels comparable with S+ and R+. Aspartokinase is an hub protein (Fig. S4), crucial in the Asp-derived amino acid pathway: regulation of Asp content, fluxes and transport has recently been recognized critical for plant to counteract biotic stresses (Han et al. 2021). Based on these observations, it seems reasonable to assume that the R genotype displays a stronger first line of defence against *C. lindemuthianum*, that is crucial to control disease progression. On the contrary, *C. lindemuthianum* infection proceeds more rapidly in the S genotype, leading to a more extensive metabolic response against fungal attack. Consistently, many I-DAPs related to plant defence induction upon pathogen infection were less abundant in R+ than in S+ plants. This list includes: two basic endochitinase B precursors (V7CH45, V7AUH2); proteins associated with the transient increase in ROS and calcium levels (MLP-like protein 43, V7AIR2; calcium-binding EF-hand family protein, V7BXX6); proteins related to protein kinase activation (mitogen-activated protein kinase kinase 4, V7ATB0), proteolysis (LON1, V7BJ03; FTSH10, V7AFJ9; peptide-N(4)-(N-acetyl-beta-glucosaminyl) asparagine amidase, V7BQ67), endomembrane trafficking and proteasome-dependent processes (golgin candidate 6, V7C0K5; vacuolar protein sorting-associated protein 29, V7B6Z5; Vacuolar Sorting Receptor 6, V7B317; RabD1, V7BRE6; Sec5, V7BGR8), secondary metabolite processing (UDP-glycosyltransferase 76F1, V7CZ85) (Ren et al. 2002, Koo et al. 2006, Fujisaki and Ishikawa 2008, Wang et al. 2016).

Also, levels of pyrroline-5-carboxylate (P5C) reductase (V7CV89) and three core enzymes of the phenylpropanoid pathway, which generates a large array of key mediators involved in plant-pathogen interactions [NADPH--cytochrome P450 reductase 1 (V7AVR7), cinnamate 4-

hydroxylase (AT2G30490.1) and chorismate mutase (V7CUM8)], were more abundant in S+ than in R+ plants. P5C catalyses the final step in proline biosynthesis and was categorized as hub protein (Supplementary Fig. S4)**.**

CONCLUSIONS

Overall, our volatilome and proteome analyses suggest that two different strategies were activated by the two bean genotypes characterized by different levels of susceptibility/resistance. The moderately resistant genotype probably reduced pathogen infection, invasion and replication investing on very highly structured epidermis and cell wall, perhaps assisted by a lower stomatal conductance. These results agree with previous experimental evidence indicating the containment of *C. lindemuthianum* infection by the activation of cell wall reinforcement-related genes in resistant plants (Padder et al. 2016). The susceptible genotype failed to reduce pathogen invasion at cell wall level and activated a wider range of defensive biochemical responses, including those involved in the release of VOC markers. The susceptible genotype also induced a quicker attainment of the fungal necrotrophic phase by the induction of a hypersensitive response involving the synthesis of GLVs and SA. Despite the volatilome of bean plants seems to be more informative as a marker of biochemical changes, without being directly involved in defensive responses, its potential for priming the neighbouring plants against *C. lindemuthianum*, as already suggested (Quintana-Rodriguez et al. 2015), deserves to be further explored.

SUPPLEMENTARY INFORMATION

Supplementary figures

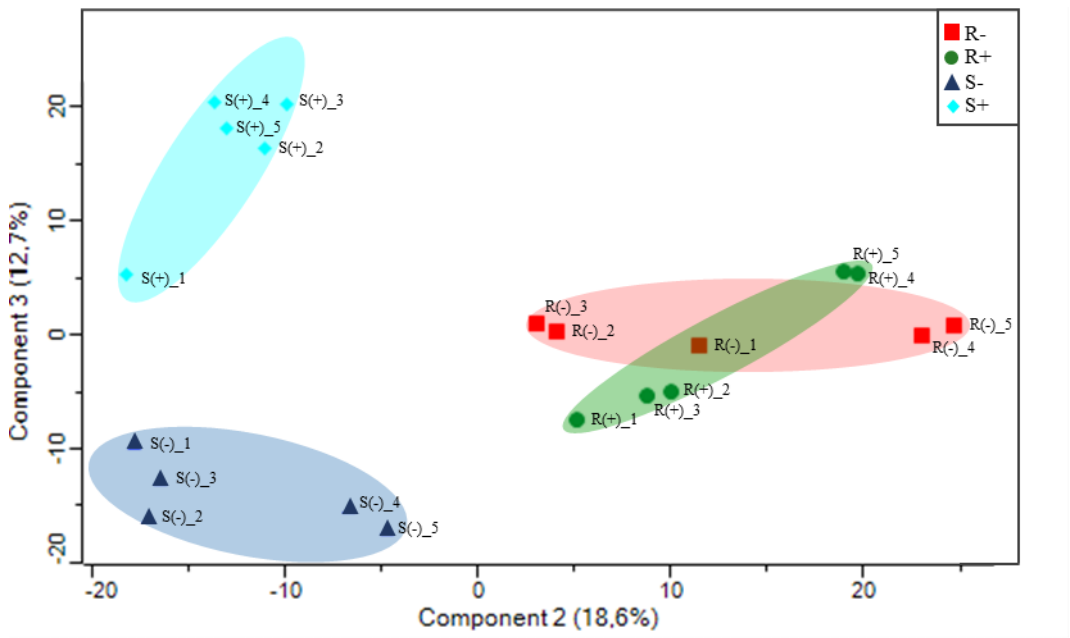

Fig. S1 Principal component analysis (PCA; Perseus V1.6) of LC-MS/MS data showing differences among proteomes of moderately resistant controls (R-, red), moderately resistant infected plants (R+, green), susceptible controls (S-, blue) and susceptible infected plants (S+, light blue). The percentage of variance explained by each component is reported in brackets. Samples were collected from five biological replicas per treatment.

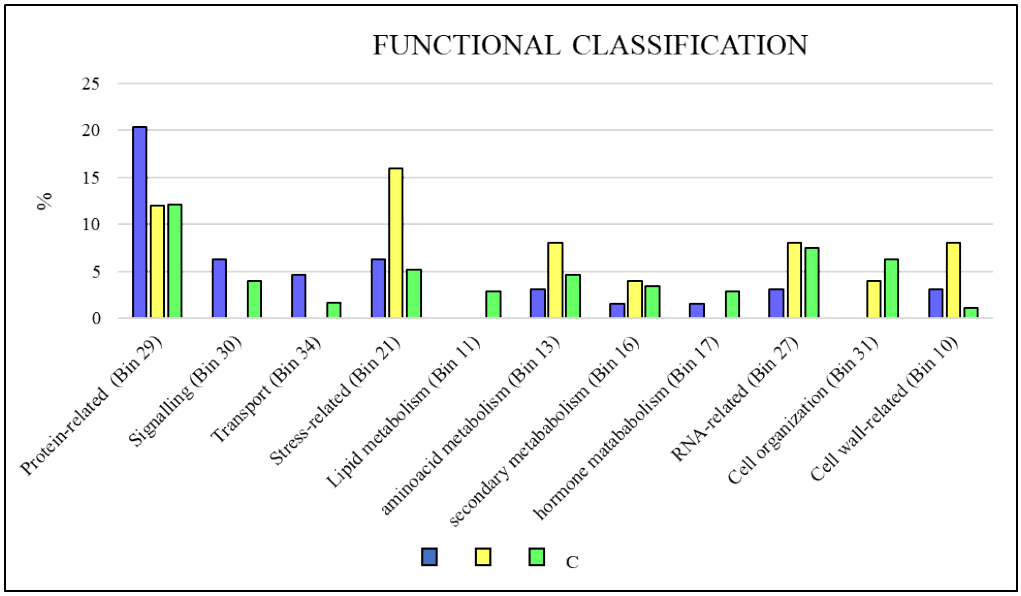

Fig. S2 Functional classification of identified differentially abundant proteins (DAPs) dependent on genotype (G, blue column), treatment (*Colletotrichum* infection, C, yellow column), or interaction (I, light green column). Samples were categorized based on MapMan V3.1, where each group refers to a specific Bin code; G, C and I proteins were grouped according to two-way ANOVA test ($p < 0.05$; Perseus V1.6).

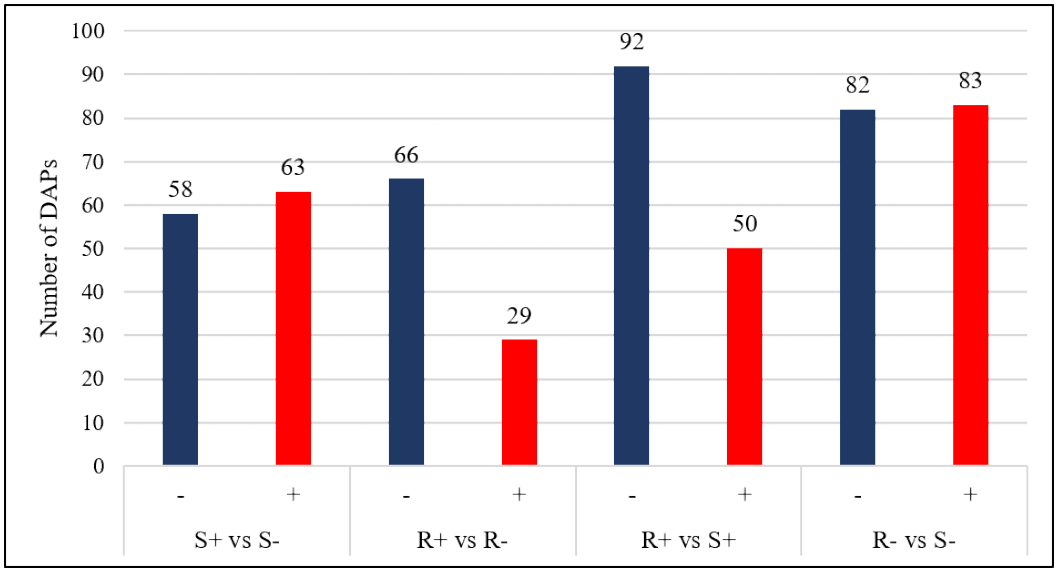

Fig. S3 Number of Differentially abundant proteins (DAPs) among moderately resistant (R) and susceptible (S) plants under control (-) and infected (+) conditions. Significant pairs obtained from one-way ANOVA test and Tuckey test (FDR adjusted value $p < 0.05$; Perseus V1.6).

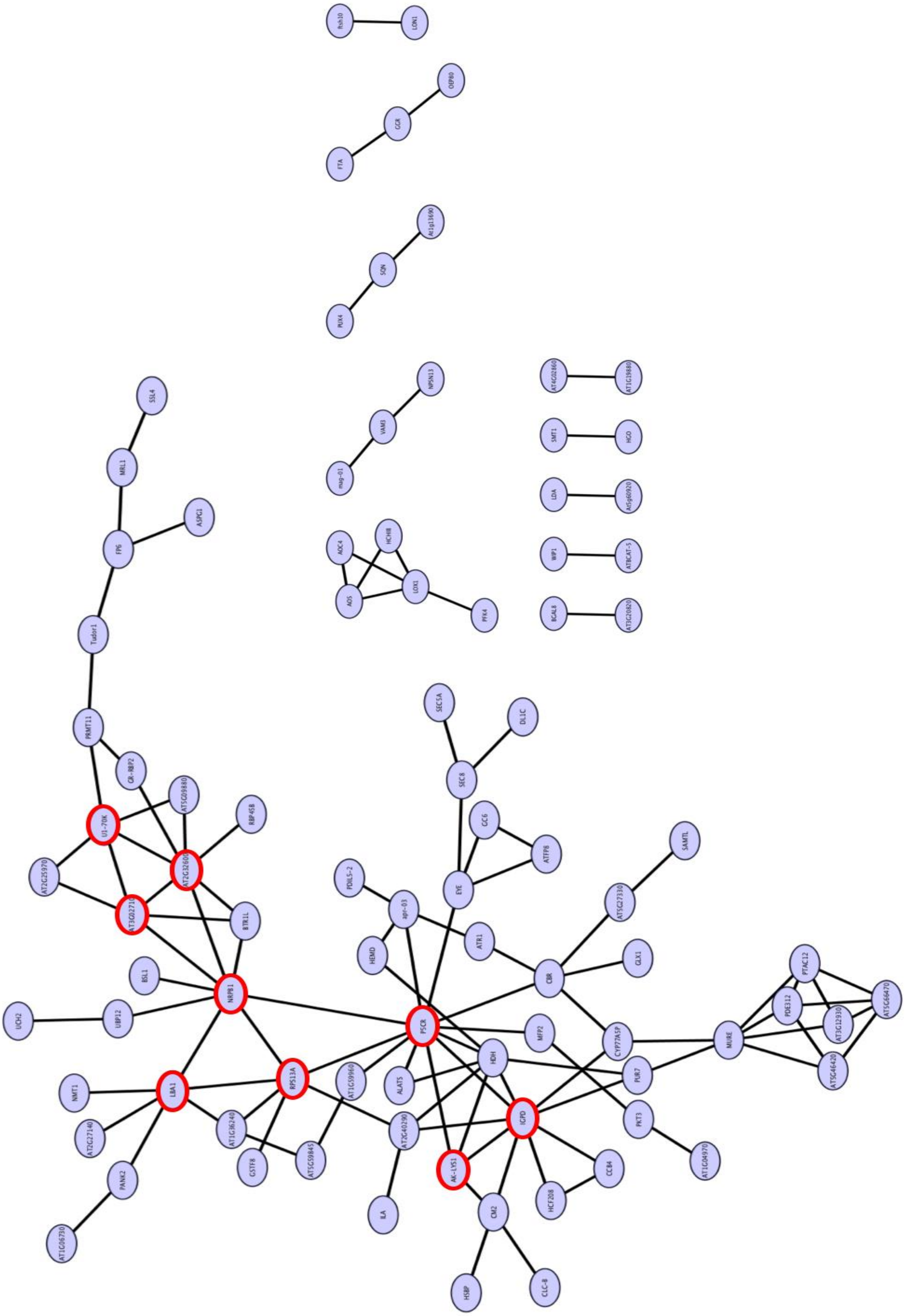

LON1
OEP80
GCR
FTA
SQN
PUX4
VAM3
NPSN13
AT4G02860
SMT1
HGO
LDA
WIP1
RCAL8
AOC4
HCHIB
LOX1
AOS
PFK4
SSL4
MRL1
ASPG1
FP6
Tudor1
PRMT11
GR-RBP2
AT5G09880
U1-70K
RBP45B
AT2G25970
BTR1L
BSL1
NRPB1
UCH2
UBP12
NMT1
LBA1
RPS13A
AT2G27140
AT1G36240
GSTF8
AT5G59845
PANK2
AT1G06730
SEC5A
DL1C
SEC8
GC6
ATFP8
EYE
SAMTL
PDIL5-2
ATR1
HEMD
AT5G27330
GLX1
CBR
PTAC12
PDE312
AT5G66470
AT3G12930
PSCR
MFP2
CYP71A5P
MURE
AT5G46420
HDH
PUR7
ALATS
IGPD
PKT3
AT2G40290
AT1G04970
AK-LYS1
CCB4
ILA
CM2
HCF208
HSBP
CLC-B

Fig. S4 Protein-protein interaction network of interaction-dependent (I) DAPs developed using STRING database and visualized with Cytoscape software. Hub proteins, identified by the CytoHubba application, are red circled.

Supplementary data[2]

Table S1: Parameters used for HPLC-MS-MS analysis. A) SA, oxylipin and standard Multiple Reaction Monitoring (MRM) conditions: metabolite, precursor ion, product ion, collision energy (CE) and fragmentor; B) Fatty acid Single Ion Monitoring (SIM) conditions: metabolite, ion mass, polarity and fragmentor.

Table S2 List of two-way ANOVA statistically significant (False discovery rate adjusted value $p < 0.05$; Metaboanalyst V5.0) genotype, treatment (*Colletotruchum* infection) and interaction-dependent VOCs, with indication of Mass/charge (m/z) ratios, protonated formulas and putative identification.

Table S3 List of Differentially abundant proteins (DAPs) dependent on genotype, treatment (Colletotrichum infection,) and interaction emerged from two-way ANOVA test (False discovery rate adjusted value $p < 0.05$; Perseus V1.6).

Dataset S1: Total VOCs detected by PTR-QiTOF-MS emitted by moderately resistant (R) and susceptible (S*) P. vulgaris* genotypes control (R-, S-) and infected by *C. lindemuthianum* (R+, S+).

Dataset S2: Total proteins identified by HPLC-MS-MS in moderately resistant (R) and susceptible (S*) P. vulgaris* genotypes control (R-, S-) and infected by *C. lindemuthianum* (R+, S+).

[2] Supplementary tables and datasets are available in the "Supplementary data_Chapter three" folder

Dataset S3: List of Differentially Abundant proteins (DAPs) based on one-way ANOVA test (False discovery rate adjusted value $p < 0.05$; Perseus V1.6).

REFERENCES

Abbas F, Ke Y, Yu R, Yue Y, Amanullah S, Jahangir MM, Fan Y (2017) Volatile terpenoids: multiple functions, biosynthesis, modulation and manipulation by genetic engineering. Planta 246(5): 803-816

Abrahám E, Rigó G, Székely G, Nagy R, Koncz C, Szabados L (2003) Light-dependent induction of proline biosynthesis by abscisic acid and salt stress is inhibited by brassinosteroid in Arabidopsis. Plant molecular biology 51(3): 363-372

Acevedo-Garcia J, Kusch S, Panstruga R (2014) Magical mystery tour: MLO proteins in plant immunity and beyond. New Phytologist 204(2): 273-281

Adebesin F, Widhalm JR, Boachon B, Lefèvre F, Pierman B, Lynch JH, Alam I, Junqueira B, Benke R, Ray S (2017) Emission of volatile organic compounds from petunia flowers is facilitated by an ABC transporter. Science 356(6345): 1386-1388

Affek HP, Yakir D (2002) Protection by isoprene against singlet oxygen in leaves. Plant Physiology 129(1): 269-277

Alagna F, Kallenbach M, Pompa A, De Marchis F, Rao R, Baldwin IT, Bonaventure G, Baldoni L (2016) Olive fruits infested with olive fly larvae respond with an ethylene burst and the emission of specific volatiles. Journal of integrative plant biology 58(4): 413-425

Albert I, Hua C, Nürnberger T, Pruitt RN, Zhang L (2020) Surface sensor systems in plant immunity. Plant Physiol 182(4): 1582-1596

Ali M, Li Q-H, Zou T, Wei A-M, Gombojab G, Lu G, Gong Z-H (2020) Chitinase gene positively regulates hypersensitive and defense responses of pepper to *Colletotrichum acutatum* infection. Internat J Mol Sci 21(18): 6624

Ali S, Ganai BA, Kamili AN, Bhat AA, Mir ZA, Bhat JA, Tyagi A, Islam ST, Mushtaq M, Yadav P (2018) Pathogenesis-related proteins and peptides as promising tools for engineering plants with multiple stress tolerance. Microbiological Research 212: 29-37

Ameye M, Allmann S, Verwaeren J, Smagghe G, Haesaert G, Schuurink RC, Audenaert K (2018a) Green leaf volatile production by plants: A meta-analysis. New Phytologist 220(3): 666-683

Ameye M, Allmann S, Verwaeren J, Smagghe G, Haesaert G, Schuurink RC, Audenaert K (2018b) Green leaf volatile production by plants: a meta-analysis. New Phytol 220(3): 666-683

Ameye M, Audenaert K, De Zutter N, Steppe K, Van Meulebroek L, Vanhaecke L, De Vleesschauwer D, Haesaert G, Smagghe G (2015) Priming of wheat with the green leaf volatile Z-3-hexenyl acetate enhances defense against Fusarium graminearum but boosts deoxynivalenol production. Plant physiology 167(4): 1671-1684

Amil-Ruiz F, Garrido-Gala J, Gadea J, Blanco-Portales R, Muñoz-Mérida A, Trelles O, de Los Santos B, Arroyo FT, Aguado-Puig A, Romero F (2016) Partial activation of SA-and JA-defensive pathways in strawberry upon Colletotrichum acutatum interaction. Frontiers in plant science 7: 1036

Andama JB, Mujiono K, Hojo Y, Shinya T, Galis I (2020) Nonglandular silicified trichomes are essential for rice defense against chewing herbivores. Plant, cell & environment 43(9): 2019-2032

Anjum SA, Xie X-y, Wang L-c, Saleem MF, Man C, Lei W (2011) Morphological, physiological and biochemical responses of plants to drought stress. African journal of agricultural research 6(9): 2026-2032

Anwar S, Ali MA, Abbas A, Wieczorek K (2019) Arabidopsis Argininosuccinate Lyase and Argininosuccinate Synthase are important for resistance against Pseudomonas syringae. Advancements in Life Sciences 7(1): 20-26

Armbruster U, Leonelli L, Correa Galvis V, Strand D, Quinn EH, Jonikas MC, Niyogi KK (2016) Regulation and levels of the thylakoid K+/H+ antiporter KEA3 shape the dynamic response of photosynthesis in fluctuating light. Plant and Cell Physiology 57(7): 1557-1567

Aslam B, Basit M, Nisar MA, Khurshid M, Rasool MH (2017) Proteomics: technologies and their applications. Journal of chromatographic science 55(2): 182-196

Athukorala SNP, Fernando WGD, Rashid KY, de Kievit T (2010) The role of volatile and non-volatile antibiotics produced by *Pseudomonas chlororaphis* strain PA23 in its root colonization and control of *Sclerotinia sclerotiorum*. Biocontrol Sci Technol 20(8): 875-890, Article

Atkinson RG (2016) Phenylpropenes: Occurrence, distribution, and biosynthesis in fruit. Journal of agricultural and food chemistry 66(10): 2259-2272

Baena-González E, Rolland F, Thevelein JM, Sheen J (2007) A central integrator of transcription networks in plant stress and energy signalling. Nature 448(7156): 938-942

Bagamboula C, Uyttendaele M, Debevere J (2004) Inhibitory effect of thyme and basil essential oils, carvacrol, thymol, estragol, linalool and p-cymene towards Shigella sonnei and S. flexneri. Food microbiology 21(1): 33-42

Baldwin IT, Schultz JC (1983) Rapid changes in tree leaf chemistry induced by damage: evidence for communication between plants. Science 221: 277 - 279

Bao Y, Song W-M, Pan J, Jiang C-M, Srivastava R, Li B, Zhu L-Y, Su H-Y, Gao X-S, Liu H (2016) Overexpression of the NDR1/HIN1-like gene NHL6 modifies seed germination in response to abscisic acid and abiotic stresses in Arabidopsis. PLoS One 11(2): e0148572

Bardas GA, Lagopodi AL, Kadoglidou K, Tzavella-Klonari K (2009) Biological control of three Colletotrichum lindemuthianum races using Pseudomonas chlororaphis PCL1391 and Pseudomonas fluorescens WCS365. Biological Control 49(2): 139-145

Barta C, Loreto F (2006) The relationship between the methyl-erythritol phosphate pathway leading to emission of volatile isoprenoids and abscisic acid content in leaves. Plant Physiology 141(4): 1676-1683

Barth C, Jander G (2006) Arabidopsis myrosinases TGG1 and TGG2 have redundant function in glucosinolate breakdown and insect defense. Plant J 46(4): 549-562

Beale MH, Birkett MA, Bruce TJ, Chamberlain K, Field LM, Huttly AK, Martin JL, Parker R, Phillips AL, Pickett JA (2006) Aphid alarm pheromone produced by transgenic plants affects aphid and parasitoid behavior. Proceedings of the National Academy of Sciences 103(27): 10509-10513

Bebber DP, Gurr SJ (2015) Crop-destroying fungal and oomycete pathogens challenge food security. Fungal Genetics and Biology 74: 62-64

Beccaccioli M, Reverberi M, Scala V (2019) Fungal lipids: Biosynthesis and signalling during plant-pathogen interaction. Front Biosci-Landmark 24: 172-185

Beccaccioli M, Salustri M, Scala V, Ludovici M, Cacciotti A, D'Angeli S, Brown DW, Reverberi M (2021) The Effect of Fusarium verticillioides Fumonisins on Fatty Acids, Sphingolipids, and Oxylipins in Maize Germlings. International journal of molecular sciences 22(5): 2435

Bednarek P, Piślewska-Bednarek M, Svatoš A, Schneider B, Doubský J, Mansurova M, Humphry M, Consonni C, Panstruga R, Sanchez-Vallet A (2009) A glucosinolate metabolism pathway in living plant cells mediates broad-spectrum antifungal defense. Science 323(5910): 101-106

Behnke K, Ehlting B, Teuber M, Bauerfeind M, Louis S, Hänsch R, Polle A, Bohlmann J, Schnitzler JP (2007) Transgenic, non-isoprene emitting poplars don't like it hot. The Plant Journal 51(3): 485-499

Behnke K, Kaiser A, Zimmer I, Brüggemann N, Janz D, Polle A, Hampp R, Hänsch R, Popko J, Schmitt-Kopplin P (2010) RNAi-mediated suppression of isoprene emission in poplar transiently impacts phenolic metabolism under high temperature and high light intensities: a transcriptomic and metabolomic analysis. Plant molecular biology 74(1-2): 61-75

Bigirimana J, Höfte M (2002) Induction of systemic resistance toColletotrichum lindemuthianum in bean by a benzothiadiazole derivative and rhizobacteria. Phytoparasitica 30(2): 159-168

Bisignano G, Lagana MG, Trombetta D, Arena S, Nostro A, Uccella N, Mazzanti G, Saija A (2001) In vitro antibacterial activity of some aliphatic aldehydes from *Olea europaea* L. FEMS Microbiol Lett 198(1): 9-13, Article

Blackburn JB, D'Souza Z, Lupashin VV (2019) Maintaining order: COG complex controls Golgi trafficking, processing, and sorting. FEBS letters 593(17): 2466-2487

Blake RS, Monks PS, Ellis AM (2009) Proton-transfer reaction mass spectrometry. Chemical reviews 109(3): 861-896

Block A, Fristedt R, Rogers S, Kumar J, Barnes B, Barnes J, Elowsky CG, Wamboldt Y, Mackenzie SA, Redding K (2013) Functional modeling identifies paralogous solanesyl-diphosphate synthases that assemble the side chain of plastoquinone-9 in plastids. Journal of Biological Chemistry 288(38): 27594-27606

Boller T, Felix G (2009) A renaissance of elicitors: perception of microbe-associated molecular patterns and danger signals by pattern-recognition receptors. Annu Rev Plant Biol 60(1): 379-406

Borges A, Melotto M, Tsai SM, Caldas DGG (2012) Changes in spatial and temporal gene expression during incompatible interaction between common bean and anthracnose pathogen. Journal of plant physiology 169(12): 1216-1220

Borges L, Santana F, Castro I, Arruda K, Ramos H, Barros E (2015) Two-dimensional electrophoresis-based proteomic analysis of Phaseolus vulgaris in response to Colletotrichum lindemuthianum. Journal of Plant Pathology 97(2)

Boubakri H, Poutaraud A, Wahab MA, Clayeux C, Baltenweck-Guyot R, Steyer D, Marcic C, Mliki A, Soustre-Gacougnolle I (2013) Thiamine modulates metabolism of the phenylpropanoid pathway leading to enhanced resistance to Plasmopara viticola in grapevine. BMC plant biology 13(1): 1-15

Bracho-Nunez A, Knothe N, Welter S, Staudt M, Costa WR, Liberato MAR, Piedade MTF, Kesselmeier J (2013) Leaf level emissions of volatile organic compounds (VOC) from some Amazonian and Mediterranean plants. Biogeosciences 10(9): 5855-5873

Bricchi I, Leitner M, Foti M, Mithöfer A, Boland W, Maffei ME (2010) Robotic mechanical wounding (MecWorm) versus herbivore-induced responses: early signaling and volatile emission in Lima bean (Phaseolus lunatus L.). Planta 232(3): 719-729

Bright J, Desikan R, Hancock JT, Weir IS, Neill SJ (2006) ABA-induced NO generation and stomatal closure in Arabidopsis are dependent on H2O2 synthesis. The Plant Journal 45(1): 113-122

Brilli F, Loreto F, Baccelli I (2019) Exploiting plant volatile organic compounds (VOCs) in agriculture to improve sustainable defense strategies and productivity of crops. Frontiers in plant science 10: 264

Brilli F, Ruuskanen TM, Schnitzhofer R, Müller M, Breitenlechner M, Bittner V, Wohlfahrt G, Loreto F, Hansel A (2011) Detection of plant volatiles after leaf wounding and darkening by proton transfer reaction “time-of-flight” mass spectrometry (PTR-TOF). PLoS One 6(5): e20419

Brilli F, Gioli B, Zona D, Pallozzi E, Zenone T, Fratini G, Calfapietra C, Loreto F, Janssens IA, Ceulemans R (2014) Simultaneous leaf-and ecosystem-level fluxes of volatile organic compounds from a poplar-based SRC plantation. Agricultural and forest meteorology 187: 22-35

Bölter B, Nada A, Fulgosi H, Soll J (2006) A chloroplastic inner envelope membrane protease is essential for plant development. FEBS letters 580(3): 789-794

Börner T, Aleynikova AY, Zubo YO, Kusnetsov VV (2015) Chloroplast RNA polymerases: Role in chloroplast biogenesis. Biochimica et Biophysica Acta (BBA)-Bioenergetics 1847(9): 761-769

Cagliari A, Margis R, dos Santos Maraschin F, Turchetto-Zolet AC, Loss G, Margis-Pinheiro M (2011) Biosynthesis of triacylglycerols (TAGs) in plants and algae. International Journal of Plant Biology 2(1): e10-e10

Camacho-Coronel X, Molina-Torres J, Heil M (2020) Sequestration of exogenous volatiles by plant cuticular waxes as a mechanism of passive associational resistance: a proof of concept. Frontiers in plant science 11: 121

Campa A, Giraldez R, Ferreira JJ (2009) Genetic dissection of the resistance to nine anthracnose races in the common bean differential cultivars MDRK and TU. Theoretical and applied genetics 119(1): 1-11

Campa A, Murube E, Ferreira J (2017) INTROGRESSION OF A POWDERY MILDEW RESISTANCE GENE INTO MARKET CLASS FABADA.

Campos L, Granell P, Tárraga S, López-Gresa P, Conejero V, Bellés JM, Rodrigo I, Lisón P (2014) Salicylic acid and gentisic acid induce RNA silencing-related genes and plant resistance to RNA pathogens. Plant physiology and biochemistry 77: 35-43

Capozzi V, Yener S, Khomenko I, Farneti B, Cappellin L, Gasperi F, Scampicchio M, Biasioli F (2017) PTR-ToF-MS coupled with an automated sampling system and tailored data analysis for food studies: bioprocess monitoring, screening and nose-space analysis. Journal of visualized experiments: JoVE(123)

Cappellin L, Loreto F, Biasioli F, Pastore P, McKinney K (2019) A mechanism for biogenic production and emission of MEK from MVK decoupled from isoprene biosynthesis. Atmospheric Chemistry and Physics 19(5): 3125-3135

Cappellin L, Loreto F, Aprea E, Romano A, Del Pulgar JS, Gasperi F, Biasioli F (2013) PTR-MS in Italy: a multipurpose sensor with applications in environmental, agri-food and health science. Sensors 13(9): 11923-11955

Castellanos-Ramos J, Guzman-Maldonado H, Kelly J, Acosta-Gallegos J (2003) Registration of'Flor de Junio Marcela'common bean.(Registrations Of Cultivars). Crop science 43(3): 1121-1123

Castillo MC, Martínez C, Buchala A, Métraux J-P, León J (2004) Gene-specific involvement of β-oxidation in wound-activated responses in Arabidopsis. Plant physiology 135(1): 85-94

Castro-Guerrero NA, Isidra-Arellano MC, Mendoza-Cozatl DG, Valdés-López O (2016) Common bean: a legume model on the rise for unraveling responses and adaptations to iron, zinc, and phosphate deficiencies. Frontiers in plant science 7: 600

Chen K, Gao J, Sun S, Zhang Z, Yu B, Li J, Xie C, Li G, Wang P, Song C-P (2020a) BONZAI Proteins Control Global Osmotic Stress Responses in Plants. Current Biology 30(24): 4815-4825. e4814

Chen S, Zhang L, Cai X, Li X, Bian L, Luo Z, Li Z, Chen Z, Xin Z (2020b) (E)-Nerolidol is a volatile signal that induces defenses against insects and pathogens in tea plants. Horticulture research 7(1): 1-15

Cheong J-J, Do Choi Y (2003) Methyl jasmonate as a vital substance in plants. TRENDS in Genetics 19(7): 409-413

Chong J, Soufan O, Li C, Caraus I, Li S, Bourque G, Wishart DS, Xia J (2018) MetaboAnalyst 4.0: towards more transparent and integrative metabolomics analysis. Nucleic Acids Research 46(W1): W486-W494

Chuwah C, van Noije T, van Vuuren DP, Stehfest E, Hazeleger W (2015) Global impacts of surface ozone changes on crop yields and land use. Atmospheric Environment 106: 11-23

Cinege G, Louis S, Hänsch R, Schnitzler J-P (2009) Regulation of isoprene synthase promoter by environmental and internal factors. Plant molecular biology 69(5): 593-604

Ciucanu I, Kerek F (1984) A simple and rapid method for the permethylation of carbohydrates. Carbohydrate research 131(2): 209-217

Ciucanu I, Costello CE (2003) Elimination of oxidative degradation during the per-O-methylation of carbohydrates. Journal of the American Chemical Society 125(52): 16213-16219

Clay NK, Adio AM, Denoux C, Jander G, Ausubel FM (2009) Glucosinolate metabolites required for an Arabidopsis innate immune response. Science 323(5910): 95-101

Coppola M, Cascone P, Madonna V, Di Lelio I, Esposito F, Avitabile C, Romanelli A, Guerrieri E, Vitiello A, Pennacchio F (2017) Plant-to-plant communication triggered by systemin primes anti-herbivore resistance in tomato. Scientific reports 7(1): 1-13

Cotrozzi L, Pellegrini E, Nali C, Lorenzini G (2019) Climate change, ozone and plant life. Agrochimica: 181

Cox J, Mann M (2008) MaxQuant enables high peptide identification rates, individualized ppb-range mass accuracies and proteome-wide protein quantification. Nature biotechnology 26(12): 1367-1372

Croft KP, Juttner F, Slusarenko AJ (1993) Volatile products of the lipoxygenase pathway evolved from Phaseolus vulgaris (L.) leaves inoculated with Pseudomonas syringae pv phaseolicola. Plant physiology 101(1): 13-24

Dai A (2013) Increasing drought under global warming in observations and models. Nature climate change 3(1): 52-58

Dalal VK, Tripathy BC (2012) Modulation of chlorophyll biosynthesis by water stress in rice seedlings during chloroplast biogenesis. Plant, cell & environment 35(9): 1685-1703

Dalin P, Ågren J, Björkman C, Huttunen P, Kärkkäinen K (2008) Leaf trichome formation and plant resistance to herbivory. In: Induced plant resistance to herbivory. Springer, pp 89-105

Dani KGS, Fineschi S, Michelozzi M, Loreto F (2016) Do cytokinins, volatile isoprenoids and carotenoids synergically delay leaf senescence? Plant, cell & environment 39(5): 1103-1111

Davydov R, Sokolov M, Hogland W, Glinushkin A, Markaryan A The application of pesticides and mineral fertilizers in agriculture. Proceedings of the MATEC web of conferences, 2018, pp 11003

De Meyer G, Audenaert K, Höfte M (1999) Pseudomonas aeruginosa 7NSK2-induced systemic resistance in tobacco depends on in planta salicylic acid accumulation but is not associated with PR1a expression. European Journal of Plant Pathology 105(5): 513-517

Dempsey DMA, Klessig DF (2017) How does the multifaceted plant hormone salicylic acid combat disease in plants and are similar mechanisms utilized in humans? BMC biology 15(1): 1-11

Deuscher Z, Andriot I, Sémon E, Repoux M, Preys S, Roger JM, Boulanger R, Labouré H, Le Quéré JL (2019) Volatile compounds profiling by using proton transfer reaction-time of flight-mass spectrometry (PTR-ToF-MS). The case study of dark chocolates organoleptic differences. Journal of Mass Spectrometry 54(1): 92-119

Di Piero RM, Garda MV (2008) Quitosana reduz a severidade da antracnose e aumenta a atividade de glucanase em feijoeiro-comum. Pesquisa Agropecuária Brasileira 43(9): 1121-1128

Dicke M, Sabelis MW (1988) How plants obtain predatory mites as bodyguards. Netherlands Journal of Zoology 38: 148-165

Dicke M, Loreto F (2010) Induced plant volatiles: from genes to climate change. Trends in plant science 15(3): 115-117

Dietz K-J, Vogel MO, Viehhauser A (2010) AP2/EREBP transcription factors are part of gene regulatory networks and integrate metabolic, hormonal and environmental signals in stress acclimation and retrograde signalling. Protoplasma 245(1): 3-14

Dietz KJ, Sauter A, Wichert K, Messdaghi D, Hartung W (2000) Extracellular β-glucosidase activity in barley involved in the hydrolysis of ABA glucose conjugate in leaves. Journal of experimental botany 51(346): 937-944

Ding P, Ding Y (2020) Stories of salicylic acid: a plant defense hormone. Trends in plant science 25(6): 549-565

Ding Z, Galván-Ampudia CS, Demarsy E, Łangowski Ł, Kleine-Vehn J, Fan Y, Morita MT, Tasaka M, Fankhauser C, Offringa R (2011) Light-mediated polarization of the PIN3 auxin transporter for the phototropic response in Arabidopsis. Nature cell biology 13(4): 447-452

Domon B, Aebersold R (2006) Mass spectrometry and protein analysis. science 312(5771): 212-217

Doncheva NT, Morris JH, Gorodkin J, Jensen LJ (2018) Cytoscape StringApp: network analysis and visualization of proteomics data. Journal of proteome research 18(2): 623-632

Dudareva N, Pichersky E, Gershenzon J (2004) Biochemistry of plant volatiles. Plant Physiol 135(4): 1893-1902

Dudareva N, Negre F, Nagegowda DA, Orlova I (2006) Plant volatiles: recent advances and future perspectives. Critical reviews in plant sciences 25(5): 417-440

Dudareva N, Klempien A, Muhlemann JK, Kaplan I (2013) Biosynthesis, function and metabolic engineering of plant volatile organic compounds. New Phytologist 198(1): 16-32

Dvořák P, Krasylenko Y, Ovečka M, Basheer J, Zapletalová V, Šamaj J, Takáč T (2020) FSD1: developmentally-regulated plastidial, nuclear and cytoplasmic enzyme with anti-oxidative and osmoprotective role. Plant, cell & environment

Eberl F, Hammerbacher A, Gershenzon J, Unsicker SB (2018) Leaf rust infection reduces herbivore-induced volatile emission in black poplar and attracts a generalist herbivore. New Phytologist 220(3): 760-772

Effah E, Holopainen JK, McCormick AC (2019) Potential roles of volatile organic compounds in plant competition. Perspectives in Plant Ecology, Evolution and Systematics 38: 58-63

Elgendy AS, Abdelrasool MK A literature review on Trypsin Enzyme.

Erb M, Glauser G, Robert CA (2012) Induced immunity against belowground insect herbivores-activation of defenses in the absence of a jasmonate burst. Journal of Chemical Ecology 38(6): 629-640

Escamilla-Treviño LL, Chen W, Card ML, Shih M-C, Cheng C-L, Poulton JE (2006) Arabidopsis thaliana β-glucosidases BGLU45 and BGLU46 hydrolyse monolignol glucosides. Phytochemistry 67(15): 1651-1660

Fahey JW, Zalcmann AT, Talalay P (2001) The chemical diversity and distribution of glucosinolates and isothiocyanates among plants. Phytochemistry 56(1): 5-51

Fall R (2003) Abundant oxygenates in the atmosphere: a biochemical perspective. Chemical reviews 103(12): 4941-4952

Farmer DK, Riches M (2020) Measuring biosphere–atmosphere exchange of short-lived climate forcers and their precursors. Accounts of Chemical Research 53(8): 1427-1435

Fernandes N, Silva FAN, de Aragão FA, Zocolo GJ, Freitas BM (2019) Volatile organic compounds role in selective pollinator visits to commercial melon types. Embrapa Agroindústria Tropical-Artigo em periódico indexado (ALICE)

Fernandez O, Béthencourt L, Quero A, Sangwan RS, Clément C (2010) Trehalose and plant stress responses: friend or foe? Trends in plant science 15(7): 409-417

Fichman Y, Mittler R (2020) Rapid systemic signaling during abiotic and biotic stresses: is the ROS wave master of all trades? Plant J 102(5): 887-896

Flor H (1955) Host-parasite interactions in flax rust-its genetics and other implications. Phytopathology 45: 680-685

Fontenelle MR, Santana MF, Cnossen A, Bazzolli DM, Bromonschenkel SH, de Araújo EF, de Queiroz MV (2017) Differential expression of genes during the interaction between Colletotrichum lindemuthianum and Phaseolus vulgaris. European Journal of Plant Pathology 147(3): 653-670

Fujioka S, Takatsuto S, Yoshida S (2002) An early C-22 oxidation branch in the brassinosteroid biosynthetic pathway. Plant Physiology 130(2): 930-939

Fujisaki K, Ishikawa M (2008) Identification of an Arabidopsis thaliana protein that binds to tomato mosaic virus genomic RNA and inhibits its multiplication. Virology 380(2): 402-411

Gabruk M, Stecka A, Strzałka W, Kruk J, Strzałka K, Mysliwa-Kurdziel B (2015) Photoactive protochlorophyllide-enzyme complexes reconstituted with PORA, PORB and PORC proteins of A. thaliana: fluorescence and catalytic properties. PloS one 10(2): e0116990

Garbeva P, Weisskopf L (2019) Airborne medicine - bacterial volatiles and their influence on plant health. The New Phytologist, ; Review

Garcia-Seco D, Chiapello M, Bracale M, Pesce C, Bagnaresi P, Dubois E, Moulin L, Vannini C, Koebnik R (2017) Transcriptome and proteome analysis reveal new insight into proximal and distal responses of wheat to foliar infection by Xanthomonas translucens. Scientific reports 7(1): 1-13

Geffroy V, Sicard D, de Oliveira JC, Sévignac M, Cohen S, Gepts P, Neema C, Langin T, Dron M (1999) Identification of an ancestral resistance gene cluster involved in the coevolution process between Phaseolus vulgaris and its fungal pathogen Colletotrichum lindemuthianum. Molecular Plant-Microbe Interactions 12(9): 774-784

Genty B, Briantais J-M, Baker NR (1989) The relationship between the quantum yield of photosynthetic electron transport and quenching of chlorophyll fluorescence. Biochimica et Biophysica Acta (BBA)-General Subjects 990(1): 87-92

Ghirardo A, Wright LP, Bi Z, Rosenkranz M, Pulido P, Rodríguez-Concepción M, Niinemets Ü, Brüggemann N, Gershenzon J, Schnitzler J-P (2014) Metabolic flux analysis of plastidic isoprenoid biosynthesis in poplar leaves emitting and nonemitting isoprene. Plant Physiology 165(1): 37-51

Gille S, Pauly M (2012) O-acetylation of plant cell wall polysaccharides. Frontiers in plant science 3: 12

Gillet LC, Leitner A, Aebersold R (2016) Mass spectrometry applied to bottom-up proteomics: entering the high-throughput era for hypothesis testing. Annual review of analytical chemistry 9: 449-472

Giraud E, Van Aken O, Ho LH, Whelan J (2009) The transcription factor ABI4 is a regulator of mitochondrial retrograde expression of ALTERNATIVE OXIDASE1a. Plant physiology 150(3): 1286-1296

Girón-Calva PS, Molina-Torres J, Heil M (2012) Volatile dose and exposure time impact perception in neighboring plants. Journal of chemical ecology 38(2): 226-228

Glas JJ, Schimmel BC, Alba JM, Escobar-Bravo R, Schuurink RC, Kant MR (2012) Plant glandular trichomes as targets for breeding or engineering of resistance to herbivores. International journal of molecular sciences 13(12): 17077-17103

Gonda I, Bar E, Portnoy V, Lev S, Burger J, Schaffer AA, Tadmor Ya, Gepstein S, Giovannoni JJ, Katzir N (2010) Branched-chain and aromatic amino acid catabolism into aroma volatiles in Cucumis melo L. fruit. Journal of experimental botany 61(4): 1111-1123

González B, Vera P (2019) Folate metabolism interferes with plant immunity through 1C methionine synthase-directed genome-wide DNA methylation enhancement. Molecular plant 12(9): 1227-1242

Gorelova V, Ambach L, Rébeillé F, Stove C, Van Der Straeten D (2017) Folates in plants: research advances and progress in crop biofortification. Frontiers in chemistry 5: 21

Gorman Z, Christensen SA, Yan Y, He Y, Borrego E, Kolomiets MV (2020) Green leaf volatiles and jasmonic acid enhance susceptibility to anthracnose diseases caused by Colletotrichum graminicola in maize. Molecular plant pathology 21(5): 702-715

Guenther A (2002) The contribution of reactive carbon emissions from vegetation to the carbon balance of terrestrial ecosystems. Chemosphere 49(8): 837-844

Guo M, Liu J-H, Ma X, Luo D-X, Gong Z-H, Lu M-H (2016) The plant heat stress transcription factors (HSFs): structure, regulation, and function in response to abiotic stresses. Frontiers in plant science 7: 114

Haider MS, Zhang C, Kurjogi MM, Pervaiz T, Zheng T, Zhang C, Lide C, Shangguan L, Fang J (2017) Insights into grapevine defense response against drought as revealed by biochemical, physiological and RNA-Seq analysis. Scientific reports 7(1): 1-15

Halliday KJ (2004) Plant hormones: the interplay of brassinosteroids and auxin. Current Biology 14(23): R1008-R1010

Hammerbacher A, Coutinho TA, Gershenzon J (2019) Roles of plant volatiles in defence against microbial pathogens and microbial exploitation of volatiles. Plant Cell Environ 42(10): 2827-2843

Han M, Zhang C, Suglo P, Sun S, Wang M, Su T (2021) l-Aspartate: An Essential Metabolite for Plant Growth and Stress Acclimation. Molecules 26(7): 1887

Hardtke CS, Dorcey E, Osmont KS, Sibout R (2007) Phytohormone collaboration: zooming in on auxin–brassinosteroid interactions. Trends in cell biology 17(10): 485-492

Harris A, Owen SM, Sleep D, Pereira MdGdS (2016) Constitutive changes in pigment concentrations: implications for estimating isoprene emissions using the photochemical reflectance index. Physiologia plantarum 156(2): 190-200

Hartikainen K, Riikonen J, Nerg A-M, Kivimäenpää M, Ahonen V, Tervahauta A, Kärenlampi S, Mäenpää M, Rousi M, Kontunen-Soppela S (2012) Impact of elevated temperature and ozone on the emission of volatile organic compounds and gas exchange of silver birch (Betula pendula Roth). Environmental and experimental botany 84: 33-43

Harvey CM, Sharkey TD (2016) Exogenous isoprene modulates gene expression in unstressed Arabidopsis thaliana plants. Plant, cell & environment 39(6): 1251-1263

Hasan SA, Hayat S, Ahmad A (2011) Brassinosteroids protect photosynthetic machinery against the cadmium induced oxidative stress in two tomato cultivars. Chemosphere 84(10): 1446-1451

Hashimoto-Sugimoto M, Higaki T, Yaeno T, Nagami A, Irie M, Fujimi M, Miyamoto M, Akita K, Negi J, Shirasu K (2013) A Munc13-like protein in Arabidopsis mediates H+-ATPase translocation that is essential for stomatal responses. Nature Communications 4(1): 1-9

He M, He C-Q, Ding N-Z (2018) Abiotic stresses: general defenses of land plants and chances for engineering multistress tolerance. Frontiers in plant science 9: 1771

Heard W, Sklenář J, Tome DF, Robatzek S, Jones AM (2015) Identification of regulatory and cargo proteins of endosomal and secretory pathways in Arabidopsis thaliana by proteomic dissection. Molecular & Cellular Proteomics 14(7): 1796-1813

Heil M (2014) Herbivore-induced plant volatiles: targets, perception and unanswered questions. New Phytol 204: 297-306

Heil M, Kost C (2006) Priming of indirect defences. Ecology letters 9(7): 813-817

Heil M, Bueno JCS (2007) Within-plant signaling by volatiles leads to induction and priming of an indirect plant defense in nature. Proceedings of the National Academy of Sciences 104(13): 5467-5472

Hemmerlin A, Hoeffler J-F, Meyer O, Tritsch D, Kagan IA, Grosdemange-Billiard C, Rohmer M, Bach TJ (2003) Cross-talk between the cytosolic mevalonate and the plastidial methylerythritol phosphate pathways in tobacco bright yellow-2 cells. Journal of Biological Chemistry 278(29): 26666-26676

Hickman DT, Rasmussen A, Ritz K, Birkett MA, Neve P (2021) Allelochemicals as multi-kingdom plant defence compounds: towards an integrated approach. Pest Management Science 77(3): 1121-1131

Hochholdinger F, Wen TJ, Zimmermann R, Chimot-Marolle P, Da Costa e Silva O, Bruce W, Lamkey KR, Wienand U, Schnable PS (2008) The maize (Zea mays L.) roothairless3 gene encodes a putative GPI-anchored, monocot-specific, COBRA-like protein that significantly affects grain yield. The Plant Journal 54(5): 888-898

Holopainen JK, Gershenzon J (2010) Multiple stress factors and the emission of plant VOCs. Trends in plant science 15(3): 176-184

Hooper CM, Castleden IR, Tanz SK, Aryamanesh N, Millar AH (2017) SUBA4: the interactive data analysis centre for Arabidopsis subcellular protein locations. Nucleic acids research 45(D1): D1064-D1074

Hoshino Y, Gaucher EA (2018) On the origin of isoprenoid biosynthesis. Molecular biology and evolution 35(9): 2185-2197

Hou S, Liu Z, Shen H, Wu D (2019) Damage-associated molecular pattern-triggered immunity in plants. Front Plant Sci 10(646): art. 646, Review

Houben M, Van de Poel B (2019) 1-Aminocyclopropane-1-carboxylic acid oxidase (ACO): the enzyme that makes the plant hormone ethylene. Frontiers in plant science 10: 695

Howe GA (2001) Cyclopentenone signals for plant defense: remodeling the jasmonic acid response. Proceedings of the National Academy of Sciences 98(22): 12317-12319

Hu S, Li Y, Shen J (2020) A Diverse Membrane Interaction Network for Plant Multivesicular Bodies: Roles in Proteins Vacuolar Delivery and Unconventional Secretion. Frontiers in Plant Science 11

Huang M, Sanchez-Moreiras AM, Abel C, Sohrabi R, Lee S, Gershenzon J, Tholl D (2012) The major volatile organic compound emitted from Arabidopsis thaliana flowers, the sesquiterpene (E)-β-caryophyllene, is a defense against a bacterial pathogen. New Phytologist 193(4): 997-1008

Huang Z, Zhang Y, Yan Q, Zhang Z, Wang X (2016) Real-time monitoring of respiratory absorption factors of volatile organic compounds in ambient air by proton transfer reaction time-of-flight mass spectrometry. Journal of hazardous materials 320: 547-555

Hwang H-S, Adhikari PB, Jo H-J, Han JY, Choi YE (2020) Enhanced monoterpene emission in transgenic orange mint (Mentha× piperita f. citrata) overexpressing a tobacco lipid transfer protein (NtLTP1). Planta 252(3): 1-12

Imran QM, Yun B-W (2020) Pathogen-induced Defense Strategies in Plants. Journal of Crop Science and Biotechnology 23(2): 97-105

Iriti M, Faoro F (2003) Benzothiadiazole (BTH) induces cell-death independent resistance in Phaseolus vulgaris against Uromyces appendiculatus. Journal of Phytopathology 151(3): 171-180

Jalakas P, Huang Y-C, Yeh Y-H, Zimmerli L, Merilo E, Kollist H, Brosché M (2017) The role of ENHANCED RESPONSES TO ABA1 (ERA1) in Arabidopsis stomatal responses is beyond ABA signaling. Plant Physiology 174(2): 665-671

Jewell JB, Tanaka K (2019) Transcriptomic perspective on extracellular ATP signaling: a few curious trifles. Plant signaling & behavior 14(11): 1659079

Jia Q, Kong D, Li Q, Sun S, Song J, Zhu Y, Liang K, Ke Q, Lin W, Huang J (2019) The function of inositol phosphatases in plant tolerance to abiotic stress. International journal of molecular sciences 20(16): 3999

Jones JD, Dangl JL (2006) The plant immune system. nature 444(7117): 323-329

Jones RJ, Mansfield T (1970) Suppression of stomatal opening in leaves treated with abscisic acid. Journal of experimental botany 21(3): 714-719

Jordan A, Haidacher S, Hanel G, Hartungen E, Märk L, Seehauser H, Schottkowsky R, Sulzer P, Märk T (2009) A high resolution and high sensitivity proton-transfer-reaction time-of-flight mass spectrometer (PTR-TOF-MS). International Journal of Mass Spectrometry 286(2-3): 122-128

Jorrin-Novo JV, Komatsu S, Sanchez-Lucas R, de Francisco LER (2019) Gel electrophoresis-based plant proteomics: Past, present, and future. Happy 10th anniversary Journal of Proteomics! Journal of proteomics 198: 1-10

Joshi R, Paul M, Kumar A, Pandey D (2019) Role of calreticulin in biotic and abiotic stress signalling and tolerance mechanisms in plants. Gene 714: 144004

Jung HW, Panigrahi GK, Jung GY, Lee YJ, Shin KH, Sahoo A, Choi ES, Lee E, Kim KM, Yang SH (2020) Pathogen-associated molecular pattern-triggered immunity involves proteolytic degradation of core nonsense-mediated mRNA decay factors during the early defense response. The Plant Cell 32(4): 1081-1101

Junker RR, Tholl D (2013) Volatile organic compound mediated interactions at the plant-microbe interface. Journal of chemical ecology 39(7): 810-825

Junker RR, Gershenzon J, Unsicker SB (2011) Floral odor bouquet loses its ant repellent properties after inhibition of terpene biosynthesis. Journal of chemical ecology 37(12): 1323-1331

Kainulainen P, Holopainen J, Palomäki V, Holopainen T (1996) Effects of nitrogen fertilization on secondary chemistry and ectomycorrhizal state of Scots pine seedlings and on growth of grey pine aphid. Journal of Chemical Ecology 22(4): 617-636

Kapoor D, Singh S, Kumar V, Romero R, Prasad R, Singh J (2019) Antioxidant enzymes regulation in plants in reference to reactive oxygen species (ROS) and reactive nitrogen species (RNS). Plant Gene 19: 100182

Kari E, Miettinen P, Yli-Pirilä P, Virtanen A, Faiola CL (2018) PTR-ToF-MS product ion distributions and humidity-dependence of biogenic volatile organic compounds. International Journal of Mass Spectrometry 430: 87-97

Kaur H, Chowrasia S, Gaur VS, Mondal TK (2021) Allantoin: Emerging Role in Plant Abiotic Stress Tolerance. Plant Molecular Biology Reporter: 1-14

Kelly JD, Vallejo VA (2004) A comprehensive review of the major genes conditioning resistance to anthracnose in common bean. HortScience 39(6): 1196-1207

Kesselmeier J, Ciccioli P, Kuhn U, Stefani P, Biesenthal T, Rottenberger S, Wolf A, Vitullo M, Valentini R, Nobre A (2002) Volatile organic compound emissions in relation to plant carbon fixation and the terrestrial carbon budget. Global Biogeochemical Cycles 16(4): 73-71-73-79

Khafif M, Balagué C, Huard-Chauveau C, Roby D (2017) An essential role for the VASt domain of the Arabidopsis VAD1 protein in the regulation of defense and cell death in response to pathogens. PloS one 12(7): e0179782

Khan Z, Midega CA, Hooper A, Pickett J (2016) Push-pull: chemical ecology-based integrated pest management technology. Journal of chemical ecology 42(7): 689-697

Kishimoto K, Matsui K, Ozawa R, Takabayashi J (2005) Volatile C6-aldehydes and allo-ocimene activate defense genes and induce resistance against *Botrytis cinerea* in *Arabidopsis thaliana*. Plant and Cell Physiology 46(7): 1093-1102

Kishimoto K, Matsui K, Ozawa R, Takabayashi J (2006) Analysis of defensive responses activated by volatile allo-ocimene treatment in Arabidopsis thaliana. Phytochemistry 67(14): 1520-1529

Klessig DF, Choi HW, Dempsey DMA (2018) Systemic acquired resistance and salicylic acid: past, present, and future. Molecular plant-microbe interactions 31(9): 871-888

Koeduka T (2014) The phenylpropene synthase pathway and its applications in the engineering of volatile phenylpropanoids in plants. Plant Biotechnology: 14.0801 a

Koo AJ, Chung HS, Kobayashi Y, Howe GA (2006) Identification of a peroxisomal acyl-activating enzyme involved in the biosynthesis of jasmonic acid in Arabidopsis. Journal of Biological Chemistry 281(44): 33511-33520

KOST C, Heil M (2006) Herbivore-induced plant volatiles induce an indirect defence in neighbouring plants. Journal of Ecology 94(3): 619-628

Kourtchenko O, Andersson MX, Hamberg M, Brunnström Å, Göbel C, McPhail KL, Gerwick WH, Feussner I, Ellerström M (2007) Oxo-phytodienoic acid-containing galactolipids in Arabidopsis: jasmonate signaling dependence. Plant physiology 145(4): 1658-1669

Krech K, Ruf S, Masduki FF, Thiele W, Bednarczyk D, Albus CA, Tiller N, Hasse C, Schöttler MA, Bock R (2012) The plastid genome-encoded Ycf4 protein functions as a nonessential assembly factor for photosystem I in higher plants. Plant Physiology 159(2): 579-591

Kroh GE, Pilon M (2020) Regulation of iron homeostasis and use in chloroplasts. International journal of molecular sciences 21(9): 3395

Lamy F, Dugravot S, Cortesero AM, Chaminade V, Faloya V, Poinsot D (2018) One more step toward a push-pull strategy combining both a trap crop and plant volatile organic compounds against the cabbage root fly Delia radicum. Environmental Science and Pollution Research 25(30): 29868-29879

Landi M, Araniti F, Flamini G, Piccolo EL, Trivellini A, Abenavoli MR, Guidi L (2020) “Help is in the air”: volatiles from salt-stressed plants increase the reproductive success of receivers under salinity. Planta 251(2): 1-15

Lantz AT, Allman J, Weraduwage SM, Sharkey TD (2019) Isoprene: New insights into the control of emission and mediation of stress tolerance by gene expression. Plant, Cell & Environment 42(10): 2808-2826

Laule O, Fürholz A, Chang H-S, Zhu T, Wang X, Heifetz PB, Gruissem W, Lange M (2003) Crosstalk between cytosolic and plastidial pathways of isoprenoid biosynthesis in Arabidopsis thaliana. Proceedings of the National Academy of Sciences 100(11): 6866-6871

Lee J-Y, Lee H-S, Song J-Y, Jung YJ, Reinbothe S, Park Y-I, Lee SY, Pai H-S (2013) Cell growth defect factor1/CHAPERONE-LIKE PROTEIN OF POR1 plays a role in stabilization of light-dependent protochlorophyllide oxidoreductase in Nicotiana benthamiana and Arabidopsis. The Plant Cell 25(10): 3944-3960

Lee S, Yap M, Behringer G, Hung R, Bennett JW (2016) Volatile organic compounds emitted by *Trichoderma species* mediate plant growth. Fungal Biology and Biotechnology 3(1): art. no 7, journal article

Lemfack MC, Nickel J, Dunkel M, Preissner R, Piechulla B (2014) mVOC: a database of microbial volatiles. Nucleic Acids Res 42(D1): D744-D748

Leng G, Hall J (2019) Crop yield sensitivity of global major agricultural countries to droughts and the projected changes in the future. Science of the Total Environment 654: 811-821

Li H-W, Zang B-S, Deng X-W, Wang X-P (2011) Overexpression of the trehalose-6-phosphate synthase gene OsTPS1 enhances abiotic stress tolerance in rice. Planta 234(5): 1007-1018

Li J, Yang P, Gan Y, Yu J, Xie J (2015) Brassinosteroid alleviates chilling-induced oxidative stress in pepper by enhancing antioxidation systems and maintenance of photosystem II. Acta Physiologiae Plantarum 37(11): 1-11

Li K, Yang F, Zhang G, Song S, Li Y, Ren D, Miao Y, Song C-P (2017) AIK1, a mitogen-activated protein kinase, modulates abscisic acid responses through the MKK5-MPK6 kinase cascade. Plant physiology 173(2): 1391-1408

Li M, Cappellin L, Xu J, Biasioli F, Varotto C (2020) High-throughput screening for in planta characterization of VOC biosynthetic genes by PTR-ToF-MS. Journal of plant research 133(1): 123-131

Li N, Alfiky A, Vaughan MM, Kang S (2016) Stop and smell the fungi: Fungal volatile metabolites are overlooked signals involved in fungal interaction with plants. Fungal Biol Rev 30(3): 134-144

Lichtenthaler HaJSaADaMR (1997) Biosynthesis of isoprenoids in higher plant chloroplasts proceeds via a mevalonate-independent pathway. FEBS Letters 400(3): 271-274

Lichtenthaler HK (1999) The 1-deoxy-D-xylulose-5-phosphate pathway of isoprenoid biosynthesis in plants. Annual review of plant biology 50(1): 47-65

Lin J-H, Chou M-S (2006) Temperature effects on Henry's law constants for four VOCs in air-activated sludge systems. Atmospheric Environment 40(14): 2469-2477

Linders PT, Peters E, Ter Beest M, Lefeber DJ, van den Bogaart G (2020) Sugary Logistics Gone Wrong: Membrane Trafficking and Congenital Disorders of Glycosylation. International Journal of Molecular Sciences 21(13): 4654

Lindinger W, Jordan A (1998) Proton-transfer-reaction mass spectrometry (PTR–MS): on-line monitoring of volatile organic compounds at pptv levels. Chemical Society Reviews 27(5): 347-375

Liu F, Wei F, Wang L, Liu H, Zhu X, Liang Y (2010) Riboflavin activates defense responses in tobacco and induces resistance against Phytophthora parasitica and Ralstonia solanacearum. Physiological and Molecular Plant Pathology 74(5-6): 330-336

Loivamäki M, Louis S, Cinege G, Zimmer I, Fischbach RJ, Schnitzler J-P (2007) Circadian rhythms of isoprene biosynthesis in grey poplar leaves. Plant Physiology 143(1): 540-551

Loreto F, Velikova V (2001) Isoprene produced by leaves protects the photosynthetic apparatus against ozone damage, quenches ozone products, and reduces lipid peroxidation of cellular membranes. Plant Physiology 127(4): 1781-1787

Loreto F, Schnitzler J-P (2010) Abiotic stresses and induced BVOCs. Trends in Plant Science 15(3): 154-166

Loreto F, Fineschi S (2015) Reconciling functions and evolution of isoprene emission in higher plants. New Phytologist 206(2): 578-582

Maccioni A, Santo A, Falconieri D, Piras A, Farris E, Maxia A, Bacchetta G (2020) Phytotoxic effects of Salvia rosmarinus essential oil on Acacia saligna seedling growth. Flora 269: 151639

Maeda H, Dudareva N (2012) The shikimate pathway and aromatic amino acid biosynthesis in plants. Annual review of plant biology 63: 73-105

Maffei ME, Gertsch J, Appendino G (2011) Plant volatiles: production, function and pharmacology. Natural product reports 28(8): 1359-1380

Maleknia SD, Bell TL, Adams MA (2007) PTR-MS analysis of reference and plant-emitted volatile organic compounds. International Journal of Mass Spectrometry 262(3): 203-210

Malinowski J, Krzymowska M, Godoń K, Hennig J, Podstolski A (2007) A new catalytic activity from tobacco converting 2-coumaric acid to salicylic aldehyde. Physiologia Plantarum 129(3): 461-471

Martins SJ, Faria AF, Pedroso MP, Cunha MG, Rocha MR, Medeiros FHV (2019) Microbial volatiles organic compounds control anthracnose (Colletotrichum lindemuthianum) in common bean (Phaseolus vulgaris L.). Biological control 131: 36-42

Matsui K (2006) Green leaf volatiles: hydroperoxide lyase pathway of oxylipin metabolism. Current opinion in plant biology 9(3): 274-280

Matsui K, Minami A, Hornung E, Shibata H, Kishimoto K, Ahnert V, Kindl H, Kajiwara T, Feussner I (2006) Biosynthesis of fatty acid derived aldehydes is induced upon mechanical wounding and its products show fungicidal activities in cucumber. Phytochemistry 67(7): 649-657

Matysik J, Alia, Bhalu B, Mohanty P (2002) Molecular mechanisms of quenching of reactive oxygen species by proline under stress in plants. Current Science: 525-532

Maurya AK (2020) Application of Plant Volatile Organic Compounds (VOCs) in Agriculture. In: New Frontiers in Stress Management for Durable Agriculture. Springer, pp 369-388

Meents AK, Mithöfer A (2020) Plant–plant communication: is there a role for volatile damage-associated molecular patterns? Frontiers in Plant Science 11: 1538

Meiri D, Tazat K, Cohen-Peer R, Farchi-Pisanty O, Aviezer-Hagai K, Avni A, Breiman A (2010) Involvement of Arabidopsis ROF2 (FKBP65) in thermotolerance. Plant molecular biology 72(1-2): 191

Merilo E, Yarmolinsky D, Jalakas P, Parik H, Tulva I, Rasulov B, Kilk K, Kollist H (2018) Stomatal VPD response: there is more to the story than ABA. Plant Physiology 176(1): 851-864

Meza I, Siebert S, Döll P, Kusche J, Herbert C, Eyshi Rezaei E, Nouri H, Gerdener H, Popat E, Frischen J (2020) Global-scale drought risk assessment for agricultural systems. Natural Hazards and Earth System Sciences 20(2): 695-712

Millet DB, Alwe HD, Chen X, Deventer MJ, Griffis TJ, Holzinger R, Bertman SB, Rickly PS, Stevens PS, Léonardis T (2018) Bidirectional ecosystem–atmosphere fluxes of volatile organic compounds across the mass spectrum: How many matter? ACS Earth and Space Chemistry 2(8): 764-777

Mohammed A (2013) An overview of distribution, biology and the management of common bean anthracnose. Journal of Plant Pathology and Microbiology 4(8): 1-6

Monson RK, Fall R (1989) Isoprene emission from aspen leaves: influence of environment and relation to photosynthesis and photorespiration. Plant Physiology 90(1): 267-274

Morales FJ (2003) Common bean. In: Virus and virus-like diseases of major crops in developing countries. Springer, pp 425-445

Muhlemann JK, Klempien A, Dudareva N (2014) Floral volatiles: from biosynthesis to function. Plant, cell & environment 37(8): 1936-1949

Mumm R, Dicke M (2010) Variation in natural plant products and the attraction of bodyguards involved in indirect plant defense. Canadian journal of zoology 88(7): 628-667

Mungalu H, Sansala M, Hamabwe S, Mukuma C, Gepts P, Kelly JD, Kamfwa K (2020) Identification of race-specific quantitative trait loci for resistance to Colletotrichum lindemuthianum in an Andean population of common bean. Crop Science 60(6): 2843-2856

Murakami Y, Tsuyama M, Kobayashi Y, Kodama H, Iba K (2000) Trienoic fatty acids and plant tolerance of high temperature. Science 287(5452): 476-479

Myers JR, Kmiecik K (2017) Common Bean: Economic importance and relevance to biological science research. In: The common bean genome. Springer, pp 1-20

Naeem M, Iqbal M, Shakeel A, Ul-Allah S, Hussain M, Rehman A, Zafar ZU, Ashraf M (2020) Genetic basis of ion exclusion in salinity stressed wheat: Implications in improving crop yield. Plant Growth Regulation: 1-18

Nagai S, Koide M, Takahashi S, Kikuta A, Aono M, Sasaki-Sekimoto Y, Ohta H, Takamiya K-i, Masuda T (2007) Induction of isoforms of tetrapyrrole biosynthetic enzymes, AtHEMA2 and AtFC1, under stress conditions and their physiological functions in Arabidopsis. Plant physiology 144(2): 1039-1051

Nathalie V, Christian H (2008) Proline accumulation in plants: a review. Amino Acids 35(4): 753-759

Nellaepalli S, Ozawa S-I, Kuroda H, Takahashi Y (2018) The photosystem I assembly apparatus consisting of Ycf3–Y3IP1 and Ycf4 modules. Nature communications 9(1): 1-10

Newton RP, Brenton AG, Smith CJ, Dudley E (2004) Plant proteome analysis by mass spectrometry: principles, problems, pitfalls and recent developments. Phytochemistry 65(11): 1449-1485

Niinemets Ü, Kännaste A, Copolovici L (2013) Quantitative patterns between plant volatile emissions induced by biotic stresses and the degree of damage. Frontiers in Plant Science 4: 262

Nishida N, Tamotsu S, Nagata N, Saito C, Sakai A (2005) Allelopathic effects of volatile monoterpenoids produced by Salvia leucophylla: inhibition of cell proliferation and DNA synthesis in the root apical meristem of Brassica campestris seedlings. Journal of chemical ecology 31(5): 1187-1203

Nishimura K, Kato Y, Sakamoto W (2017) Essentials of proteolytic machineries in chloroplasts. Molecular plant 10(1): 4-19

Nuvolone D, Petri D, Voller F (2018) The effects of ozone on human health. Environmental Science and Pollution Research 25(9): 8074-8088

Oblessuc PR, Borges A, Chowdhury B, Caldas DGG, Tsai SM, Camargo LEA, Melotto M (2012) Dissecting Phaseolus vulgaris innate immune system against Colletotrichum lindemuthianum infection. PLoS One 7(8): e43161

Oblessuc PR, Baroni RM, da Silva Pereira G, Chiorato AF, Carbonell SAM, Brinez B, Luciano Da Costa ES, Garcia AAF, Camargo LEA, Kelly JD (2014) Quantitative analysis of race-specific resistance to Colletotrichum lindemuthianum in common bean. Molecular Breeding 34(3): 1313-1329

Padder B, Sharma P, Awale H, Kelly J (2017) Colletotrichum lindemuthianum, the causal agent of bean anthracnose. Journal of Plant Pathology: 317-330

Padder BA, Kamfwa K, Awale HE, Kelly JD (2016) Transcriptome profiling of the Phaseolus vulgaris-Colletotrichum lindemuthianum pathosystem. PLoS One 11(11): e0165823

Pan X, Welti R, Wang X (2010) Quantitative analysis of major plant hormones in crude plant extracts by high-performance liquid chromatography–mass spectrometry. Nature protocols 5(6): 986-992

Paniagua C, Bilkova A, Jackson P, Dabravolski S, Riber W, Didi V, Houser J, Gigli-Bisceglia N, Wimmerova M, Budínská E (2017) Dirigent proteins in plants: modulating cell wall metabolism during abiotic and biotic stress exposure. Journal of experimental botany 68(13): 3287-3301

Paradiso A, Domingo G, Blanco E, Buscaglia A, Fortunato S, Marsoni M, Scarcia P, Caretto S, Vannini C, de Pinto MC (2020) Cyclic AMP mediates heat stress response by the control of redox homeostasis and ubiquitin-proteasome system. Plant, Cell & Environment 43(11): 2727-2742

Patel N, Desai P, Patel N, Jha A, Gautam HK (2014) Agronanotechnology for plant fungal disease management: a review. Int J Curr Microbiol App Sci 3(10): 71-84

Penuelas J, Llusià J (2001) The complexity of factors driving volatile organic compound emissions by plants. Biologia plantarum 44(4): 481-487

Perez-Riverol Y, Csordas A, Bai J, Bernal-Llinares M, Hewapathirana S, Kundu DJ, Inuganti A, Griss J, Mayer G, Eisenacher M (2019) The PRIDE database and related tools and resources in 2019: improving support for quantification data. Nucleic acids research 47(D1): D442-D450

Peñuelas J, Llusià J (2002) Linking photorespiration, monoterpenes and thermotolerance in Quercus. New Phytologist 155(2): 227-237

Peñuelas J, Munné-Bosch S (2005) Isoprenoids: an evolutionary pool for photoprotection. Trends in plant science 10(4): 166-169

Peñuelas J, Staudt M (2010) BVOCs and global change. Trends in plant science 15(3): 133-144

Phillips MA, León P, Boronat A, Rodríguez-Concepción M (2008) The plastidial MEP pathway: unified nomenclature and resources. Trends in plant science 13(12): 619-623

Pichersky E, Gershenzon J (2002) The formation and function of plant volatiles: perfumes for pollinator attraction and defense. Current opinion in plant biology 5(3): 237-243

Pichersky E, Noel JP, Dudareva N (2006) Biosynthesis of plant volatiles: nature's diversity and ingenuity. Science 311(5762): 808-811

Pieterse CM, Van der Does D, Zamioudis C, Leon-Reyes A, Van Wees SC (2012) Hormonal modulation of plant immunity. Annual review of cell and developmental biology 28: 489-521

Pinfield-Wells H, Rylott EL, Gilday AD, Graham S, Job K, Larson TR, Graham IA (2005) Sucrose rescues seedling establishment but not germination of Arabidopsis mutants disrupted in peroxisomal fatty acid catabolism. The Plant Journal 43(6): 861-872

Planas-Riverola A, Gupta A, Betegón-Putze I, Bosch N, Ibañes M, Caño-Delgado AI (2019) Brassinosteroid signaling in plant development and adaptation to stress. Development 146(5)

Plesse M (2020) Global Food and Water Security in 2050: Demographic Change and Increased Demand. Future Directions International,

Pollastri S, Tsonev T, Loreto F (2014) Isoprene improves photochemical efficiency and enhances heat dissipation in plants at physiological temperatures. Journal of experimental botany 65(6): 1565-1570

Pollastri S, Baccelli I, Loreto F (2021) Isoprene: An Antioxidant Itself or a Molecule with Multiple Regulatory Functions in Plants? Antioxidants 10(5): 684

Pollastri S, Jorba I, Hawkins TJ, Llusià J, Michelozzi M, Navajas D, Peñuelas J, Hussey PJ, Knight MR, Loreto F (2019) Leaves of isoprene-emitting tobacco plants maintain PSII stability at high temperatures. New Phytologist 223(3): 1307-1318

Porta H, Rocha-Sosa M (2002) Plant lipoxygenases. Physiological and molecular features. Plant physiology 130(1): 15-21

Portillo-Estrada M, Okereke CN, Jiang Y, Talts E, Kaurilind E, Niinemets Ü (2021) Wounding-Induced VOC Emissions in Five Tropical Agricultural Species. Molecules 26(9): 2602

Portillo-Estrada M, Van Moorleghem C, Janssenswillen S, Cooper RJ, Birkemeyer C, Roelants K, Van Damme R (2021) Proton-transfer-reaction time-of-flight mass spectrometry (PTR-TOF-MS) as a tool for studying animal volatile organic compound (VOC) emissions. Methods in Ecology and Evolution 12(4): 748-766

Price PW, Bouton CE, Gross P, McPheron BA, Thompson JN, Weis AE (1980) Interactions among three trophic levels: influence of plants on interactions between insect herbivores and natural enemies. Annual review of Ecology and Systematics 11(1): 41-65

Pérez-Gil J, Rodríguez-Concepción M (2013) Metabolic plasticity for isoprenoid biosynthesis in bacteria. Biochemical journal 452(1): 19-25

Qamar A, Mysore K, Senthil-Kumar M (2015) Role of proline and pyrroline-5-carboxylate metabolism in plant defense against invading pathogens. Frontiers in plant science 6: 503

Qi X, Kaneda M, Chen J, Geitmann A, Zheng H (2011) A specific role for Arabidopsis TRAPPII in post-Golgi trafficking that is crucial for cytokinesis and cell polarity. The Plant Journal 68(2): 234-248

Qian Y, Lynch JH, Guo L, Rhodes D, Morgan JA, Dudareva N (2019) Completion of the cytosolic post-chorismate phenylalanine biosynthetic pathway in plants. Nature communications 10(1): 1-15

Quintana Rodríguez E, Rivera Macías LE, Adame Álvarez RM, Molina-Torres J, Heil M (2018) Shared weapons in fungus-fungus and fungus-plant interactions? Volatile organic compounds of plant or fungal origin exert direct antifungal activity *in vitro*. Fungal Ecol 33: 115-121

Quintana-Rodriguez E, Rivera-Macias LE, Adame-Alvarez RM, Torres JM, Heil M (2018) Shared weapons in fungus-fungus and fungus-plant interactions? Volatile organic compounds of plant or fungal origin exert direct antifungal activity in vitro. Fungal Ecology 33: 115-121

Quintana-Rodriguez E, Morales-Vargas AT, Molina-Torres J, Ádame-Alvarez RM, Acosta-Gallegos JA, Heil M (2015) Plant volatiles cause direct, induced and associational

resistance in common bean to the fungal pathogen C olletotrichum lindemuthianum. Journal of Ecology 103(1): 250-260

Rakusová H, Abbas M, Han H, Song S, Robert HS, Friml J (2016) Termination of shoot gravitropic responses by auxin feedback on PIN3 polarity. Current Biology 26(22): 3026-3032

Redillas MC, Park S-H, Lee JW, Kim YS, Jeong JS, Jung H, Bang SW, Hahn T-R, Kim J-K (2012) Accumulation of trehalose increases soluble sugar contents in rice plants conferring tolerance to drought and salt stress. Plant Biotechnology Reports 6(1): 89-96

Ren D, Yang H, Zhang S (2002) Cell death mediated by MAPK is associated with hydrogen peroxide production in Arabidopsis. Journal of Biological Chemistry 277(1): 559-565

Rendón-Anaya M, Montero-Vargas JM, Saburido-Álvarez S, Vlasova A, Capella-Gutierrez S, Ordaz-Ortiz JJ, Aguilar OM, Vianello-Brondani RP, Santalla M, Delaye L (2017) Genomic history of the origin and domestication of common bean unveils its closest sister species. Genome biology 18(1): 1-17

Rhoades DF (1983) Responses of alder and willow to attack by tent caterpillars and webworms: evidence for pheromonal sensitivity of willows. In: Hedin PA (ed) Plant Resistance to Insects. American Chemical Society, Washington DC, USA, pp 55-68

Rinnan R, Steinke M, McGenity T, Loreto F (2014) Plant volatiles in extreme terrestrial and marine environments. Plant, cell & environment 37(8): 1776-1789

Robert-Seilaniantz A, Grant M, Jones JD (2011) Hormone crosstalk in plant disease and defense: more than just jasmonate-salicylate antagonism. Annual review of phytopathology 49: 317-343

Rodríguez A, Alquézar B, Peña L (2013) Fruit aromas in mature fleshy fruits as signals of readiness for predation and seed dispersal. New Phytologist 197(1): 36-48

Rontein D, Basset G, Hanson AD (2002) Metabolic engineering of osmoprotectant accumulation in plants. Metabolic engineering 4(1): 49-56

Rosado A, Schapire AL, Bressan RA, Harfouche AL, Hasegawa PM, Valpuesta V, Botella MA (2006) The Arabidopsis tetratricopeptide repeat-containing protein TTL1 is required for osmotic stress responses and abscisic acid sensitivity. Plant Physiology 142(3): 1113-1126

Rosenkranz M, Schnitzler JP (2016) Plant volatiles. eLS: 1-9

Rosquete MR, Worden N, Ren G, Sinclair RM, Pfleger S, Salemi M, Phinney BS, Domozych D, Wilkop T, Drakakaki G (2019) AtTRAPPC11/ROG2: a role for TRAPPs in maintenance of the plant trans-Golgi network/early endosome organization and function. The Plant Cell 31(8): 1879-1898

Ryan AC, Hewitt CN, Possell M, Vickers CE, Purnell A, Mullineaux PM, Davies WJ, Dodd IC (2014) Isoprene emission protects photosynthesis but reduces plant productivity during drought in transgenic tobacco (Nicotiana tabacum) plants. New phytologist 201(1): 205-216

Sakr S, Wang M, Dédaldéchamp F, Perez-Garcia M-D, Ogé L, Hamama L, Atanassova R (2018) The sugar-signaling hub: overview of regulators and interaction with the hormonal and metabolic network. International journal of molecular sciences 19(9): 2506

Samuels L, McFarlane HE (2012) Plant cell wall secretion and lipid traffic at membrane contact sites of the cell cortex. Protoplasma 249(S1): 19-23

Sasaki K, Ohara K, Yazaki K (2005) Gene expression and characterization of isoprene synthase from Populus alba. FEBS letters 579(11): 2514-2518

Sasaki K, Saito T, Lämsä M, Oksman-Caldentey K-M, Suzuki M, Ohyama K, Muranaka T, Ohara K, Yazaki K (2007) Plants utilize isoprene emission as a thermotolerance mechanism. Plant and Cell Physiology 48(9): 1254-1262

Sato K, Ueda T, Nakano A (1999) The Arabidopsis thaliana RER1 gene family: its potential role in the endoplasmic reticulum localization of membrane proteins. Plant molecular biology 41(6): 815-824

Scala A, Allmann S, Mirabella R, Haring MA, Schuurink RC (2013) Green leaf volatiles: a plant's multifunctional weapon against herbivores and pathogens. Internat J Mol Sci 14(9): 17781-17811

Schiestl FP, Huber FK, Gomez JM (2011) Phenotypic selection on floral scent: trade-off between attraction and deterrence? Evolutionary Ecology 25(2): 237-248

Schilmiller AL, Koo AJ, Howe GA (2007) Functional diversification of acyl-coenzyme A oxidases in jasmonic acid biosynthesis and action. Plant Physiology 143(2): 812-824

Schmidt R, Etalo DW, de Jager V, Gerards S, Zweers H, de Boer W, Garbeva P (2016) Microbial small talk: volatiles in fungal–bacterial interactions. Front Microbiol 6: art. no 1495, Original Research

Schmitt-Keichinger C (2019) Manipulating cellular factors to combat viruses: a case study from the plant eukaryotic translation initiation factors eIF4. Frontiers in microbiology 10: 17

Schmutz J, McClean PE, Mamidi S, Wu GA, Cannon SB, Grimwood J, Jenkins J, Shu S, Song Q, Chavarro C (2014) A reference genome for common bean and genome-wide analysis of dual domestications. Nature genetics 46(7): 707-713

Schneider A, Steinberger I, Strissel H, Kunz HH, Manavski N, Meurer J, Burkhard G, Jarzombski S, Schünemann D, Geimer S (2014) The Arabidopsis Tellurite resistance C protein together with ALB 3 is involved in photosystem II protein synthesis. The Plant Journal 78(2): 344-356

Schrick K, Mayer U, Martin G, Bellini C, Kuhnt C, Schmidt J, Jürgens G (2002) Interactions between sterol biosynthesis genes in embryonic development of Arabidopsis. The Plant Journal 31(1): 61-73

Schröder F, Lisso J, Müssig C (2011) EXORDIUM-LIKE1 promotes growth during low carbon availability in Arabidopsis. Plant physiology 156(3): 1620-1630

Schurr U, Schulze ED (1995) The concentration of xylem sap constituents in root exudate, and in sap from intact, transpiring castor bean plants (Ricinus communis L.). Plant, Cell & Environment 18(4): 409-420

Schwab W, Davidovich-Rikanati R, Lewinsohn E (2008) Biosynthesis of plant-derived flavor compounds. The plant journal 54(4): 712-732

Shafiq S, Akram NA, Ashraf M (2015) Does exogenously-applied trehalose alter oxidative defense system in the edible part of radish (Raphanus sativus L.) under water-deficit conditions? Scientia Horticulturae 185: 68-75

Shams E, Javan-Nikkhah M, Gohari AM (2020) Dissecting molecular events and gene expression signatures involved in Colletotrichum lindemuthianum-Phaseolus vulgaris pathosystem in compatible and incompatible interactions. European Journal of Plant Pathology 156(3): 925-937

Sharifi R, Lee SM, Ryu CM (2018) Microbe-induced plant volatiles. New Phytologist 220(3): 684-691

Sharkey TD (2013) Is it useful to ask why plants emit isoprene? Plant, Cell & Environment 36(3): 517-520

Sharkey TD, Singsaas EL (1995) Why plants emit isoprene. Nature 374(6525): 769-769

Sharkey TD, Yeh S (2001) Isoprene emission from plants. Annual review of plant biology 52(1): 407-436

Sharkey TD, Chen X, Yeh S (2001) Isoprene increases thermotolerance of fosmidomycin-fed leaves. Plant Physiology 125(4)

Sharkey TD, Gray DW, Pell HK, Breneman SR, Topper L (2013) Isoprene synthase genes form a monophyletic clade of acyclic terpene synthases in the Tps-b terpene synthase family. Evolution: International Journal of Organic Evolution 67(4): 1026-1040

Sharma P, Sharma O, Padder B, Kapil R (2008) Yield loss assessment in common bean due to anthracnose (Colletotrichum lindemuthianum) under sub temperate conditions of North-Western Himalayas. Indian Phytopathology 61(3): 323

Sheoran IS, Ross AR, Olson DJ, Sawhney VK (2009) Compatibility of plant protein extraction methods with mass spectrometry for proteome analysis. Plant Science 176(1): 99-104

Shi C, Baldwin IT, Wu J (2012) Arabidopsis plants having defects in nonsense-mediated mRNA decay factors UPF1, UPF2, and UPF3 show photoperiod-dependent phenotypes in development and stress responses. Journal of integrative plant biology 54(2): 99-114

Shiojiri K, Kishimoto K, Ozawa R, Kugimiya S, Urashimo S, Arimura G, Horiuchi J, Nishioka T, Matsui K, Takabayashi J (2006) Changing green leaf volatile biosynthesis in plants: An approach for improving plant resistance against both herbivores and pathogens. Proc Natl Acad Sci USA 103(45): 16672-16676

Shu S, Tang Y, Yuan Y, Sun J, Zhong M, Guo S (2016) The role of 24-epibrassinolide in the regulation of photosynthetic characteristics and nitrogen metabolism of tomato seedlings under a combined low temperature and weak light stress. Plant Physiology and Biochemistry 107: 344-353

Sicard D, Michalakis Y, Dron M, Neema C (1997) Genetic diversity and pathogenic variation of Colletotrichum lindemuthianum in the three centers of diversity of its host, Phaseolus vulgaris. Phytopathology 87(8): 807-813

Siegrist J, Orober M, Buchenauer H (2000) β-Aminobutyric acid-mediated enhancement of resistance in tobacco to tobacco mosaic virus depends on the accumulation of salicylic acid. Physiological and Molecular Plant Pathology 56(3): 95-106

Silva NF, Goring DR (2002) The proline-rich, extensin-like receptor kinase-1 (PERK1) gene is rapidly induced by wounding. Plant molecular biology 50(4): 667-685

Singh M, Kumar J, Singh S, Singh VP, Prasad SM (2015) Roles of osmoprotectants in improving salinity and drought tolerance in plants: a review. Reviews in Environmental Science and Bio/Technology 14(3): 407-426

Singh P, Pandey AK (2021) Dysphania ambrosioides essential oils: from pharmacological agents to uses in modern crop protection—a review. Phytochemistry Reviews: 1-19

Singsaas EL, Lerdau M, Winter K, Sharkey TD (1997) Isoprene increases thermotolerance of isoprene-emitting species. Plant physiology 115(4): 1413-1420

Smart RE, Bingham GE (1974) Rapid estimates of relative water content. Plant physiology 53(2): 258-260

Song GC, Ryu C-M (2013) Two volatile organic compounds trigger plant self-defense against a bacterial pathogen and a sucking insect in cucumber under open field conditions. International journal of molecular sciences 14(5): 9803-9819

Souter M, Topping J, Pullen M, Friml J, Palme K, Hackett R, Grierson D, Lindsey K (2002) hydra mutants of Arabidopsis are defective in sterol profiles and auxin and ethylene signaling. The Plant Cell 14(5): 1017-1031

Steindel F, Beauchamp J, Hansel A, Kesselmeier J, Kleist E, Kuhn U, Wisthaler A, Wildt J Stress induced VOC emissions from mildew infested oak. Proceedings of the Geophys Res Abstr, 2005, pp EGU05-A-03010

Strizhov N, Ábrahám E, Ökrész L, Blickling S, Zilberstein A, Schell J, Koncz C, Szabados L (1997) Differential expression of two P5CS genes controlling proline accumulation during salt-stress requires ABA and is regulated by ABA1, ABI1 and AXR2 in Arabidopsis. The Plant Journal 12(3): 557-569

Subba P, Narayana Kotimoole C, Prasad TSK (2019) Plant proteome databases and bioinformatic tools: an expert review and comparative insights. Omics: a journal of integrative biology 23(4): 190-206

Sulkowska A, Auber A, Sikorski PJ, Silhavy D, Auth M, Sitkiewicz E, Jean V, Merret R, Bousquet-Antonelli C, Kufel J (2020) RNA helicases from the DEA (D/H)-box family contribute to plant NMD efficiency. Plant and Cell Physiology 61(1): 144-157

Szklarczyk D, Franceschini A, Wyder S, Forslund K, Heller D, Huerta-Cepas J, Simonovic M, Roth A, Santos A, Tsafou KP (2015) STRING v10: protein–protein interaction networks, integrated over the tree of life. Nucleic acids research 43(D1): D447-D452

Taheri P, Tarighi S (2011) A survey on basal resistance and riboflavin-induced defense responses of sugar beet against Rhizoctonia solani. Journal of Plant Physiology 168(10): 1114-1122

Takemiya A, Sugiyama N, Fujimoto H, Tsutsumi T, Yamauchi S, Hiyama A, Tada Y, Christie JM, Shimazaki K-i (2013) Phosphorylation of BLUS1 kinase by phototropins is a primary step in stomatal opening. Nature communications 4(1): 1-8

Tan F-C, Cheng Q, Saha K, Heinemann IU, Jahn M, Jahn D, Smith AG (2008) Identification and characterization of the Arabidopsis gene encoding the tetrapyrrole biosynthesis enzyme uroporphyrinogen III synthase. Biochemical Journal 410(2): 291-299

Tanaka K, Heil M (2021a) Damage-Associated Molecular Patterns (DAMPs) in Plant Innate Immunity: Applying the Danger Model and Evolutionary Perspectives. Annual Review of Phytopathology 59

Tanaka K, Heil M (2021b) Damage-associated molecular patterns (DAMPs) in plant innate immunity: applying the danger model and evolutionary perspectives. Annu Rev Phytopathol 59: posted online on April 26, 2021

Tani A, Mochizuchi T (2021) Exchanges of volatile organic compounds between terrestrial ecosystems and the atmosphere. Journal of Agricultural Meteorology 77(1): 66-80

Tattini M, Loreto F, Fini A, Guidi L, Brunetti C, Velikova V, Gori A, Ferrini F (2015) Isoprenoids and phenylpropanoids are part of the antioxidant defense orchestrated daily by drought-stressed P latanus× acerifolia plants during Mediterranean summers. New Phytologist 207(3): 613-626

Tattini M, Velikova V, Vickers C, Brunetti C, Di Ferdinando M, Trivellini A, Fineschi S, Agati G, Ferrini F, Loreto F (2014) Isoprene production in transgenic tobacco alters isoprenoid, non-structural carbohydrate and phenylpropanoid metabolism, and protects photosynthesis from drought stress. Plant, Cell & Environment 37(8): 1950-1964

Thalmann M, Santelia D (2017) Starch as a determinant of plant fitness under abiotic stress. New Phytologist 214(3): 943-951

Thellmann M, Rybak K, Thiele K, Wanner G, Assaad FF (2010) Tethering factors required for cytokinesis in Arabidopsis. Plant physiology 154(2): 720-732

Thimm O, Bläsing O, Gibon Y, Nagel A, Meyer S, Krüger P, Selbig J, Müller LA, Rhee SY, Stitt M (2004) MAPMAN: a user-driven tool to display genomics data sets onto diagrams of metabolic pathways and other biological processes. The Plant Journal 37(6): 914-939

Tissier A, Morgan JA, Dudareva N (2017) Plant volatiles: going 'in'but not 'out'of trichome cavities. Trends in plant science 22(11): 930-938

Toribio R, Mangano S, Fernández-Bautista N, Muñoz A, Castellano M (2020) HOP, a Co-chaperone Involved in Response to Stress in Plants. Frontiers in Plant Science 11: 1657

Torres RO, Henry A (2018) Yield stability of selected rice breeding lines and donors across conditions of mild to moderately severe drought stress. Field crops research 220: 37-45

Trouvelot S, Héloir M-C, Poinssot B, Gauthier A, Paris F, Guillier C, Combier M, Trdá L, Daire X, Adrian M (2014) Carbohydrates in plant immunity and plant protection: roles and potential application as foliar sprays. Frontiers in plant science 5: 592

Turan S, Tripathy BC (2015) Salt-stress induced modulation of chlorophyll biosynthesis during de-etiolation of rice seedlings. Physiologia plantarum 153(3): 477-491

Turlings TCJ, Erb M (2018) Tritrophic interactions mediated by herbivore-induced plant volatiles: mechanisms, ecological relevance, and application potential. In: Berenbaum MR (ed) Annual Review of Entomology, Vol 63. Annual Reviews, Palo Alto, pp 433-452

Tyanova S, Temu T, Sinitcyn P, Carlson A, Hein MY, Geiger T, Mann M, Cox J (2016) The Perseus computational platform for comprehensive analysis of (prote) omics data. Nature methods 13(9): 731-740

Türkan I, Demiral T (2009) Recent developments in understanding salinity tolerance. Environmental and Experimental Botany 67(1): 2-9

ul Hassan MN, Zainal Z, Ismail I (2015) Green leaf volatiles: biosynthesis, biological functions and their applications in biotechnology. Plant Biotechnology Journal 13(6): 727-739

Ungar D, Oka T, Krieger M, Hughson FM (2006) Retrograde transport on the COG railway. Trends in cell biology 16(2): 113-120

van Dijk M, Morley T, Rau ML, Saghai Y (2021) A meta-analysis of projected global food demand and population at risk of hunger for the period 2010–2050. Nature Food 2(7): 494-501

Vanzo E, Merl-Pham J, Velikova V, Ghirardo A, Lindermayr C, Hauck SM, Bernhardt J, Riedel K, Durner J, Schnitzler J-P (2016) Modulation of protein S-nitrosylation by isoprene emission in poplar. Plant physiology 170(4): 1945-1961

Velikova V, Loreto F (2005) On the relationship between isoprene emission and thermotolerance in Phragmites australis leaves exposed to high temperatures and during the recovery from a heat stress. Plant, Cell & Environment 28(3): 318-327

Velikova V, Edreva A, Loreto F (2004) Endogenous isoprene protects Phragmites australis leaves against singlet oxygen. Physiologia Plantarum 122(2): 219-225

Velikova V, Ghirardo A, Vanzo E, Merl J, Hauck SM, Schnitzler J-P (2014) Genetic manipulation of isoprene emissions in poplar plants remodels the chloroplast proteome. Journal of proteome research 13(4): 2005

Velikova V, Várkonyi Z, Szabó M, Maslenkova L, Nogues I, Kovács L, Peeva V, Busheva M, Garab G, Sharkey TD (2011) Increased thermostability of thylakoid membranes in isoprene-emitting leaves probed with three biophysical techniques. Plant Physiology 157(2): 905-916

Ventura I, Brunello L, Iacopino S, Valeri MC, Novi G, Dornbusch T, Perata P, Loreti E (2020) Arabidopsis phenotyping reveals the importance of alcohol dehydrogenase and pyruvate decarboxylase for aerobic plant growth. Scientific reports 10(1): 1-14

Verhage A, van Wees SC, Pieterse CM (2010) Plant immunity: it's the hormones talking, but what do they say? Plant Physiology 154(2): 536-540

Veyrat N, Robert CAM, Turlings TCJ, Erb M (2016) Herbivore intoxication as a potential primary function of an inducible volatile plant signal. J Ecol 104(2): 591-600, Article

Vickers CE, Gershenzon J, Lerdau MT, Loreto F (2009) A unified mechanism of action for volatile isoprenoids in plant abiotic stress. Nature chemical biology 5(5): 283-291

Vranová E, Coman D, Gruissem W (2013) Network analysis of the MVA and MEP pathways for isoprenoid synthesis. Annual review of plant biology 64: 665-700

Vukašinović N, Žárský V (2016) Tethering complexes in the Arabidopsis endomembrane system. Frontiers in cell and developmental biology 4: 46

Wang Q, Yu F, Xie Q (2020a) Balancing growth and adaptation to stress: Crosstalk between brassinosteroid and abscisic acid signaling. Plant, Cell & Environment 43(10): 2325-2335

Wang R-S, Pandey S, Li S, Gookin TE, Zhao Z, Albert R, Assmann SM (2011) Common and unique elements of the ABA-regulated transcriptome of Arabidopsis guard cells. BMC genomics 12(1): 1-24

Wang S, Kurepa J, Smalle JA (2009) The Arabidopsis 26S proteasome subunit RPN1a is required for optimal plant growth and stress responses. Plant and Cell Physiology 50(9): 1721-1725

Wang X, Xu M, Gao C, Zeng Y, Cui Y, Shen W, Jiang L (2020b) The roles of endomembrane trafficking in plant abiotic stress responses. Journal of integrative plant biology 62(1): 55-69

Wang Y, Yang L, Chen X, Ye T, Zhong B, Liu R, Wu Y, Chan Z (2016) Major latex protein-like protein 43 (MLP43) functions as a positive regulator during abscisic acid responses and confers drought tolerance in Arabidopsis thaliana. Journal of experimental botany 67(1): 421-434

War AR, Paulraj MG, Ahmad T, Buhroo AA, Hussain B, Ignacimuthu S, Sharma HC (2012) Mechanisms of plant defense against insect herbivores. Plant signaling & behavior 7(10): 1306-1320

Wasternack C, Feussner I (2018) The Oxylipin Pathways: Biochemistry and Function. In: Merchant SS (ed) Annual Review of Plant Biology, Vol 69. Annual Reviews, Palo Alto, pp 363-386

Watanabe S, Matsumoto M, Hakomori Y, Takagi H, Shimada H, Sakamoto A (2014) The purine metabolite allantoin enhances abiotic stress tolerance through synergistic activation of abscisic acid metabolism. Plant, cell & environment 37(4): 1022-1036

Way DA, Ghirardo A, Kanawati B, Esperschütz J, Monson RK, Jackson RB, Schmitt-Kopplin P, Schnitzler JP (2013) Increasing atmospheric CO 2 reduces metabolic and physiological differences between isoprene-and non-isoprene-emitting poplars. New Phytologist 200(2): 534-546

Wheatley R, Hackett C, Bruce A, Kundzewicz A (1997) Effect of substrate composition on production of volatile organic compounds from Trichoderma spp. inhibitory to wood decay fungi. International biodeterioration & biodegradation 39(2-3): 199-205

Widhalm JR, Dudareva N (2015) A familiar ring to it: biosynthesis of plant benzoic acids. Molecular plant 8(1): 83-97

Widhalm JR, Jaini R, Morgan JA, Dudareva N (2015) Rethinking how volatiles are released from plant cells. Trends in plant science 20(9): 545-550

Wilkins K (1996) Volatile metabolites from actinomycetes. Chemosphere 32(7): 1427-1434

Wilkinson S, Davies WJ (2002) ABA-based chemical signalling: the co-ordination of responses to stress in plants. Plant, cell & environment 25(2): 195-210

Winter G, Todd CD, Trovato M, Forlani G, Funck D (2015) Physiological implications of arginine metabolism in plants. Frontiers in plant science 6: 534

Wiśniewski JR (2016) Quantitative Evaluation of Filter Aided Sample Preparation (FASP) and Multienzyme Digestion FASP Protocols. Analytical Chemistry 88(10): 5438-5443

Wiśniewski JR, Zougman A, Nagaraj N, Mann M (2009) Universal sample preparation method for proteome analysis. Nature methods 6(5): 359-362

Wong LH, Gatta AT, Levine TP (2019) Lipid transfer proteins: the lipid commute via shuttles, bridges and tubes. Nature reviews Molecular cell biology 20(2): 85-101

Wu X, Xiong E, Wang W, Scali M, Cresti M (2014) Universal sample preparation method integrating trichloroacetic acid/acetone precipitation with phenol extraction for crop proteomic analysis. Nature protocols 9(2): 362

Wu X, Qiao Z, Liu H, Acharya BR, Li C, Zhang W (2017) CML20, an Arabidopsis calmodulin-like protein, negatively regulates guard cell ABA signaling and drought stress tolerance. Frontiers in plant science 8: 824

Xu J, Trainotti L, Li M, Varotto C (2020) Overexpression of isoprene synthase affects ABA-and drought-related gene expression and enhances tolerance to abiotic stress. International journal of molecular sciences 21(12): 4276

Yi H-S, Heil M, Adame-Alvarez RM, Ballhorn DJ, Ryu C-M (2009) Airborne induction and priming of plant defenses against a bacterial pathogen. Plant Physiology 151(4): 2152-2161

You J, Zhang Y, Liu A, Li D, Wang X, Dossa K, Zhou R, Yu J, Zhang Y, Wang L (2019) Transcriptomic and metabolomic profiling of drought-tolerant and susceptible sesame genotypes in response to drought stress. BMC plant biology 19(1): 1-16

Yáñez-Serrano AM, Nölscher AC, Bourtsoukidis E, Derstroff B, Zannoni N, Gros V, Lanza M, Brito J, Noe SM, House E (2016) Atmospheric mixing ratios of methyl ethyl ketone (2-butanone) in tropical, boreal, temperate and marine environments. Atmospheric Chemistry and Physics 16(17): 10965-10984

Zabel F, Delzeit R, Schneider JM, Seppelt R, Mauser W, Václavík T (2019) Global impacts of future cropland expansion and intensification on agricultural markets and biodiversity. Nature communications 10(1): 1-10

Zhang JJ, Wei Y, Fang Z (2019) Ozone pollution: a major health hazard worldwide. Frontiers in immunology 10: 2518

Zhang S, Yang X, Sun M, Sun F, Deng S, Dong H (2009) Riboflavin-induced priming for pathogen defense in Arabidopsis thaliana. Journal of Integrative Plant Biology 51(2): 167-174

Zhao C, Liu B, Piao S, Wang X, Lobell DB, Huang Y, Huang M, Yao Y, Bassu S, Ciais P (2017) Temperature increase reduces global yields of major crops in four independent estimates. Proceedings of the National Academy of Sciences 114(35): 9326-9331

Zhao N, Guan J, Ferrer J-L, Engle N, Chern M, Ronald P, Tschaplinski TJ, Chen F (2010) Biosynthesis and emission of insect-induced methyl salicylate and methyl benzoate from rice. Plant Physiology and Biochemistry 48(4): 279-287

Zhao S, Erbilgin N (2019) Larger resin ducts are linked to the survival of lodgepole pine trees during mountain pine beetle outbreak. Frontiers in plant science 10: 1459

Zheng Z, Nonomura T, Appiano M, Pavan S, Matsuda Y, Toyoda H, Wolters A-MA, Visser RG, Bai Y (2013) Loss of function in Mlo orthologs reduces susceptibility of pepper and tomato to powdery mildew disease caused by Leveillula taurica. PloS one 8(7): e70723

Zuo Z, Weraduwage SM, Lantz AT, Sanchez LM, Weise SE, Wang J, Childs KL, Sharkey TD (2019) Isoprene Acts as a Signaling Molecule in Gene Networks Important for Stress Responses and Plant Growth. Plant Physiol 180(1): 124-152

Šimpraga M, Verbeeck H, Demarcke M, Joó É, Pokorska O, Amelynck C, Schoon N, Dewulf J, Van Langenhove H, Heinesch B (2011) Clear link between drought stress, photosynthesis and biogenic volatile organic compounds in Fagus sylvatica L. Atmospheric Environment 45(30): 5254-5259